Theses and Dissertations

2010

Properties associated with filoviral-glycoprotein-mediated entry events in permissive cells

Catherine Leta Miller
University of Iowa

Recommended Citation

Miller, Catherine Leta. "Properties associated with filoviral-glycoprotein-mediated entry events in permissive cells." PhD (Doctor of Philosophy) thesis, University of Iowa, 2010.
http://ir.uiowa.edu/etd/1028.

PROPERTIES ASSOCIATED WITH FILOVIRAL-GLYCOPROTEIN-MEDIATED

ENTRY EVENTS IN PERMISSIVE CELLS

by

Catherine Leta Miller

<u>An Abstract</u>

Of a thesis submitted in partial fulfillment of the
requirements for the Doctor of Philosophy degree
in Microbiology
in the Graduate College of
The University of Iowa

May 2010

Thesis Supervisor: Associate Professor Wendy J Maury

ABSTRACT

To enter cells, the filovirus, ebolavirus (EBOV), must bind to target cells and internalize into an endocytic vesicle. The properties surrounding filoviral entry into permissive cells remain poorly studied. To date, the kinetics associated with filoviral-glycoprotein (GP)-mediated entry have never been investigated past 6 hours. We observed that less than half of the retroviral based pseudovirions pre-bound to the cell surface were internalized by 7 hours at 37ºC indicating that virion internalization was a slow process. Consistent with slow internalization of retroviral particles, we observed that, while virus entry lost sensitivity to ammonium chloride treatment with time, 50% of the virions remained sensitive to low pH neutralization for at least 7 hours. These slow entry kinetics for filoviruses have not been appreciated thus far, and could have significant implications in the timing and types of treatments that could be administered to filoviral infected individuals.

We also determined the impact of specific carbohydrate linkages on host cell plasma membrane proteins involved in filoviral entry, by using a series of Chinese hamster ovary (CHO) cell lines deficient in one or more enzymes required for N- and O-linked glycosylation. The LdlD CHO cell line that expresses normal surface N-linked glycans but has abbreviated O-linked surface glycans showed a 50% reduction in transduction by both Zaire (ZEBOV) and Lake Victoria MARV-GP pseudotyped particles as compared to the control wild type parental CHO cell line (Pro5). Use of the novel O-linked inhibitor drug 1-68A allowed us to confirm the necessity of O-linked glycans in efficient ZEBOV entry into additional permissive cells types. Interestingly, loss of terminal sialic acids (Lec2 cells) or galactose (Lec8 cells) on both N- and O-linked sugars resulted in a 2-fold enhancement of filoviral GP mediated entry compared to control. However, Lec1 cells that have wild type O-linked glycans but highly abbreviated N-linked glycans had similar levels of transduction to control Pro5 cells. Further studies indicated that binding of ZEBOV pseudovirions to Pro5 and all mutant

CHO cells was equal, indicating that a post-binding defect or enhancement in ZEBOV internalization may be occurring. These data identify the importance of host cell O-linked glycosylation during the initial steps of filovirus infection.

While the receptor(s) used by filoviruses for productive binding and entry into cells remains to be identified, several proteins have been shown to enhance filoviral entry into cells. Axl, a plasma membrane associated Tyro3/Axl/Mer (TAM) family member, is necessary for optimal ZEBOV-GP-dependent entry into some permissive cells, but not others. To date, the precise role of Axl in virion entry is unknown. Through the use of biochemical inhibitors, RNAi, and dominant-negative constructs, we set out to characterize entry pathways used for ZEBOV uptake in cells that require Axl for optimal transduction (Axl-dependent cells) and to define the role of Axl in these processes. We demonstrate that ZEBOV-GP-dependent entry into Axl-dependent cells occurs through multiple pathways including both clathrin-dependent and caveolae/lipid raft-mediated endocytosis. Surprisingly, both dynamin-dependent and -independent fluid-phase uptake (FPU) pathways mediated ZEBOV-GP entry into the Axl-dependent cells as well. Reduction of Axl expression by RNAi treatment resulted in abrogation of ZEBOV entry by FPU-dependent pathways, but had no effect on receptor-mediated endocytosis mechanisms. Our findings demonstrate for the first time that Axl enhances FPU, thereby increasing productive ZEBOV entry, and providing insight into the mechanisms surrounding filoviral entry.

Abstract Approved: _____

                                                    Thesis Supervisor

         _____

                                               Title and Department

         _____

                                                         Date

PROPERTIES ASSOCIATED WITH FILOVIRAL-GLYCOPROTEIN-MEDIATED

ENTRY EVENTS IN PERMISSIVE CELLS

by

Catherine Leta Miller

A thesis submitted in partial fulfillment
of the requirements for the Doctor
of Philosophy degree in Microbiology
in the Graduate College of
The University of Iowa

May 2010

Thesis Supervisor: Associate Professor Wendy J Maury

Graduate College
The University of Iowa
Iowa City, Iowa

CERTIFICATE OF APPROVAL

_____

PH.D. THESIS

_____

This is to certify that the Ph. D. thesis of

Catherine Leta Miller

has been approved by the Examining Committee
for the thesis requirement for the Doctor of
Philosophy degree in Microbiology
at the May 2010 graduation.

Thesis Committee: _____
                         Wendy Maury, Thesis Supervisor

                         _____
                         Lee-Ann Allen

                         _____
                         Anton McCaffrey

                         _____
                         Steve Varga

                         _____
                         Paul McCray Jr.

To Jason R. Hunt, Kathleen A. Miller and David L. Miller

ACKNOWLEDGEMENTS

TABLE OF CONTENTS

LIST OF TABLES

LIST OF FIGURES

Figure

LIST OF ABBREVIATIONS

RNA   Ribonucleic acid

EBOV   Ebolavirus

MARV   Marburgvirus

LVMARV   Lake Victoria Marburgvirus

ZEBOV   Zaire ebolavirus

SEBOV   Sudan ebolavirus

REBOV   Reston ebolavirus

CIEBOV   Côte d'Ivoire ebolavirus

BEBOV   Bundibugyo ebolavirus

GP   Glycoprotein

NP   Nucleoprotein

VP30   Viral protein 30

VP40   Viral protein 40

VP24   Viral protein 24

sGP   Secreted glycoprotein

ssGP   Secondary secreted glycoprotein

$GP_{1,2}$ Spike glycoprotein

VP35   Viral protein 24

L   Polymerase protein

M   Matrix protein

preGP   Precursor glycoprotein

HSV-1   Herpes simplex virus 1

HIV-1   Human immunodeficiency virus 1

VSV   Vesicular stomatitis virus

SARS   Severe-acute respiratory syndrome coronavirus

MuLV	Murine leukemia virus
SFV	Semliki Forest virus
RBD	Receptor binding domain
MLD	Mucin-like domain
EBOVΔO-GP	Mucin-like domain deleted form of ebolavirus glycoprotein
FPU	Fluid-phase uptake
EGFR	Extracellular growth-factor-receptor
PLC	Phospholipase C
PI3K	Phosphatidylinositol 3-kinase
CIE	Clathrin-independent endocytosis
CME	Clathrin-mediated endocytosis
GPI	Glycosylphosphatidylinositol
CAV1	Caveolin 1
CAV2	Caveolin 2
SV40	Simian virus-40
CCP	Clathrin-coated pit
RNAi	Ribonucleic acid interference
EIAV	Equine infectious anemia virus
CRD	Carbohydrate recognition domain
FR-α	Folate receptor α
TAM	Tyro3 family of receptor tyrosine kinases
CGA	Comparative genomic analysis
Gla	γ-carboxyglutamic acid
LG	Laminin G-like
Ig	Immunoglobulin-like
BSL-4	Biosafety level four
FIV	Feline immunodeficiency virus

β-gal   Beta-galactosidase

GFP   Green fluorescent protein

Hff   Human foreskin fibroblast

HuVEC   Human umbilical vein endothelial cell

MOI   Multiplicity of infection

CHO   Chinese hamster ovary

PS   Phosphatidylserine

TIM   T-cell/immunoglobulin/mucin-like domain molecule

CHAPTER ONE: INTRODUCTION

Filoviruses

The family *Filoviridae* belongs to the phylogenetic order *Mononegavirales* and thus contains a negative sense, single stranded RNA genome. Other members of the *Mononegavirales* order include *Bornaviridae*, *Paramyxoviridae* and *Rhabdoviridae* families. These families encompass such viral species as Borna disease virus, measles virus, mumps virus and rabies virus and are known throughout the world for causing debilitating infections. It is believed that the *Filoviridae* family is evolutionarily linked to both the *vesiculovirus* genus of the *Rhabdoviridae* as well as the *Pneumovirinae* subfamily of the family *Paramyxoviridae* [1-3]. However, it was only relatively recently, within the past 7,000 to 8,000 years, that the *Filoviridae* family diverged to form two distinct genera, *Ebolavirus* (EBOV) and *Marburgvirus* (MARV) [3].

The first and only species of MARV, Lake Victoria (LVMARV) was discovered in 1967, followed by the discovery of the first EBOV species, Zaire (ZEBOV) in 1976. Genetic analysis of subsequent filoviral isolates following the discovery of ZEBOV showed the existence of 4 additional EBOV species including Sudan (SEBOV), Reston (REBOV), Côte d'Ivoire (CIEBOV) and the most recently discovered species Bundibugyo (BEBOV).

Lake Victoria MARV

LVMARV was officially discovered in Marburg, Germany in 1967 after laboratory workers became ill in different geographic locations after processing tissues of infected African green monkeys imported from Uganda. LVMARV is antigenically different form each of the EBOV species [4, 5]. At the nucleotide level, the LVMARV genome is approximately 30% similar to the recognized EBOV species (excluding BEBOV) [6]. Between LVMARV and EBOV species, the viral glycoproteins (GPs) differ by at least 55% at the nucleotide level and by approximately 67% at the amino acid level

[7]. Infections of LVMARV have resulted in an 80-83% case fatality rate since the year of its discovery, with the most recent LVMARV outbreak occurring in Uganda in 2007.

ZEBOV

ZEBOV is the most pathogenic species of the EBOV genera, with an average case fatality rate of 80-90% [8]. ZEBOV shares an identity of approximately 60% at the nucleotide level with the other species of EBOV (excluding BEBOV) [6]. The GPs of the different EBOV species (excluding BEBOV) differ by at least 37-41% at the nucleotide level and at least 34-43% at the amino acid level [7]. Phylogenetic analysis of ZEBOV, SEBOV, REBOV and CIEBOV has suggested that ZEBOV is the oldest species of EBOV, and that ZEBOV gave rise to all of the other EBOV species, beginning up to 2,100 years ago [3]. The last known ZEBOV outbreak occurred in Congo in the summer of 2006.

SEBOV

SEBOV was first isolated in 1976, the same year ZEBOV was discovered. SEBOV mortality rates average around 80-85%, and the last known SEBOV outbreak occurred in 2004 in Sudan. Phylogenetic analysis of SEBOV isolates has suggested that it, along with the REBOV species, diverged from ZEBOV approximately 1,600 years ago [3].

REBOV

REBOV is the only filovirus to infect humans but not cause significant pathology or disease. It was first introduced to the United States in the fall of 1989 through importation of non-human primates (cynomolgus macaques) from the Philippines. Approximately 8% (42/550) of the American workers who had come into contact with the monkeys were seropositive for one or more antigens of REBOV, ZEBOV, SEBOV or Lake Victoria MARV [9]. REBOV is more closely related to SEBOV than the other ebolaviruses, however differences in the genomic sequence of REBOV, particularly the

GP gene, have not provided information as to why REBOV is non-pathogenic in humans [10, 11].

CIEBOV

To date, only one confirmed human case of CIEBOV has ever been recorded, and occurred in 1994 in the Ivory Coast region of Africa as the result of contact with CIEBOV infected chimpanzees. The infected individual did not die from the infection, and the symptoms exhibited by the infected individual were quite mild compared to infection with LV MARV, ZEBOV or SEBOV [12, 13]. CIEBOV is thought have diverged from the ZEBOV as little as 700 years ago [3].

BEBOV

Sequencing of viral isolates from a winter, 2007 hemorrhagic fever outbreak in Bundibugyo District in Western Uganda yielded the discovery of a distinct, previously unidentified ebolavirus species [14]. This new isolate of EBOV isolate was very distantly related to CIEBOV, and resulted in an approximate 36% mortality rate in the infected individuals [14]. Additional studies concerning BEBOV tropism, pathogenicity and pathology in humans and non-human primates have yet to be performed.

Filoviral particles

All filoviruses exhibit a characteristic filamentous branched or "shepherd's crook" type morphology when viewed under electron microscopy (**Fig. 1**). While all filovirions are roughly equivalent in diameter (80 nm), viral particles generated *in vitro* and those observed in tissue samples from infected individuals have a heterogeneous appearance, as virus length may vary slightly depending on the exact time and position of budding from the infected cell [9]. MARV and EBOV particles range in size from 800 nm (MARV) to greater than 1 μm (EBOV species) in length. The degree of branching differs among the four most studied EBOV species, with SEBOV producing the straightest and least branched viral particles, and ZEBOV producing viral particles with significantly more branching during *in vitro* tissue culture propagation of virus [15].

Filovirus genome

The genomes of each MARV and EBOV species are approximately 19 kb in length. The genomes are composed of linear RNA of negative polarity and are single-stranded. Each EBOV species genome is arranged similarly, and contains 7 genes (**Fig. 2A**), that through co-transcriptional editing, yield a total of 9 known proteins. These proteins include the primary and secondary structural nucleoproteins (NP and VP30), the primary and secondary structural matrix proteins (VP40 and VP24), two EBOV-GP secreted forms (sGP and ssGP), a non-secreted, viral membrane bound form of the EBOV-GP (GP$_{1,2}$), and two non-structural proteins (VP35 and L). The MARV genome is arranged identically to the EBOV genome, and also contains 7 genes. However, the MARV genome only encodes for 7 known proteins, as only one form of the viral membrane bound glycoprotein (GP$_{1,2}$) has been identified to date.

EBOV structural protein NP. The EBOV nucleoprotein (NP) is the second largest EBOV protein at approximately 740 amino acids in length and forms hexagonal, helical structures that complexes with both negative-sense and positive-sense genomic RNA (**Fig. 2B**). NP is abundant in the cytoplasm during EBOV replication and alone, is necessary but not sufficient to form functional ribonucleoprotein complexes that are capable of serving as the template for EBOV genome synthesis [16-19].

EBOV structural protein VP30. EBOV protein 30 (VP30) is the minor NP and is capable of binding to itself as well as to EBOV NP (**Fig. 2B**). Expression of VP30 and NP simultaneously allows for the formation of NP and VP30 inclusion bodies within eukaryotic cells [20]. VP30 functions as a transcriptional activator during EBOV infection [21] and binds specifically to EBOV single-stranded RNA, and not other, non-specific or host derived single-stranded RNAs. The specificity of VP30 binding and subsequent viral transcription is enhanced by low pH and also depends on the ability of VP30 to bind to zinc ions via a zinc-binding motif [22].

EBOV structural protein VP40. The filoviral protein 40 (VP40) genes are the most conserved genes among all of the filovirus species, and encode for the most abundant filoviral protein found in infectious filoviral virions [23]. VP40 is the major structural protein in filovirions (**Fig. 2B**) and its functions are analogous to the matrix (M) protein of other viruses within the *mononegavirales* order. EBOV VP40 is a hydrophobic protein and binds to cellular membranes during infection via its C-terminal region [24, 25]. The N-terminal region of EBOV VP40 allows for VP40 oligomerization, which appears to be necessary for formation of infectious EBOV, but not for EBOV egress [26-28]. EBOV VP40 binds to microtubules at the plasma membrane as well as viral single-stranded RNA during EBOV budding to mediate the formation and release of EBOV virions [18, 29, 30].

EBOV structural protein VP24. EBOV protein 24 (VP24) protein does not have known sequence homology to any other known viral protein [29]. VP24 has been reported to also function as a structural matrix-like protein, but a direct interaction with VP40 has not been shown [23, 31]. However, it has been determined that VP24 co-localizes with VP40 at the plasma membrane during filovirion release and is also found in newly budded virions [32]. VP24 protein is capable of binding to EBOV NP, and appears to be necessary to generate infectious EBOV particles [9]. Additionally, VP24 has been shown to block interferon responses during infection [33, 34].

EBOV non-structural protein VP35. The filoviral protein 35 (VP35) protein is capable of binding to itself as well as NP and the filoviral polymerase protein (L) (**Fig. 2B**) [35]. The formation of EBOV VP35 homo-oligomers is believed to be necessary for EBOV replication and transcription [9]. During viral replication, EBOV VP35 binds to L to form a complex that functions as the EBOV replicase-transcriptase holoenzyme thus allowing EBOV genome transcription [36]. EBOV VP35 aids in genome transcription by specifically binding filoviral genomic RNA directly [37]. In addition to its functions involving filoviral transcription, the ability of EBOV VP35 to bind single and double-stranded RNA also allows VP35 to act as an RNA-silencing suppressor [38]. This RNA-

silencing ability allows EBOV VP35 to inhibit both double-stranded and virus-mediated induction of interferon-responsive promoters and is thought to be one of the most important virulence factors harbored by EBOV [39-41].

EBOV non-structural protein L. The EBOV RNA-dependent RNA polymerase protein (L) is the largest protein encoded by the filoviral genome and is composed of approximately 2,000 amino-acids [42, 43]. EBOV L is the catalytic portion of the EBOV holoenzyme complex that is necessary for transcription of the filoviral genome [36]. EBOV L protein utilizes a 3'-5' transcription initiation site before the beginning of each gene and a 3'-5' transcription termination site at the end of each gene to guide transcription of each of the EBOV genes. These transcription initiation and termination sites are the most highly conserved portions of the genome among MARV and EBOV species.

MARV and EBOV glycoproteins. The filoviral genome encodes one gene that is responsible for the production of the viral GP. The MARV genome *GP* gene encodes a single glycoprotein (preGP) that is N-glycosylated in the endoplasmic-reticulum. As the preGP reaches the Golgi apparatus, it gains additional N- and O-linked glycans. It is further processed in the Golgi by furin into GP_1 and GP_2 which remain attached to each other by a single disulfide bond to form MARV-$GP_{1,2}$ heterodimers. The mature MARV-$GP_{1,2}$ consists of three $GP_{1,2}$ heterodimers that associate in the host plasma membrane as the viral spike glycoprotein and are incorporated into the filovirion structure as it buds during replication.

The glycoprotein-encoding transcripts generated from EBOV genome are more complex. Three separate and distinct GP gene products are produced from a single gene. These EBOV-GP gene products differ in size, structure and the abundance. The different EBOV-GP gene products are transcribed from the single EBOV *GP* gene via co-transcriptional editing, involving polymerase stuttering that can lead to the addition or subtraction of specific residues and are discussed in detail below [7, 44].

EBOV sGP. The primary EBOV-GP gene product encoded by the EBOV *GP* gene is a secreted form termed secreted GP, or sGP. This GP form is 364 amino acids in length and does not contain a membrane anchor and is secreted from the infected cell [7, 44, 45]. EBOV sGP is a homodimer of two sGP molecules linked by two disulfide bonds [45-48]. EBOV sGP is glycosylated and contains N-linked glycans as well as a rare modification, C-mannosylation [49]. During EBOV infection, large amounts of sGP are detectable in the blood [7], however, the exact physiological role of sGP *in vivo* remains to be determined. However, it has been speculated that sGP acts as a decoy during infection, and may bind to antibodies secreted by an infected individual [50]. This has been suggested, as sGP contains approximately 300 amino acids that are identical to the N-terminal region of the mature $GP_{1,2}$ [7, 44].

EBOV ssGP. Transcriptional modifications involving the addition of two non-genomic adenosine residues or the subtraction of one adenosine residue during transcription of the primary EBOV-*GP* gene can allow for the production of a sGP variant [44]. The EBOV secondary soluble variant (ssGP) is only 297 amino acids in length and is secreted as a monomer. Although ssGP also contains the 295 N-terminal residues that sGP and $GP_{1,2}$, it is not known if ssGP can bind to antibodies specific to $GP_{1,2}$. The amount of ssGP secreted by replicating EBOV *in vitro* represents less than one percent of the total EBOV-GP produced. To date, functional role for ssGP during EBOV infection has not been determined.

EBOV $GP_{1,2}$. The secondary expression product of the EBOV-*GP* gene is the spike GP ($GP_{1,2}$), which is present on the plasma membrane of infected cells and on the membrane of budded filovirions. Mature $GP_{1,2}$ is produced from a 676 amino acid protein precursor. The production of the $GP_{1,2}$ precursor transcript involves the co-transcriptional addition of one non-template adenosine residue by the EBOV L protein [7, 44]. Following translation of the transcript, the precursor protein is transported to the rough endoplasmic reticulum, where the signal peptide is removed and the protein begins to acquire N-

glycans. EBOV preGP is then transported to the Golgi apparatus, where N- and O-linked glycosylation is completed. Cleavage of EBOV precursor GP by the host enzyme furin results in the formation of two GP subunits, GP_1 and GP_2 which are linked by a disulfide bond to generate a $GP_{1,2}$ heterodimer [51]. It should be noted that the furin cleavage of the mature EBOV-$GP_{1,2}$ is not necessary for EBOV-GP-mediated entry [50, 52]. Three $GP_{1,2}$ heterodimers then associate to form the $GP_{1,2}$ homotrimer that eventually becomes the final spike GP expressed on the surface of EBOV virions (**Fig. 2*B***), acquired during EBOV virion budding from the infected cell [46].

<u>**Viral glycoprotein/fusion protein mediated entry**</u>

The release of a viral genome from the confines of a viral particle is necessary for productive viral infection to proceed. For enveloped viruses, the lipid viral membrane stands between productive and non-productive viral infection. Many RNA viruses, including filoviruses, replicate within the cytosol and utilize one or more surface exposed proteins (GPs and/or fusion proteins) to get their RNA into the cytoplasm [53]. Although viral GPs/fusion proteins are necessary for successful viral entry, properties associated with the host are often necessary to "activate" the viral proteins so that they are ready and capable of promoting viral/host membrane fusion. These GP/fusion protein "activating" host attributes include pH-independent processes such as induction of viral-GP/fusion protein conformational change, as well as pH-dependent processes including viral-GP/fusion protein proteolysis that can also induce viral-GP/fusion protein conformational changes [54-56]. The induction of one or more viral-GP/fusion protein conformational changes is critical for membrane fusion events of enveloped viruses.

pH-independent viral entry

The GPs/fusion proteins of other enveloped RNA viruses, including herpes simplex virus 1 (HSV-1), Sendai virus, human immunodeficiency virus-1 (HIV-1) and other retroviruses, can fuse directly with the plasma membrane [57]. This direct fusion occurs at neutral pH, and abrogates the need for these viruses to enter the endocytic

pathway within eukaryotic cells. The conformational change or changes that occur in these viral proteins that triggers them for fusion occurs when the viral protein(s) engage attachment factors and/or receptors on the surface of cells. Other, non-enveloped viruses are also capable of direct membrane fusion that is not dependent on pH, and include polio virus, other picornaviruses and polyomaviruses [57]. Virus penetration by direct membrane fusion allows viral genomes to enter the cytoplasm, but other viral proteins within the viral membrane, including the viral GPs/fusion proteins remain exposed on the surface of the cell where they are subject to immune surveillance.

pH-dependent viral entry

The GPs/fusion proteins of certain viruses, including vesicular stomatitis virus (VSV), severe acute respiratory syndrome-associated coronavirus (SARS) and EBOV, require low pH conditions to become primed for membrane fusion [54, 55, 58]. Other viruses, such as avian leukosis virus require both low pH conditions and simultaneous interaction with a host receptor for optimal priming [59-61]. However, even after exposure to lower pH in the presence of a receptor, many viruses still are not primed for fusion and need more processing and modification before they are truly activated. Viruses including MARV, EBOV, SARS, the non-enveloped mammalian reoviruses, murine leukemia virus (MuLV) and Semlike forest virus (SFV) need low pH and the activity of one or more host proteolytic proteins to process and expose the fusion-capable portions of the viral membrane proteins [54, 58, 62, 63]. The requirement for low pH and other host factors necessary for viral/host membrane fusion can be met when a virus is taken up into the endocytic pathway.

Each of the recognized portals of entry into the eukaryotic cell have the ability to provide the low pH and other host protein factors needed for productive viral entry of most pH-dependent viruses. Viral internalization into an endosome is followed by the trafficking of the endosome into the interior cytoplasm of the cell. As the vesicle travels deeper into the cell, the endosome fuses with vesicles of gradually decreasing pH that

also contain various host proteins, including the proteolytic enzymes that some viruses

need for further viral protein processing that will result in membrane fusion. Many of

these host proteolytic enzymes also have a requirement for low pH to be active thereby

processing viral membrane proteins and changing viral GPs into the fusion-ready state.

Viral entry via endocytosis also allows the viral evasion of the host immune system by

means of removal of all viral proteins and lipids from the surface of the infected cell upon

endocytosis. Interestingly, some viruses that are known to fuse directly with the host

plasma membrane such as HIV-1 are also capable of utilizing endocytosis to gain entry

into host cells [64]. However, the extent to which each mechanism (direct plasma

membrane fusion versus endocytosis) leads to productive infection is controversial [57, 65].

EBOV-GP: type I transmembrane protein

The EBOV-GP is an example of a type I transmembrane protein. As a $GP_{1,2}$

heterodimer, the GP_1 portion contains the receptor binding domain (RBD) located within

the first 200 amino acids of the N-terminal region [66-68] (**Fig. 3***A* **and 3***B*). This RBD is

located within GP_1 of both MARV and the EBOV GPs. The RBD is believed to be

responsible for binding to an as yet unidentified receptor(s) that allows filoviral

internalization into permissive cells.

The GP_2 portion of the mature filoviral $GP_{1,2}$ contains the fusion peptide domain

as well as the coiled/coil domain that are responsible for enabling fusion of the viral

membrane and the host membrane (**Fig. 3***A* **and 3***B*). Current evidence suggests that the

mature $GP_{1,2}$ must be processed by the pH dependent host cysteine proteases cathepsins

B and L as well as at least one other host cysteine protease, to generate a GP that

activated for membrane fusion [54, 55].

The mature $EBOV-GP_{1,2}$ contains a region, termed the mucin-like domain (**Fig.**

3*A* **and 3***C*), (MLD) that is heavily glycosylated with both N- and O-linked glycans, and

is believed to be responsible for the cytopathic effects (cell rounding/detachment)

observed by $EBOV-GP_{1,2}$ expression *in vitro* [69-71]. Because the MLD does not contain

the putative RBD, deletion of the MLD and expression of a truncated form of EBOV-GP$_{1,2}$ (EBOVΔO-GP) is sufficient to allow viral entry [72]. Expression of EBOVΔO-GP on surrogate systems actually allows for significantly increased viral titers that do not elicit any cytopathic effects associated with full length EBOV-GP$_{1,2}$ [72].

Based on studies of other type I transmembrane viral GPs, a multi-step mechanism has been proposed for EBOV-GP$_{1,2}$ induced membrane fusion (**Fig. 4**). In the metastable state, the GP$_2$ fusion portion of EBOV-GP$_{1,2}$ is hidden by residues in the GP$_1$ RBD. The fusion peptide of GP$_2$ portion is exposed following GP-mediated binding, internalization and subsequent cathepsin cleavage of GP1 in the acidified endosomal compartment [54, 55]. The removal of a substantial portion of EBOV-GP$_1$ by cathepsin L generates an approximate 18 kDa form of GP$_{1,2}$ that is then destabilized by the activity of cathepsin B to form a new 17 kDa intermediate [54, 55]. The activity of another, unidentified cysteine protease is then necessary to further trim the 17 kDa GP$_{1,2}$ intermediate, thus fully activating EBOV-GP$_{1,2}$ and allowing the fusion peptide to insert into the host endosomal membrane [54, 55].

The insertion of the activated EBOV-GP$_2$ leads to the formation of a bridge between the viral and host endosomal membrane. EBOV-GP$_2$ then collapses on itself, bring the membranes in close enough proximity that hemifusion of the membranes occurs, eventually leading to complete fusion of the viral and host endosomal membranes, and an opening through which the viral RNA and its associated proteins can be released into the host cell cytoplasm, where the viral life cycle continues. Proper function of the filoviral-GP is critical for the virus to initiate productive infection during the filoviral life cycle.

Endocytic pathways utilized for viral entry

Many viruses utilize the normal mammalian host cellular machinery involved in endocytic pathways to enter permissive cells. Viral entry into mammalian cells via endocytic events is generally thought to occur by both specific (requiring a viral and host

receptor interaction) and non-specific means (not requiring a viral and host receptor interaction) (**Fig. 5**). These endocytic pathways are normally used during cellular metabolism to transport extracellular material of varying size and state (soluble and non-soluble) into the interior of the host cell. Via evolution, some viruses have generated specific surface proteins, including surface GPs, which allow them to attach to a host cell and then use one or more of these endocytic pathways for productive infection. Currently, there are at least five recognized endocytic pathways within the eukaryotic cell that have been identified to be utilized by known animal viruses to elicit productive viral infection [57].

Macropinocytosis

Macropinocytosis, a form of fluid-phase uptake (FPU), occurs spontaneously as well as in the presence of extracellular growth-factor-receptor (EGFR) stimulation [73]. Growth-factor stimulation occurs as a result of cell-surface ruffles that close at the host plasma membrane and thus engulf growth factors along with extracellular fluid [73]. Therefore, specific receptor engagement by a viral particle at the cell surface is not necessarily required for macropinocytosis to take place.

Macropinocytotic vesicle formation is dependent upon actin, with vesicles ranging in size from 0.2 μM to 10 μM. Macropinosomes thus have the potential to engulf extracellular fluid or large non-soluble particles such as viruses [73]. Vesicles generated by this uptake pathway can become acidified and interact with endocytic vesicles [74] and therefore could serve as a mechanism of filovirus uptake as it fulfills the requirement of a low pH step [54, 55]. A growing number of animal viruses have been shown to utilize macropinocytosis as means of entry during infection. These include human adenovirus, coxsackievirus, baculovirus, rubella virus, HIV-1, echovirus 1, HSV-1 and vaccinia virus [75-83].

Signaling through EGFR after ligand binding can result in the subsequent stimulation and re-localization of actin, leading to the formation of additional

macropinosomes at the surface of the cell [73]. Signaling events that can stimulate actin have been shown to be mediated through Src-family kinases, the tyrosine kinase Syk, the adapter protein GRB2, phospholipase C (PLC) and phosphatidylinositol 3-kinase (PI3K) [73, 84-86]. The spontaneous formation of macropinosomes also requires the activation and activity of the signaling molecules mentioned above and actin for successful macropinosome formation [73].

Clathrin-independent endocytosis

Clathrin-independent endocytosis (CIE) pathways do not require clathrin, and include the involvement of a different set of proteins that are also capable of facilitating viral endosomal entry into host cells. It is generally believed that these CIE pathways are activated through receptor-mediated endocytosis and do not occur spontaneously. Additionally, it is known that cargo entry through a CIE pathway occurs more slowly than does cargo entry through the clathrin-mediated endocytosis (CME) pathway [87]. During normal eukaryotic cell metabolism, these pathways are responsible for internalizing lipids such as cholesterol from the extracellular milieu, as well as glycosylphosphatidylinositol (GPI) -anchored proteins and lipid rafts within the plasma membrane. Not surprisingly, many animal viruses have found a way to utilize CIE pathways to gain entry into host cells. The three most common forms of CIE include endocytosis mediated by host caveolin, endocytosis mediated by host plasma membrane cholesterol-rich regions (lipid rafts), and endocytosis mediated by dynamin 2 alone. The small GTPase dynamin1 and/or dynamin 2 is required for each of these CIE pathways, and it is believed that CIE uptake ultimately results in the delivery of extracellular cargo to a caveosome within the host cell cytoplasm [57].

Dynamin 2-dependent fluid phase endocytosis. Recently, it was recognized that a portion of fluid-phase endocytosis was dependent upon the small host GTPase dynamin 2 [88]. This dynamin 2 dependent pinocytosis mechanism is a form of clathrin-independent endocytosis and has been termed "micropinocytosis" to differentiate it from

macropinocytosis, which does not require dynamin [88]. In addition to dynamin 2, other small GTPases of the Ras family that have been shown to be involved in macropinocytosis, are also assumed to be necessary for micropinocytosis. To date, entry of a virus has not been attributed to micropinocytosis. However, it is likely that viruses that use multiple mechansims for entry, including receptor-mediated and non-receptor-mediated are also using micropinocytosis to some degree [81]. It is also not clear whether cargo taken up by micropinocytosis is actually delivered to an endosome. Thus far, micropinocytosis has not been linked to uptake of a virus and is recognized as a novel form of CIE [88].

Caveolin-mediated endocytosis. Caveolin molecules reside in the plasma membrane of virtually all animal cell types where they associate directly with cholesterol [89]. The two most common forms of caveolin, caveolin-1 (CAV1) and caveolin-2 (CAV2), are abundantly expressed and facilitate the formation of caveosomes, or membrane invaginations ranging in diameter from 60 nm to 80 nm. Caveolae-containing endocytic vesicles are also rich in other lipids, including glycosphingolipids and sphingomyelin [89], however depletion of plasma membrane cholesterol alone results in the disruption of caveolae-driven endocytosis. Viruses that have been established to utilize caveolins for uptake include the non-enveloped simian virus-40 (SV40) and other related polyomaviruses, coxsackie B virus and Echo 1 virus [57]. Previous studies have also indicated that EBOV is capable of utilizing caveolae for uptake into permissive cells [90, 91].

Cholesterol/lipid raft-dependent endocytosis. Although plasma membrane cholesterol is necessary for caveolin-mediated endocytosis, portions of the host plasma membrane exist that have only cholesterol-rich lipid rafts, and do not include caveolin molecules. These lipid raft portions of the membrane are capable of eliciting endocytosis and result in the formation of endocytic vesicles that are slightly smaller in diameter that caveolae vesicles [87]. Endocytic pathways that do not require caveolae have been shown to be utilized by SV40 and polyomavirus [57].

Clathrin-mediated endocytosis

Clathrin-mediated endocytosis (CME) represents the most well studied form of receptor-mediated endocytosis. The hallmark of CME is the formation of clathrin-coated pits, or CCPs. CCPs are made up of repeating units of clathrin, termed triskelions, which are arranged to form a polygon cage around specific cargo. Active CME requires the engagement of specific receptors by their specific ligand or ligands. The correct formation and release of clathrin-coated vesicles requires the activity of both dynamin 1 and dynamin 2. Clathrin-coated vesicles have an average diameter of approximately 100 nm [87].

Uptake by CME is used by many viruses, as CME provides an extremely fast and efficient route of entry into a permissive cell [87]. The study of the transferrin receptor has been key to understanding much of what we know today concerning CME and endocytic recycling in general [92]. Because of this, the transferrin receptor has become an important tool for studying events associated specifically with CME.

Inhibition of CME can be achieved through the use of biochemicals as well as RNA interference (RNAi) against clathrin, and expression of dominant-negative forms of either Dynamin 1 or 2, or expression of dominant-negative forms of specific adaptor proteins such as Eps15 that link receptors bound with ligand to the clathrin lattice. These means of CME inhibition have been successfully used to show the dependence of many animal viruses upon CME for entry into permissive host cells. These viruses include the non-enveloped mammalian reoviruses, equine infectious anemia virus (EIAV), SFV, influenza virus, SARS, avian leukosis virus and VSV [57, 93]. Studies have also suggested that EBOV utilizes CME to access certain cell populations [90, 94].

Current knowledge of filoviral-GP-mediated

entry kinetics in permissive cells

The kinetics of filoviral binding and subsequent internalization into permissive host cells remains poorly studied. Gaining a better understanding of these initial entry

events may lead to the development of novel antiviral therapies targeting such events during filoviral infection. Additionally, understanding the timing of these events would expand the current knowledge base of *when* existing antiviral filoviral agents would be most effectively administered post-filoviral infection. To date, a study investigating filoviral-GP-mediated entry kinetics has not been carried out past 2 or 6 hours [72, 91]. If the entry kinetics associated with the filoviral-GP were actually quite slow, this time frame could skew the kinetics considerably. Additionally, it is not known if the entry kinetics associated with the filoviral-GP differed among cell type and species origin.

Current knowledge of the impact of glycosylation patterns on host plasma membrane proteins in filoviral-GP-mediated entry into permissive cells

It has been shown that pronase treatment of permissive cells inhibits filovirus-GP-dependent entry, indicating that one or more cell surface proteins are involved in filovirus-GP-dependent entry [95, 96]. However, these studies do not rule out the possibility that carbohydrates on plasma membrane proteins are serving as attachment factors or receptors.

The glycan composition of the filoviral-GP and how the glycans impact host/virus interactions has been investigated [97-99]. The ease of generating various filoviral-GP mutants that eliminate N-linked glycosylation sites combined with the use of surrogate systems to study the effects of these mutations on the filoviral-GP-dependent entry has made such studies possible. Interestingly, it was found that the heavily glycosylated mucin-like domain of the EBOV-GP was dispensable for GP-mediated entry into permissive cells [99]. In fact, pseudovirion titers generated using the mucin-domain deleted form of EBOV-GP were considerably higher than those generated using the full length EBOV-GP [99]. Other studies have shown that N-linked glycans on EBOV-GP can modulate the antigenicity of the GP [97] as well as its interaction with the C-type lectin DC-SIGN [98]. However, host plasma membrane proteins identified thus far that are important

for or enhance filoviral-GP-mediated entry into certain cell populations appear to function as viral attachment factors, and are not considered to be receptors for the virus [100]. To date, a role for host plasma membrane protein glycosylation in filoviral-GP-mediated entry has not been investigated.

Current knowledge of proteins reported as
potential receptors for filoviral-GP-mediated
entry into permissive cells

Early studies have demonstrated that protease treatment of permissive cells reduced filovirus entry [95], indicating that one or more plasma membrane proteins are involved in entry. However, because of the wide cell tropism of these viruses, identification of a receptor(s) responsible for virus internalization has proven difficult and has led to the general assumption within the field that multiple cellular receptors may be used by filoviruses for entry [101]. While cellular receptors that bind to and mediate filovirus entry into cells have yet to be identified, host cell proteins have been identified that at least bind to one or more filoviral glycoproteins and/or enhance filoviral-GP mediated entry into certain cell types. These proteins include the C-type lectins, the β1-integrins, folate receptor α and the Tyro3 family receptor tyrosine kinases.

C-type lectins containing carbohydrate
recognition domains (CRDs)

The C-type lectin family of transmembrane proteins are important in allowing immune system recognition of viral, bacterial, fungal and parasitic pathogens that express specific glycans on their surface [102]. This recognition is calcium dependent and involves binding of the host C-type lectin to the specific pathogenic glycan(s) through regions termed carbohydrate recognition domains (CRDs) [102]. For the binding of CRDs to pathogenic glycans, it is crucial that the CRDs recognize conserved microbial glycosylated regions. To date, the filoviral GP_1 mucin domain appears to be responsible for mediating filovirus attachment to members of the C-type lectin family [103-109].

However, the binding of filoviral GP$_1$ to C-type lectins does not allow for productive virus internalization into cells, and therefore eliminates the possibility that these molecules are filoviral receptors [103-109]. Additionally, the mucin domain of EBOV is dispensable for infection, and thus does not include the receptor binding domain [99].

The β1 integrin adhesion receptors

The β1 integrin adhesion receptors are a family of heterodimeric cell-surface receptors that mediate cell-cell adhesion, cell contact with the extracellular matrix, cell migration, cell proliferation, cell differentiation and apoptosis [110]. B1 integrins are expressed on a wide range of mammalian cells and bind to matrix substrates including collagen, fibronectin and laminin. Neutralizing antibodies against cell surface β1 integrin as well as a soluble form of β1 integrin effectively inhibited EBOV-GP-mediated entry of pseudovirions into permissive cells [110]. Although β1 integrins have not been shown to directly interact with any filoviral-GP, it has recently been shown that that they modulate host cysteine protease (cathepsin) activity that is necessary for efficient filoviral-GP-mediated entry into permissive cells [111]. Because cathepsin activity is necessary for efficient filoviral-GP-mediated viral/host membrane fusion activities that are well downstream of viral internalization [54, 55], it is apparent that the β1 integrins are also not receptors for the filovirus family.

Folate receptor α (FR-α)

The most controversial of the proteins identified to enhance filoviral entry, folate receptor-α (FR-α) is expressed on a wide variety of mammalian cells, but not on every cell that is permissive for filoviral infection [112]. FR-α binds specifically to its natural ligand, folic acid, but has never been shown to bind to any filoviral family GP. Later studies attempting to confirm the necessity of FR-α in filoviral-GP-mediated entry using infectious filovirus or surrogate systems have failed [113, 114]. To date, the necessity for FR-α in filoviral entry into any cell population remains questionable.

Tyro3 family of receptor tyrosine kinases

(TAM) family members and Gas6 interactions

The tyro3 family of receptor tyrosine kinases (TAM) subfamily of tyrosine kinase receptors include three members, Tyro3 (Dtk), Mer and Axl. Axl is appreciated to enhance filovirus infection, as overexpression of Axl increased filovirus infection in poorly permissive Jurkat T cells [115, 116]. Axl has also been strongly implicated as being important for filoviral entry in two independent screens, including a comparative genomic analysis (CGA) screen in this laboratory. The first screen was carried out in the Kawaoka lab [115] utilized a cDNA library from filoviral permissive VeroE6 cells. The library was transduced into filoviral non-permissive Jurkat cells and the Jurkat cells were subsequently transduced with pseudovirions bearing the ZEBOVΔO-GP [115]. This screen was successful in identifying the tyrosine kinase Axl as the cDNA that allowed transduction of the Jurkat cells by ZEBOVΔO-GP pseudovirions. Our more recent screen assessed ZEBOV-GP-dependent entry into a large panel of cell lines and identified cellular genes whose expression positively correlated with ZEBOV-GP-dependent entry. In our screen we found that Axl expression correlated well with ZEBOV-GP dependent entry.

TAMs bind to and are activated by the common ligand, Gas6 [117, 118]. TAMs also bind to and are activated by a molecule called Protein S in a limited number of cell populations [117]. Gas6 contains multiple γ-carboxyglutamic acid (Gla) residues in its N-terminal domain that are responsible for binding to lipid membranes containing negatively charged membrane phospholipids, including PS. The C-terminal region of Gas6 is composed of two globular laminin G-like (LG) domains that are necessary for binding to Axl. This structural organization of Gas6 allows for simultaneous binding of Gas6 to Axl and to PS containing membranes, leading to Axl activation and signaling in many different cells types [119, 120]. Gas6 is relatively abundant protein in human and fetal calf serum and is secreted by many cells [118].

The TAM family members are capable of regulating normal cellular processes and promote cell survival, cellular growth, cellular differentiation, cellular adhesion and cellular motility [117]. Each family member contains a conserved tyrosine kinase domain in the cytoplasmic tail, two immunoglobulin-like (Ig) and two fibronectin type III domains in the ectodomain that are responsible for ligand binding [117]. While all three TAM family members have been implicated in enhancing EBOV entry into some cell populations [115], the role of Axl has been studied most extensively [116]. However, a direct interaction between Axl, Tyro3 or Mer with a filoviral-GP has never been shown. The role or roles of Axl or any of the other TAM family members during filoviral-GP-mediated entry into permissive cells that require Axl for optimal entry has not been determined. Similarly, the precise mechanism or mechanisms of entry utilized during filoviral-GP-mediated entry into cells that require Axl for optimal entry have also not been determined.

Surrogate systems as a tool for filoviral-GP
related studies

As the members of the filoviridae family are highly infectious to many mammalian species and are recognized by the Centers for Disease Control as Class A Priority Pathogens, it is required that they be studied within the confines of a biosafety level four (BSL-4) facility. Because of the risk, cost and time associated with BSL-4 study, multiple surrogate systems have been developed in the recent past to study filoviral life cycle events in a lower biosafety level laboratory setting. As the earliest events in the filoviral entry process such as attachment, binding, internalization into and fusion with an endocytic vesicle are solely associated with the filoviral-GP, surrogate systems expressing the filoviral-GP can serve as tools to study these processes.

Many different non-pathogenic and non-replicating viral cores or "backbones" that can facilitate the presentation of the correct, trimeric form of the filoviral type I transmembrane GP have been developed. For instance, a reverse genetics approach is commonly used by this laboratory to produce feline immunodeficiency virus (FIV)

pseudovirions bearing the ZEBOV-GP protein [121]. Plasmids expressing the FIV structural and enzymatic proteins (Gag-Pol) and filoviral-GP are transfected into producer cells such as 293T cells. An additional plasmid encoding a viral (i.e. FIV) specific packaging signal as well as a reporter gene such as the *β-galactosidase* (*β-gal*) gene is also introduced, providing an easily detectable readout signal post-virion entry [121]. Recent studies with EBOV or LVMARV-GP pseudovirions have provided significant insights into steps involved with productive entry of this deadly pathogen into cells and therefore represent valuable and safe tools for assessing viral properties associated with a specific viral-GPs [54, 55, 66, 68, 72, 111, 115, 121-123].

Rationale and objectives for current study

The current understanding of early events associated with the filoviral life cycle is lacking. Additionally, confusing and conflicting information concerning the route or routes of entry that are used by filoviruses in different cell populations. To this end, we studied basic characteristics of filoviral-GP-mediated entry in permissive mammalian cell populations and more closely examined the properties of host cell plasma membrane proteins and their effect on filoviral-GP-dependent entry.

The data presented here represent a collection of studies aimed at gaining a more complete understanding of the properties associated with filoviral-GP-mediated entry into permissive cells. These findings will provide a much more detailed understanding of the time frame involved in filoviral-GP-mediated entry as well as the glycan patterns associated with optimal entry. Additionally, these studies will begin to elucidate how Axl is used by the filoviral-GP to gain entry into some permissive cell populations but not others.

List of Specific Aims

1.   Determine the kinetics of filoviral entry into permissive cells.

2.   Determine the glycosylation patterns on membrane proteins of permissive cells that facilitate filoviral entry into permissive cells.

3.   Determine the mechanism (s) of filoviral entry into permissive cells.

4.   Determine the role host membrane protein Axl plays in the filoviral entry process.

Knowledge gained by the current study

1.   The binding of retrovirions bearing filoviral-GPs to permissive cells is inefficient.
Following binding, retrovirion internalization into a variety of permissive cells
(including human, non-human primate and fruit bat cells) occurs slowly but
linearly over time, as the virions remain stable for extended periods of time. In
contrast, rhabdoviral based pseudovirions bearing filoviral-GPs internalize into
permissive cells in a non-linear fashion, with internalization kinetics stalling
within 1-4 hours after the onset of the experiment. Additionally, retrovirions
bearing filoviral-GPs remain sensitive to the lysosomaltropic agent ammonium
chloride for up to 7 hours, indicating that the virus was within a vesicle that
required low pH for extended time periods. Combined we show that the entry of
filoviral-GP bearing pseudovirions is relatively inefficient and slow and depends
on the pseudovirion background used.

2.   O-linked glycans on host proteins in the plasma membrane are necessary for
optimal filoviral-GP-mediated entry into permissive cells post-viral-GP binding to
the cell surface. Interestingly, filoviral-GP-dependent entry into cells post-
binding is enhanced by the removal of either sialic acid or galactose from both N-
and O-linked membrane protein glycans. These data represent the first time that
glycans on host plasma membrane proteins have been shown to play a role in
filoviral-GP-dependent entry.

3.   Filoviral entry into some permissive cells is dependent upon the TAM family
receptor tyrosine kinase Axl. Within these Axl-dependent cell populations,
filoviral entry occurs through multiple mechanisms, including both clathrin-
mediated and caveolin/lipid raft-mediated pathways. We also show that filoviral

entry into Axl-dependent cells occurs through FPU. This is the first time that FPU has been identified as a route of filoviral entry.

4. Within Axl-dependent cell populations, Axl facilitates FPU of ZEBOV-GP bearing pseudovirions and infectious ZEBOV and is necessary for efficient ZEBOV-GP bearing pseudovirion internalization. Signaling through PLC but not PI3K is necessary for efficient filoviral-GP-mediated entry in Axl-dependent cells. The Axl ligand Gas6 is capable of binding to ZEBOV-GP expressing pseudovirions, thereby providing preliminary evidence for a possible mechanism by which filoviral-GP-expressing virions interact indirectly with Axl through Gas6.
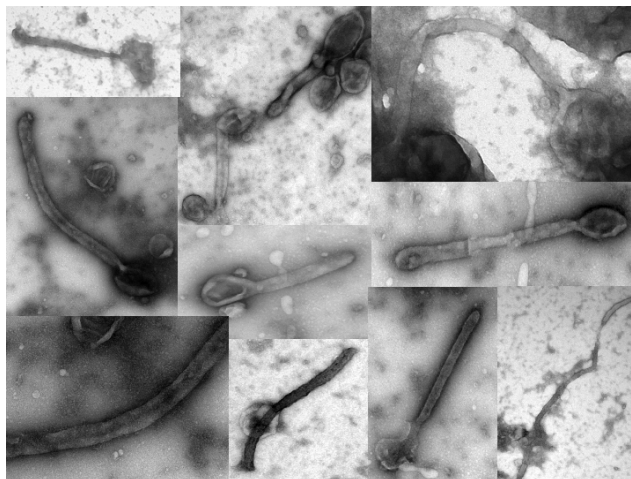
Figure 1. Micrographs of ZEBOV virus like particles. Filovirions measure approximately 80nm in diameter and range from 800nm to greater than 1000nm in length.
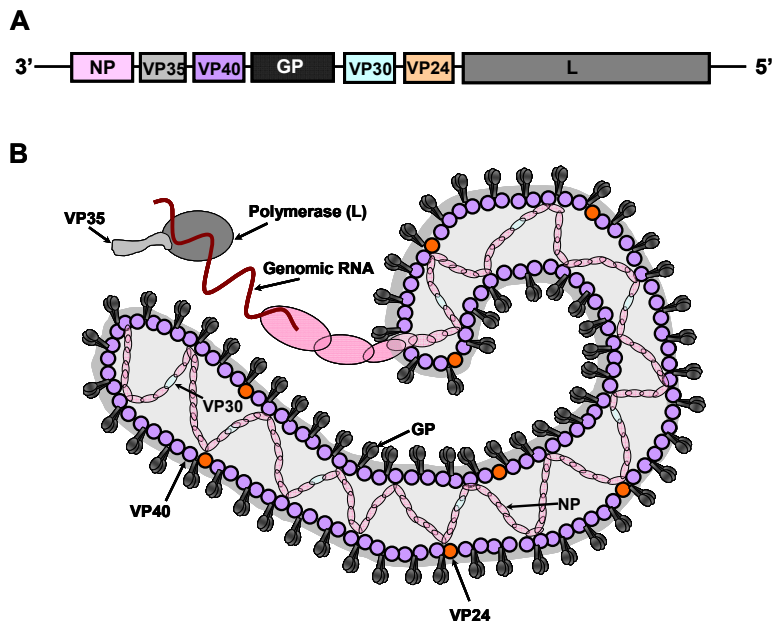
Figure 2. Filoviral genome and protein structure organization. A) The negative sense, single-stranded RNA genome of each EBOV species is approximately 19 kb in size and is organized into seven different genes, encoding a total of nine known proteins. Three forms of the EBOV glycoprotein (GP) are known to be expressed from the one EBOV-GP gene, via co-transcriptional editing. *NP*: nucleoprotein gene; gene product is major protein enveloping the viral genome. *VP35*: VP35 gene; gene product interacts with the viral polymerase and is also the major suppressor of host interferon response. *VP40*: VP40 gene; gene product is major matrix protein. *VP30*: VP30 gene; gene product is minor nucleoprotein and a transcriptional activator during infection. *VP24*: VP24 gene; gene product is minor matrix protein. *L*: polymerase gene; gene product is RNA-dependent RNA polymerase. **B)** The EBOV virion is composed of the viral genome in contact with viral proteins L and VP35 and is enveloped by NP and VP30. VP40 is the major structural protein of EBOV, and gives it the typical filamentous appearance. The GP protein exists as a homotrimer embedded within the viral envelope and in contact with VP40. The exact location of VP24 within the virion is unknown.
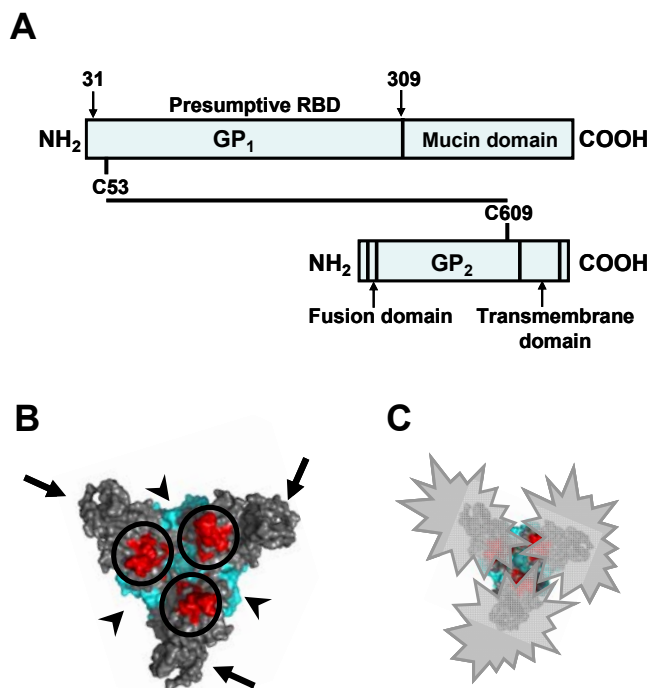
Figure 3. The ZEBOV spike glycoprotein (GP$_{1,2}$). **A)** Schematic representing the monomeric form of GP$_{1,2}$, which exists as two distinct subunits, GP$_1$ and GP$_2$. The two subunits are generated after furin cleavage of the GP poly-protein in the Golgi, and remain linked by a disulfide bond. The GP$_1$ portion of the GP$_{1,2}$ heterodimer contains the presumptive receptor binding domain (RBD) as well as a highly glycosylated portion termed the mucin domain. The GP$_2$ portion of the heterodimer contains the fusion domain as well as the transmembrane domain. Three GP$_{1,2}$ heterodimers associated to form the mature GP trimer that exists within the virion as the spike GP. **B)** The crystal structure of the EBOV-GP (lacking its mucin domain) has been solved and is shown. The GP$_1$ portions of the protein are depicted by arrows. The GP$_2$ portions of the protein are depicted by arrow heads. Residues within the RBD that are important for GP binding to permissive cells are depicted by black circles. The view shown is a top view, looking down into the "chalice" that is formed by the homotrimer. GP$_1$ is located at the top of this cup, and GP$_2$ is located at the base. The RBD lies within GP$_1$ and near the interface between GP$_1$ and GP$_2$ at the base of the "chalice". **C)** The GP$_{1,2}$ trimer depicted with its bulky mucin domains intact as represented by gray stars. The mucin domain is located at the C-terminus of GP$_1$ and is heavily O-glycosylated. Removal of the mucin domain was necessary for crystallization; however, removal of the mucin domain will not impact EBOV entry or replication.
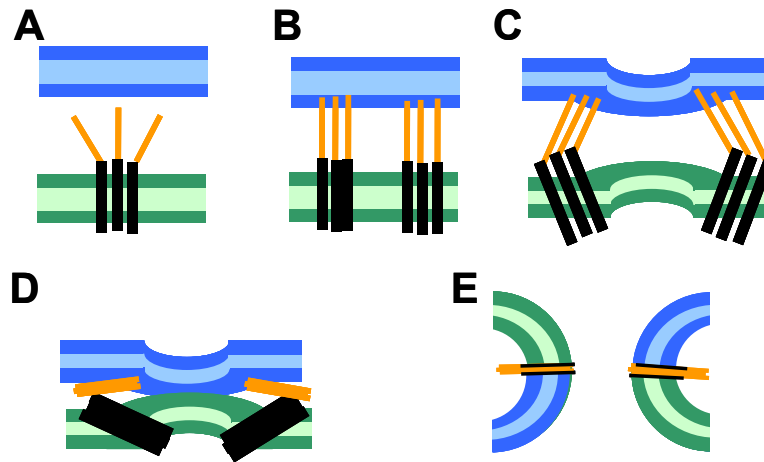
Figure 4. General model for class I fusion protein induced viral/cellular membrane fusion. The viral trimeric transmembrane domain sits in the viral envelope. **A)** The TM contains two helical domains, orange and black. **B)** Conformation changes are triggered by receptor binding or low pH, causing insertion of the hydrophobic domain into the cellular membrane. **C)** The helical domains begin to fold up on each other. **D)** The folding into the six-helical bundle produces first a hemi-fusion state, where only the outer leaflet of the viral and cellular membranes fuse. **E)** Finally, both leaflets of the membranes fuse producing a fusion pore.
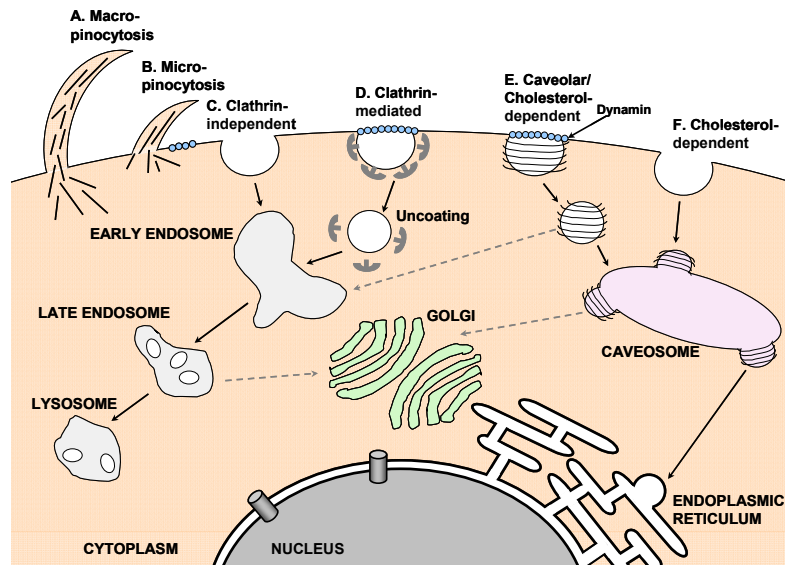
Figure 5. Endocytosis pathways used by viruses in mammalian cells. In mammalian cells, many different mechanisms are available for the endocytic internalization of virus particles. Some of these mechanisms, such as clathrin-mediated endocytosis, are ongoing, whereas others, such as caveolae, are ligand and cargo induced. Currently, five pathways are recognized to facilitate productive virus entry in mammalian cells: **A)** Macropinocytosis, **C)** clathrin-independent endocytosis, **D)** clathrin-mediated endocytosis, **E)** Caveolae/cholesterol-mediated endocytosis and **F)** a cholesterol-dependent endocytic pathway devoid of clathrin and caveolin-1. **B)** Micropinocytosis a pathway similar to A) except dependent on dynamin-2 potentially utilized by filoviruses for productive entry into Axl-dependent cells.

CHAPTER TWO: KINETICS OF FILOVIRAL-
GP-MEDIATED ENTRY EVENTS INTO
PERMISSIVE CELLS

Abstract

Information about the kinetics of filoviral-GP-dependent entry is incomplete. To gain a better understanding of this aspect of filoviral entry, we investigated the timing of entry events using filovirus pseudovirions. Initial entry studies with filoviral-GP pseudotyped retrovirions at 37°C indicated that virions entered permissive cells with a half-time (T_{50}) of 7.5 to 8 hours. We found that 10 to 20% of retroviral based virions bound to cells in over a one hour period at 4°C suggesting that virion binding was relatively inefficient. The low level of binding was not a result of limiting numbers of viral receptor(s) available on the cell surface. Surprisingly, we also observed that less than half of the retroviral based pseudovirions pre-bound to the cell surface were internalized by 7 hours indicating that virion internalization was a slow process. Consistent with slow internalization of retroviral particles, we observed that, while virus entry lost sensitivity to ammonium chloride treatment with time, 50% of the virions remained sensitive to low pH neutralization for at least 7 hours. Entry and internalization kinetics assessed using vesicular stomatitis virus (VSV) based pseudovirions bearing filoviral-GPs showed an initial uptake of >25% of the virions within 1 hour compared to controls. The retroviral system based entry and internalization increased linearly for the duration of the experiment, whereas the VSV system stalled after the initial 1 hour uptake of virions. Combined, these data indicate that entry and internalization of pseudovirions bearing filoviral-GP is relatively inefficient, and depends on the pseudovirion system used.

Introduction

The filoviral entry process is mediated by the filoviral GPs that protrude from the infectious filovirion or from the surrogate pseudovirion. The GP exists as a trimer within

the viral envelope and is solely responsible for allowing virion attachment to and internalization into an endosome within a permissive cell [54, 55, 68]. Once the virion is internalized into an endosome, the endosome becomes gradually acidified as it makes its way deeper into the cytoplasm and away from the host plasma membrane. The acidic environment within the endosome allows filoviral-GP fusion with the endosomal membrane and release of the viral RNA into the cytoplasm, where the life cycle of the filovirus continues [54, 55]. Fusion of viral and host membranes driven by the filoviral-GP is critical and absolutely necessary for the infection process to continue. The work herein was designed to measure the timing of these entry events, including filoviral-GP-mediated binding, filoviral-GP-mediated internalization and the time within the host cell endosome following filoviral-GP-mediated internalization.

We first investigated the kinetics of filovirus-GP-dependent virion entry into a variety of permissive cell populations by utilizing retroviral based pseudovirions, including feline immunodeficiency virus (FIV), human immunodeficiency virus (HIV) and murine leukemia virus (MuLV), as well as rhabdovirus based vesicular stomatitis virus (VSV) virions. The limited, previous EBOV entry studies have only investigated the kinetics of EBOV-GP mediated entry for as long as 2 or 6 hours [72, 91]. Setting a 100% point at only 2 or 6 hours could skew the entry kinetics of the virus if the entry kinetics were actually much slower. By evaluating virion entry for longer times, we have determined the kinetics involved in filoviral-GP-mediated entry, including both binding and subsequent internalization, into multiple permissive mammalian cells.

Although differences in kinetics existed between the different retroviral-based pseudovirions systems, all systems clearly showed that filoviral-GP-mediated entry into the cell populations examined was an inefficient process. Analysis of virion binding using the FIV system showed that this was not due to a limited availability of receptors or attachment factors on the host plasma membrane. In addition to poor binding, retroviral based filoviral-GP-mediated internalization was slow, with the filoviral-GPs remaining

sensitive to lysosomaltropic agents for up to 7 hours post-binding. Interestingly, the entry and internalization kinetics of the filoviral systems into multiple filoviral permissive cell types showed some variation between the cell populations, indicating there is some level of dependence upon cell type for filoviral-GP-dependent entry. Together, these data clearly show that the entry process mediated by the filoviral-GP using retroviral based pseudovirion systems is sub-optimal and slow.

We also examined the entry and internalization kinetics of the rhabdoviral (VSV) based pseudovirion system bearing filoviral-GPs. Surprisingly, we found that VSV-filoviral-GP-dependent entry and internalization processes initially occurred much more quickly than with the retroviral systems. At least 25% of the VSV/filoviral-GP pseudovirions had entered or been internalized into all of the cells tested by 1 hour. However, entry and internalization beyond 1 hour seemed to slow considerably or stall, whereas retroviral entry and internalization remained linear throughout the entire time course. This data indicates that the surrogate system(s) bearing the filoviral-GP as well as the cell populations used in analysis may each affect filoviral-GP entry and/or internalization to some degree. In total, these results suggest that filoviral-GP-dependent entry is at the least, an inefficient process relative to the initial inoculum applied to cells. Additionally, these findings indicate that the filoviral entry process may be much slower than previously thought [72, 91]. A slow filoviral entry process could allow for a greater window during which viral entry could be blocked or decreased.

Materials and methods

Cell lines

Human embryonic kidney cells 293T (CRL-11268; ATCC), a human glioblastoma line, SNB19 (NCI 0502596), a human fibrosarcoma cell line, HT-1080 (CCL-121; ATCC) and an African green monkey kidney cell line, Vero (CCL-81; ATCC) were maintained in high-glucose Dulbecco's modified Eagle's medium (DMEM) (Invitrogen) supplemented with 100 units/ml of penicillin and 100 µg/ml streptomycin

(1% P/S) and 10% fetal calf serum (FBS) (HyClone). A human renal cancer cell line, 786-0 (NCI 0505780) was maintained in Roswell Park Memorial Institute media 1640 (RPMI) with 1% P/S and 5% FBS. The 293T cell line stably expressing the gag-pol proteins from the murine leukemia virus (MLV) and an RNA plasmid expressing GFP [124] was maintained in DMEM supplemented with 10% FBS, 1% P/S and 0.4 mg/ml G418. Primary human foreskin fibroblasts (Hffs) isolated from fresh penile foreskin, and primary Egyptian fruit bat, *Rousettus aegyptiacus*, fibroblasts were isolated from fresh ear punches obtained from healthy animals from the Oregon Zoo and were maintained in DMEM supplemented with 1% P/S and 15% FBS. Primary human umbilical vein macrovascular endothelial cells (HuVECs) isolated from a fresh umbilical cord were maintained in Endothelial Cell Basal Medium (EBM) supplemented with bovine brain extract, hEGF, hydrocortisone, gentamicin, amphotericin B and 5% fetal calf serum (Lonza/Cambrex). Cells were maintained at 37ºC with 5% CO_2.

Plasmids used

All plasmids used to generate feline immunodeficiency virus (FIV) and VSV core pseudovirions have been previously described [121, 125]. All plasmids used to generate HIV and murine leukemia virus (MuLV) core pseudovirions are commercially available from Invitrogen and Clontech, respectively. EBOV nucleocapsid protein (NP) and VP40 plasmids were kindly provided by R. Harty (Department of Pathobiology, School of Veterinary Medicine, University of Pennsylvania) and have been previously described [126].

Viral pseudovirion particle production

Production of ZEBOV-GP pseudotyped FIV-β-galactosidase particles. FIV virions were generated as previously described [121]. Virus was produced by transfection of three plasmids into 80% confluent HEK 293T cells in a total of 75 µg of plasmid DNA. The transfected plasmids consisted of the following at a ratio of 1:2:3, respectively: pCMV/EBOVΔO that expresses Zaire (ZEBOV-GP) with a deletion of the mucin

domain, pCMV/FIV∆∆ that expresses FIV gag-pol, and pFIV𝚿βgal. Full length forms of the ZEBOV-GP and MARV-GP were also used in place of the pCMV/EBOV∆O expression plasmid. The DNA was transfected into 15-cm diameter dishes of 293T cells using calcium phosphate precipitation [127]. After 12 h the cells were washed, and fresh medium was added (DMEM, 2% [vol/vol] FBS, 1% [vol/vol] Pen-Strep). Supernatants were collected at 24, 36, 48, 60, and 72 h post-transfection and frozen at −80°C. The supernatants were thawed, filtered through a 0.45-μm-pore-size filter, and pelleted by a 16-h centrifugation step (7,700 x g at 4°C in a Sorvall GSA rotor). The viral pellet was resuspended in DMEM for an approximate 200-fold concentration, and the virus was either used immediately for infection or stored at −80°C until use.

Production of VSV/VSV-eGFP and EBOV/VSV-eGFP particles. VSV encoding an enhanced green fluorescent protein (VSV-eGFP) reporter gene was pseudotyped with either the native GP or ZEBOV-GP as previously described [128]. Briefly, 15-cm diameter plates of 80% confluent 293T cells were transfected with 75 μg of pcDNA3.1 plasmid expressing VSV-G or ZEBOV∆O-GP using the calcium phosphate precipitation procedure [127]. Cells were rinsed with phosphate-buffered saline (PBS) 12 h later to remove the transfection reagents. At 24 h following transfection, cells were transduced with VSV-G pseudotyped VSV∆G-eGFP (multiplicity of infection [MOI] of ∼0.1). Viral inoculum was removed 12 h later, and supernatants were collected at 24 h following transduction for viral stocks. Stocks were serially diluted on the desired target cells, cells were lifted in Accumax (Fisher) and analyzed with a FACScan cytometer (BD Biosciences) for FL-1 intensity.

Production of EBOV-GP and VSV-G pseudotyped MuLV-eGFP particles. Producer 2E6 cells that were derived from 293T cells stably express MuLV Gag/Pol proteins and MuLV𝚿eGFP. 2E6 cells were plated in 15-cm plates and transfected with 75 μg of either pCMV/EBOV∆O or pCMV/VSV-G using the calcium phosphate transfection procedure, and supernatant was harvested and concentrated as described above. Stocks were serially

diluted on the desired target cells, cells were lifted in Accumax and analyzed with a FACScan cytometer for FL-1 intensity.

Production of EBOV-GP and VSV-G pseudotyped HIV-eGFP particles. Protocols to generate HIV-based particles were similar to the FIV-based virion production described above except that the transfection was composed of a four-plasmid system that included the following at a ratio of 1:2:1:3, respectively: pCMV/EBOV∆O, pCMV/HIV gag-pol, pCMV/Rev, and pHIV♣eGFP. Stocks were serially diluted on the desired target cells, cells were lifted in Accumax and analyzed with a FACScan cytometer for FL-1 intensity.

Detection of β-galactosidase based
pseudovirion entry

FIV transduction studies were performed in a 48 well format using a MOI of ~0.005 (resulting in approximately 200 β-gal positive cells/40,000 cells/well in control wells). FIV pseudovirion transduction was detected by fixing cells in 3.7% formalin and evaluating for β-gal activity using the substrate 5-bromo-4-chloro-3-indolyl-β-D-galactopyranoside. All FIV transduction evaluation was done 48 h after initial FIV pseudovirion addition to cells. The number of β-gal-positive cells was enumerated by microscopic visual inspection.

Detection of GFP based pseudovirion entry

For detection of GFP based pseudovirion transduction, cells were lifted in Accumax (Fisher) and analyzed with a FACScan cytometer (BD Biosciences) for FL-1 intensity. GFP encoding pseudovirions were applied to cells to yield approximately 1,000 GFP positive cells for every 20,000 cells analyzed by flow cytometry. This gives an MOI of approximately 0.05 for all studies using a GFP based readout system.

Chemical reagents

Ammonium chloride and citric acid were obtained from Sigma (St. Louis, MO). The ammonium chloride solution was prepared from a 1 M stock, pH 7.4, in DMSO. The concentrations of ammonium chloride used did not affect the pH of the cell culture

medium. Citric acid buffer contained 40 mM citric acid, 10 mM KCl and 135 mM NaCl in ddH$_2$O at a pH of 3.0.

Ammonium chloride addition studies

SNB19 cells were transduced with FIV pseudovirions expressing full length ZEBOV-GP in the absence of ammonium chloride. At various time points post-transduction, 1 M ammonium chloride stock was added to the SNB19 culture medium to a final concentration of 25 mM. The cells were fixed and stained 96 h post-transduction as described above.

Virion binding studies

All binding studies were preformed in a 48-well format using ~3 x 10^4 cells per well. Pseudovirions were incubated with cells for the indicated time(s) at 4ºC to allow virion binding but not internalization. After binding, the media containing non-bound virus was removed, and new media was added. The cells were then shifted to 37ºC to allow internalization of the bound virions. Cells were analyzed for pseudovirion transduction 96 hours post-transduction.

Virion entry studies

All binding studies were preformed in a 48-well format using ~3 x 10^4 cells per well. Pseudovirions were applied to cells at time zero and incubated with the cells at 37ºC to allow virion entry into the cells. At the indicated times post-transduction, media containing virus was refreshed with media not containing virus. Cells were analyzed for pseudovirion transduction 96 hours post-transduction.

Virion stability studies

FIV pseudovirion stocks bearing filoviral-GPs were incubated in DMEM containing 10% fetal calf serum and 1% P/S. The virion stock was maintained at 37°C and used to transduce SNB19 cells at various time points post-initial transduction. The number of β-gal positive cells at the various time points following 37°C incubation was

compared to the number of positive cells when the virus was immediately used for transduction.

Virion internalization studies

All internalization studies were preformed in a 48-well format using ~3 x 10^4 cells per well. Pseudovirions were incubated with cells for the one hour at 4ºC to allow virion binding but not internalization. After binding, the media containing non-bound virus was removed, and new media was added. The cells were then shifted to 37ºC to allow internalization of the bound virions. At the indicated time points, cells were treated with pH 3.0 citric acid buffer for 30 seconds to inactivate all non-internalized pseudovirions. After citric acid buffer treatment, cells were washed in media three times to restore the pH, and fresh media was added to the cells, and the cells were again incubated at 37ºC. Cells were analyzed for pseudovirion transduction 96 hours post initial pseudovirion addition.

Statistical analysis

The T_{50} mean values calculated in Table 1 were used to determine statistical significance between the two samples using a Poisson distribution analysis. Data in Figures 9 and 14 were analyzed for statistical significance using Student's *t* test, utilizing the two-tailed distribution and two-sample equal-variance conditions. A significant difference was determined by a *P* value of <0.05. If the *P* value was >0.05, the data were not considered significant.

Results

Entry of retroviral pseudovirions bearing
ZEBOV-GP into permissive cells is
a slow and inefficient process

For enveloped viruses, including filoviruses, entry into a permissive cell after the viral glycoprotein has engaged its receptor is the next step in the infection process. The length of time that is required to do this may be crucial in determining how successful the

virus is at evading the host immune response against it. We first investigated the kinetics

of virion entry into a variety of permissive cell populations by utilizing retroviral

pseudovirions (FIV, MuLV and HIV) or rhabdoviral vesicular stomatitis virus (VSV)

pseudovirions.

Retroviral pseudovirions (FIV and MuLV) bearing either Zaire ebolavirus mucin

domain deleted GP (ZEBOVΔO-GP) or vesicular stomatitis virus-GP (VSV-G-GP) were

applied to filoviral (and VSV) permissive cells, including SNB19 cells, in a 48-well

format. SNB19 cells are the most filoviral-GP permissive cell population that we have

found to date [121]. Other cell lines that were filoviral and VSV permissive that were tested

included a human renal carcinoma cell line, 786-0, and a human fibrosarcoma cell line,

HT-1080.

Virus was incubated with the cells at 37°C from one to 72 hours. At the time

points noted, the media was removed from the cells and fresh media was added.

Changing the media allowed for the removal of virions that were not bound and/or

internalized. Ninety-six hours after the initial application of virions to the cells (at time

zero), the cells were assessed for pseudovirion entry. Virion transduction was expressed

as a percentage of the transduction observed when virions were added at time zero and

not removed. Shown are the findings where virus was removed during the first 24 hours.

We were surprised to see that both the all of the retrovirions expressing

ZEBOVΔO-GP entered the cells populations tested slowly, with greater than 50% of

virus remaining extracellular at 8 to10 hours following transduction (**Fig. 6; Table 1**).

Interestingly, we also observed that the FIV-ZEBOVΔO-GP pseudovirions reached 50%

entry (T_{50}) at 11.25 hours whereas MuLV-ZEBOVΔO-GP pseudovirions reached 50%

entry slightly faster at 8.4 hours. This suggested that the background of the particle (FIV

versus MuLV) may impact the kinetics of entry into SNB19 cells. Additionally, the T_{50}

entry times for the retrovirions bearing ZEBOVΔO-GP varied from 8.4-18.3 hours in the

different cell types, and indicated that the entry kinetics were also influenced by the cell population tested.

Also surprising was the entry time for VSV-G-GP bearing pseudovirions in the SNB19 and 786-0 cells (**Fig. 6A-6C; Table 1**) as previously published kinetics of VSV particles demonstrated that this virus entered HeLa cells in 3 minutes or less [129]. In SNB19 and 786-0 cells, the T_{50} of VSV-G-GP-dependent retrovirion entry ranged from 7.5-13.2 hours (**Fig. 6A-6C; Table 1**), again indicating that the background of the pseudovirion as well as the cell population tested may each impact the entry kinetics. This was confirmed when we tested the entry kinetics of FIV-VSV-G-GP in HT-1080 cells (**Fig. 6D; Table 1**). FIV-VSV-G-GP entry was considerably faster ($T_{50} = 4.2$ hours) in this cell line compared to the other cell lines. FIV-VSV-G-GP entry was also significantly faster than FIV-ZEBOVΔO-GP entry in the HT1080 cell line. Together, these results suggest that the kinetics of ZEBOVΔO-GP- and VSV-G-GP-mediated entry into cells is dependent on the pseudovirion background as well as the cell population tested.

<div align="center">

Entry of rhabdovirus based pseudovirions

bearing ZEBOV-GP into permissive cells

occurs relatively rapidly, but then stalls

</div>

Because the shape of retroviral particles (spherical; approximately 100 nM in diameter) differs from rhabdoviral particles (bullet shaped; approximately 200 nM in length) or filoviral particles (filamentous; approximately 1 μM in length), we next tested the entry kinetics of VSVΔG pseudovirions bearing ZEBOVΔO-GP or VSV-G-GP. In contrast to the retroviral based pseudovirions, both ZEBOVΔO-GP and VSV-G-GP VSVΔG pseudovirions entered the cell populations tested much more rapidly, with 30-40% of the virions entering the cells within 1 hour (**Fig. 7A and 7B, Table 1**). Entry of VSVΔG bearing ZEBOVΔO-GP in SNB19s reached a level of 50% after approximately 5.7 hours (**Fig. 7A**), and a level of 50% less than 1 hour in the filoviral permissive

African green monkey Vero cell line (**Fig. 7*B*; Table 1**). Interestingly, entry of the virions did not increase linearly over the remainder of the time course as did the retrovirions bearing ZEBOVΔO-GP. The T_{50} for entry of VSV-G-GP pseudotyped VSVΔG virions was similar to VSVΔG-ZEBOVΔO-GP in both cell lines tested, and we observed a similar "stalling" effect with the VSVΔG-VSV-G-GP pseudovirions as well.

These rapid initial entry kinetics are the fastest that we have observed in our laboratory with any surrogate system expressing either the ZEBOV-GP or the VSV-G-GP to date. This data clearly suggests that there are differences between the rhabdovirus based and retroviral based pseudovirion systems used to present the viral GPs that affect the rate of filoviral-GP-mediated entry. Additionally, it appears that the cell population used can affect the entry kinetics as well.

The filoviral-GPs remain capable of facilitating
productive pseudovirion entry into permissive
cells for extended time periods

Because the entry kinetics of ZEBOV-GP-bearing retrovirions were found to be so surprisingly slow (**Fig. 6**), we next wanted to determine the length of time ZEBOV-GP pseudovirions remained competent for productive entry. Virus was incubated in media alone (without cells) and then added at the indicated time points to cells (**Fig. 8**). Approximately 25% of the virus added to the SNB19 cells after 9 to12 hours was still able to transduce the cells (**Fig. 8**). These data show that filoviral-GPs are more than capable of remaining stable enough to allow productive viral entry for extended time periods, and that this occurs independently of viral-GP engagement of host cell plasma membrane factors.

Filoviral-GP-dependent binding to permissive
cells at 4°C is inefficient

Because the entry process mediated by filoviral-GP bearing retropseudovirions was so slow, we next wanted to examine the efficacy of filoviral-GP binding to SNB19

cells. FIV pseudovirions bearing ZEBOVΔO-GP, full length ZEBOV-GP (FL-ZEBOV-GP) or full length LVMARV (FL MARV-GP) were applied to cells in a 48-well format at 4°C. In some of the wells, the virus added initially was left on for the remainder of the experiment and determined the "100%" control values. Alternatively, after the 1 hour binding step, we removed media containing unbound virus and applied this media to fresh cells to determine the amount of virus not bound in 1 hour. We then washed these cells and applied the media from this wash media to fresh cells to determine how well the virus remained bound to the cells. This wash step would allow for the removal of virions that were not tightly bound to the surface of the cells, but would not affect the binding of those virions that were more tightly bound.

The majority of the pseudovirions initially applied to the SNB19 cells at 4ºC did not bind within the 1 hour time period (**Fig. 9**). These data indicate that all of the filoviral-GPs tested bind inefficiently to the highly transducible SNB19 cell line. However, these data also indicate that the FIV-ZEBOVΔO-GP virions that did bind to the host cell plasma membrane were bound relatively tightly, and were not disturbed by the wash step following removal of the unbound virus (**Fig. 9**). Interestingly, the wash step also revealed that the FIV pseudovirions expressing the full length filoviral-GPs were not as tightly bound as the ZEBOVΔO-GP virions. The LVMARV-GP expressing pseudovirions were bound with significantly lesser affinity than were the ZEBOVΔO-GP bearing pseudovirions. Together these data suggest that the lack of the MLD on the filoviral-GP may aid in allowing a higher binding affinity for GP and attachment factors and/or receptor(s).

Binding of filoviral-GP expressing pseudovirions

to the surface of permissive cells is not

limited by the amount of available attachment

factor(s)/receptor(s)

From these initial studies, it was evident that both filoviral GP and VSV-G transduction of SNB19 cells required many hours, despite the fact that SNB19 cells were one of the most permissive lines for filovirus transduction that has been identified. Thus, we sought to determine the limiting factor(s) in filoviral-GP-mediated entry into SNB19 cells. To test if filoviral-GP-dependent binding at the surface of SNB19 cells was limiting, we bound either about 1200 transducing FIV pseudovirions (1X) or 6000 transducing virions (5X) to cells at 4°C for 1, 4 or 8 hours. VSV-G-GP pseudovirion binding studies were performed in parallel. At each time point, we removed any unbound virions and assessed the transduction levels at 96 hours after initial viral addition to the cells.

We compared the binding of 1X as well as 5X concentrations of virions, with the total amount of transducing virions used for the 1X concentration of virions (**Fig. 10**). The number of ZEBOVΔO-GP and VSV-G-GP virions binding to SNB19 cells at each time point was about 15% of the total number initially added, indicating that as previously seen for EBOV-GP (**Fig. 9**), binding of virus to permissive cells is extremely inefficient. However, the addition of 5X the amount of either FIV-ZEBOVΔO-GP or VSV-G-GP virions allowed an approximate 5X increase in virion binding to SNB19s (**Fig. 10**), indicating that filoviral-GP and VSV-G-GP-mediated binding to permissive cells is not limited. Interestingly, we also observed that over time, the binding of both the ZEBOVΔO-GP and VSV-G-GP pseudovirions did not change, indicating that the viral-GP binding to the SNB19 cells was not a dynamic process at 4ºC (**Fig. 10**).

Retroviral based pseudovirions bearing

ZEBOVΔO-GP mediate internalization into

permissive cells slowly

As virions bind at 4˚C, but only internalize at higher temperatures, we can determine the rate of virion internalization by pre-binding virus in the cold. FIV or human immunodeficiency virus (HIV) pseudovirions bearing ZEBOVΔO-GP or VSV-G-GP were bound to SNB19 cells at 4°C (**Fig. 11*A* and 11*B***). Media heated to 37˚C was refreshed to remove any unbound virus and allow internalization of the bound virus. Extracellular virus was inactivated with a low pH citric acid buffer at time points ranging from 1 to 24 hours post binding and transduction levels were evaluated 96 hours after initial virus binding.

The internalization kinetics of pre-bound retrovirions bearing either ZEBOVΔO-GP or VSV-G-GP was linear over a 24 hour period, but occurred slowly in the cell populations tested (**Fig. 11**). Internalization of 50% of FIV-ZEBOVΔO-GP and HIV-ZEBOVΔO-GP retrovirions into SNB-19 cells occurred at 13.5 hours and 8.7 hours, respectively. Similarly, FIV-VSV-G-GP internalization into SNB19 occurred more slowly than HIV-VSV-G-GP internalization, suggesting that for the viral GPs tested, the pseudovirion core impacted the kinetics of internalization (**Fig. 11*A* and 11*B***). Analysis of HIV-ZEBOVΔO-GP and HIV-VSV-G-GP internalization into a different cell population, 786-0 cells, yielded significantly faster internalization kinetics for HIV-VSV-G-GP pseudovirions compared to HIV-ZEBOVΔO-GP pseudovirions (**Fig. 11*C***). These internalization rates suggest that the cell type used in the analysis also affected the internalization kinetics of the pseudovirions.

Internalization of rhabdovirus based pseudovirions

bearing ZEBOVΔO-GP stalls shortly after

initial virion internalization flux

We next evaluated the internalization kinetics of VSVΔG psuedovirions bearing ZEBOVΔO-GP and VSV-G-GP into Vero and SNB19 cells to confirm that pseudovirion background and cell type were impacting ZEBOVΔO-GP internalization kinetics. We observed that the internalization kinetics of both VSVΔG-ZEBOVΔO-GP and VSVΔG-VSV-G-GP were not linear, as was observed with retro-pseudovirion internalization kinetics. Because of this, the T_{50} times for VSVΔG-ZEBOVΔO-GP pseudovirion internalization into the cells tested occurred at 20.1 hours or later (**Fig. 12**). The non-linear internalization kinetics also impacted the T_{50} (>24 hours) of VSVΔG-VSV-G-GP in SNB19 cells (**Fig. 12***A*). Interestingly, although VSVΔG-VSV-G-GP internalization kinetics into Vero cells also did not occur in a linear fashion, VSVΔG-VSV-G-GP pseudovirions were internalized into Veros significantly faster than VSVΔG-ZEBOVΔO-GP pseudovirions. However, internalization of the VSVΔG-VSV-G-GP virions in Veros stalled shortly after the T_{50} was reached. Combined, these results confirm that the internalization of pseudovirions is dependent upon both the pseudovirion system as well as the cell type tested.

The full-length forms of the filoviral-GPs

also mediate virion internalization into

SNB19 cells slowly

We next determined the kinetics of internalization mediated by pseudovirions bearing the full length forms of filoviral-GPs. It was found that internalization mediated by either the full length ZEBOV-GP or by the full length MARV-GP into SNB19s occurred even more slowly than did FIV-ZEBOVΔO-GP internalization into SNB19s (**Fig. 6***A* **versus Fig. 13**). Interestingly, pseudovirions bearing full length MARV-GP internalized into SNB19s at a slower rate than pseudovirions bearing full length ZEBOV-

GP (**Fig. 13**). 50% of the full length ZEBOV-GP bearing pseudovirions were internalized into the SNB19s after approximately 17.45 hours (black lines; **Fig. 13**). However, the T_{50} for pseudovirions bearing full length MARV-GP was not reached even after the 24 hour time period (gray lines; **Fig. 13**). These results show that internalization events associated with the full length forms of the filoviral-GP may be considerably slower than those associated with the mucin-domain deleted form of ZEBOV-GP. Lastly, it was observed that differences in internalization rates may exist between species of filovirus, as the internalization kinetics of the full length MARV-GP were considerably slower than those observed for full length ZEBOV-GP.

Following filoviral-GP-mediated internalization

into an endosome, the virus remains there

for an extended period of time

As a final confirmation that filoviral-GP-dependent internalization into permissive cells is indeed a very slow process, we sought to determine the time, post-internalization, that filoviral-GP expressing virions spend within a host endosomal compartment. It is known that the filoviral-GP mediates internalization of the virion from the cell surface into an endosome that gradually lowers in pH as it travels further into the host cell cytoplasm [53-55, 100]. The low pH within the endosome is necessary to trigger the activity of host derived proteases on the filoviral-GP and ultimately allow fusion of the filoviral and host endosomal membranes [54, 55]. Thus, ammonium chloride treatment of cells will prevent late endosomal events that are required for virion membrane/endosomal membrane fusion.

The addition of 25 mM ammonium chloride to SNB19 cells at 1 h completely (and significantly) prevented transduction despite attachment or internalization of about 1/3 of the virions used in this study (**Fig. 14**). At 4, 7, and 12 hours post-transduction initiation, ammonium chloride caused an approximate 50% reduction in the number of transducing virions (**Fig. 14**). For instance, at the 7 hour and 12 hour time point, 25/50

and 22/46 of transducing virions were still significantly affected by the ammonium chloride, respectively. This indicates that even 12 hours after binding, half of the filovirus-GP pseudovirions initially bound to the cell remain within endosome and are ammonium chloride sensitive.

Together, the data presented here indicate that the binding of the filoviral-GP to the surface of permissive mammalian cells is extremely inefficient. The data also suggest that after this inefficient binding to one or more proteins on the host plasma membrane, internalization into an endosomal vesicle is a very slow process. Once the internalized virus is inside of the endosomal vesicle, it remains within there for an extended period of time before the viral and host endosomal membranes fuse.

Filoviral-GP-mediated internalization into primary

human and reservoir cell populations is slow

These surprising kinetics results combined with the recent appreciation that the Egyptian fruit bat (*Rousettus aegyptiacus*) is capable of serving as a reservoir for filoviruses in the wild led us to determine if filovirion-GP-mediated internalization into fruit bat cells was faster than internalization into human cell populations [130-139]. To determine this, we cultivated primary fruit bat fibroblasts from ear punches, primary human fibroblasts from fresh penile foreskin (Hff) and primary human endothelial cells from fresh umbilical cords (HuVEC). We then measured filoviral-GP-mediated internalization into these primary cell populations.

Surprisingly, we observed no difference observed between the internalization kinetics of FIV-ZEBOVΔO-GP pseudovirions into the bat and human primary fibroblast cell populations (**Fig. 15***A*). Internalization of 50% of the virions into the primary Hffs occurred around 5 hours (black line; **Fig. 15***A***, Table 1**). The internalization rate of the FIV-ZEBOVΔO-GP pseudovirions into the separate fruit bat fibroblast cell populations was similar to the kinetics in the Hff cells, with 50% of the virions being internalized into

the bat cells between approximately 4.7 hours and 8.3 hours (gray lines; **Fig. 15*B*, Table 1**).

We then confirmed the slow internalization kinetics mediated by the filoviral-GP in another primary human cell population, HuVECs (**Fig. 15*B***). Internalization of 50% of the virions occurred after approximately 18 hours, whereas internalization of 100% of the virions initially bound to the HuVECs was complete only after 48-72 hours (**Fig. 15*B*, Table 1**). When compared to the internalization kinetics of ZEBOVΔO-GP expressing pseudovirions in Hffs, the internalization of pseudovirions into HuVECs was significantly slower. These internalization kinetics are consistent with the filoviral-GP entry kinetics observed in the other human cell lines, and also mirror the internalization kinetics observed in the other human cell populations.

Discussion

The current literature concerning the kinetics of filoviral-GP related binding and internalization events in permissive cells leaves many questions unanswered. Past kinetic experiments using pseudotyped virions have not addressed the possibility that filoviral-GP-dependent entry events may take place over longer than a 6 h time period. Here, we demonstrate that in the highly filoviral permissive SNB19 cell line, retrovirions bearing the filoviral-GP exhibited inefficient binding and slow internalization kinetics (**Fig. 6*A*-6*B* and Fig. 11*A*-11*B***). Additionally, filoviral-GP retrovirions stayed for an extended time period within an endosome in SNB19s post-internalization (**Fig. 14**). The assessment of filoviral-GP pseudotyped retrovirion stability showed that particles remained capable of mediating transduction for extended periods of time (**Fig. 8**), thus supporting the data that retrovirion based filoviral-GP-mediated entry events also occur over extended periods of time.

We first determined that the binding of retroviral pseudovirions bearing either filoviral-GPs or VSV-G-GP to SNB19 cells was not limiting (**Fig. 10**). Binding of retrovirions bearing either viral-GP to the SNB19s at 4ºC increased accordingly when 5X

the amount of virus was added, indicating that the SNB19 cells had enough binding spots to facilitate the increased viral load. However, when we assessed the total amount of virus bound to the cells compared to the total amount initially added (the control value), it becomes clear that the binding mediated by both VSV-G and the filoviral-GP are inefficient (**Fig. 10**).

When we assessed binding of retrovirions bearing the full length forms of ZEBOV- and MARV-GPs, we confirmed that the binding of all forms of the filoviral-GPs including the mucin-domain deleted form of ZEBOV-GP, were inefficient at binding to SNB19s at 4ºC (**Fig. 9**). By subsequently washing the cells once after the removal of this supernatant, we were also able to determine that the ZEBOVΔO-GP virus remained nearly completely bound, indicating a relatively high affinity of binding. Compared to the mucin-domain deleted form of the filoviral-GP, the full length forms seemed not bind to the SNB19 cells as tightly. In fact, full length ZEBOV-GP bound significantly more poorly to SNB19s than did ZEBOVΔO-GP (**Fig. 9**). Full length MARV-GP also bound less well to the SNB19s as compared to ZEBOVΔO-GP (**Fig. 9**). These preliminary results indicate that the mucin domain may be important for more high-affinity filoviral-GP-mediated interactions with the surface of permissive cells.

The assessment of full length ZEBOV-GP- and full length MARV-GP-mediated internalization in SNB19s was also determined using the retrovirion based system. Internalization mediated by full length ZEBOV-GP (black lines; **Fig. 13**) and full length MARV-GP (gray lines; **Fig. 13**) was slower than internalization mediated by the mucin-domain deleted ZEBOV-GP (**Fig. 11***A*). However, full length filoviral-GP-mediated internalization exhibited an overall linear progression of virion internalization similar to ZEBOVΔO-GP (**Fig. 13**). Unexpectedly, we observed that the kinetics of full length MARV-GP virions was considerably slower than that observed with full length ZEBOV-GP (**Fig. 13**). At each time point tested, the percentage of FIV-MARV-GP virions

internalized was approximately half of the amount of FIV-FL ZEBOV-GP virions relative to the controls for each (**Fig. 13**).

It is not clear why one full length filoviral-GP would mediate internalization into the same cell population more quickly than the other. It is possible that the mucin domains present on the full length forms of the filoviral-GP may interfere sterically with viral attachment factors and/or viral receptors on SNB19s. Because the MARV and EBOV species-GPs are not identical within their RBD, it is also possible that ZEBOV-GP and MARV-GP may each use a different set of attachment factors or receptors that allow virion internalization with different kinetics or through different mechanisms. Further exploration of properties associated with MARV-GP-mediated interaction with and entry into certain cell populations will help in understanding these differences.

We lastly determined the internalization kinetics of filoviral-GP bearing retrovirions into three primary cell populations, including two human cell populations, and cells from the reported filoviral reservoir, the Egyptian fruit bat. We were surprised to learn that retrovirions bearing ZEBOVΔO-GP were internalized into primary fruit bat fibroblasts with nearly identical kinetics as ZEBOVΔO-GP internalization into primary human fibroblasts (**Fig. 15***A*). Comparison of these kinetics with ZEBOVΔO-GP-mediated internalization kinetics into an additional primary human cell population, yielded no differences (**Fig. 15***A* **versus 15***B*).

In total, our data indicate that both the binding step and the subsequent internalization step mediated by the filoviral-GPs and by the VSV-G-GPs are inefficient in SNB19s and likely contributing to the overall kinetics of entry observed with the retroviral pseudovirions. We can also conclude that an extended stay in endosomal compartments also contributes to the slow entry observed with retrovirions expressing filoviral-GPs in SNB19s. Although we did not test the binding properties of all of the pseudovirion background systems expressing the filoviral- and VSV-G-GPs, it is likely that those virions are also inefficient in their binding to many of the cell populations

tested. Inefficient binding could therefore also be playing a role in the overall slow and inefficient entry kinetics seen in the majority of cell populations with the majority of pseudovirion systems expressing either the filoviral- or VSV-G-GP.

Additionally, it is possible that these results indicate that even in its reservoir, filovirus entry leading to productive infection is truly a slow event. Slow filoviral replication in the fruit bat may be essential for the virus to effectively manage the host immune system, to remain relatively undetected over time and to not cause overt disease. Understanding the timing of filoviral entry events is crucial in understanding the overall pathogenesis of this deadly family of viruses, and may aid in the development of future treatments targeted at these early events in the filoviral life cycle. Additionally, the appreciation of the timing of these events may help determine more efficacious ways of using current therapies to treat and prevent filoviral infections.

Table 1. T$_{50}$ values for pseudovirion cell association and internalization.

Event	Pseudo-type System	Cell Type	T$_{50}$	Viral-GP	*P* value between T$_{50}$ means
Cell Association	FIV	SNB19	11.25 hr	ZEBOVΔO	0.3865
			7.5 hr	VSV-G	
Cell Association	MuLV	SNB19	8.4 hr	ZEBOVΔO	0.3018
			13.2 hr	VSV-G	
Cell Association	FIV	HT1080	18.3 hr	ZEBOVΔO	0.0030 **
			4.2 hr	VSV-G	
Cell Association	HIV	786-0	13.125 hr	ZEBOVΔO	1.0000
			13.125 hr	VSV-G	
Cell Association	VSVΔG	SNB19	5.7 hr	ZEBOVΔO	0.6336
			4.2 hr	VSV-G	
Cell Association	VSVΔG	Vero	<1 hr	ZEBOVΔO	1.0000
			<1 hr	VSV-G	
Internalization	FIV	SNB19	13.5 hr	ZEBOVΔO	0.6739
			11.4 hr	VSV-G	
Internalization	HIV	SNB19	8.7 hr	ZEBOVΔO	0.6344
			10.8 hr	VSV-G	
Internalization	HIV	786-0	15.9 hr	ZEBOVΔO	0.0417 *
			6.3 hr	VSV-G	
Internalization	VSVΔG	SNB19	>24 hr	ZEBOVΔO	1.0000
			>24 hr	VSV-G	
Internalization	VSVΔG	Vero	20.1 hr	ZEBOVΔO	0.0039 **
			6 hr	VSV-G	
Internalization	FIV	SNB19	17.45 hr	FL ZEBOV	0.3091
			>24 hr	FL MARV	
Internalization	VSVΔG	Hff	5.14 hr	ZEBOVΔO	(between Hffs and bat fibroblasts) 0.6902
Internalization	VSVΔG	Bat fibroblasts	4.7 hr- 8.3 hr	ZEBOVΔO	
Internalization	FIV	HuVECs	18.33 hr	ZEBOVΔO	(Between Hffs and HuVECs) 0.0065 *

Note: *****, *P* <0.05; ******, *P* <0.005
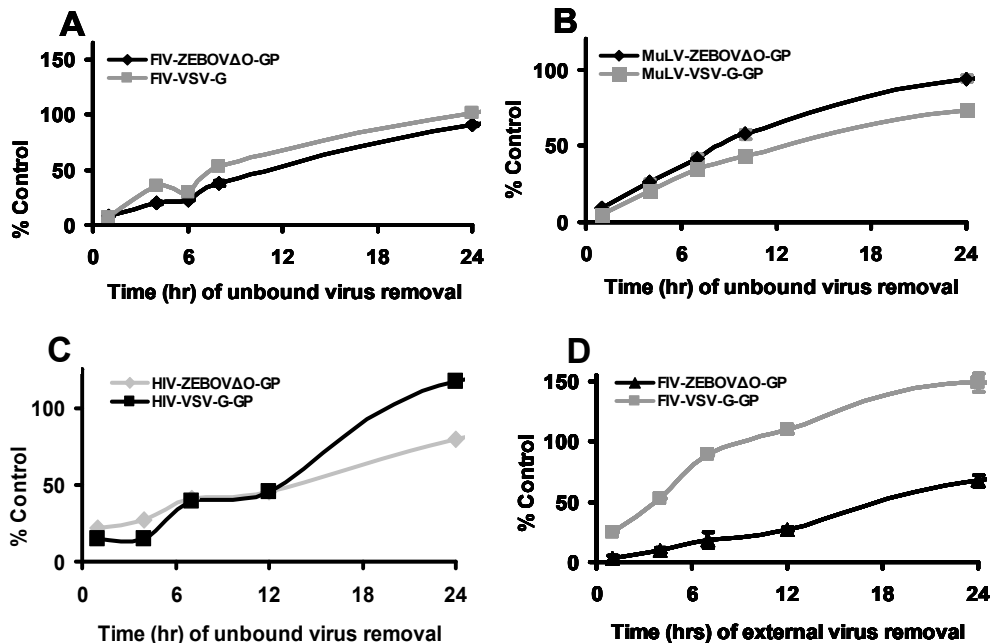
Figure 6. Entry of retroviral pseudovirions bearing ZEBOVΔO-GP into permissive cells is a slow and inefficient process. Pseudotyped virions bearing ZEBOVΔO-GP and VSV-G-GP were applied to 3 x 10⁴ adherent SNB19 cells **(A-B)**, 786-0 cells **(C)** or HT1080 cells **(D)** in a 48-well plate at an MOI of 0.005. The plates were then incubated at 37ºC until the indicated time point. At the time points, the media was removed (along with all unbound virions) and fresh media was added. 96 h post-transduction, all cells were either fixed and stained for β-gal activity, or lifted and analyzed for GFP positivity. The number of β-gal or GFP positive cells when transducing particles were not removed was set to 100% to calculate the percentage of control values. Data in panels A-C represent the means and standard errors of the means from three independent experiments performed in triplicate. Data in panel D represents the means from one experiment performed in triplicate.
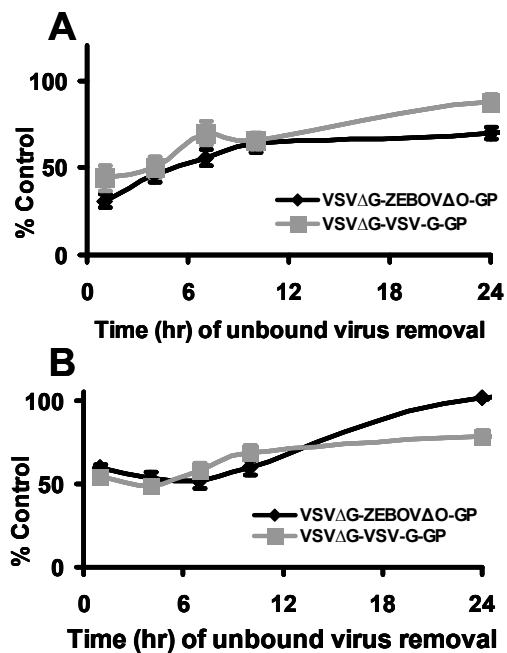
Figure 7. Entry of rhabdovirus based pseudovirions bearing ZEBOV-GP into permissive cells occurs relatively rapidly, but then stalls. Pseudotyped virions bearing ZEBOVΔO-GP and VSV-G-GP were applied to 3 x 10^4 adherent SNB19 cells **(A)** or Vero cells **(B)** in a 48-well plate at an MOI of 0.05. The plates were then incubated at 37ºC until the indicated time point. At the time points, the media was removed (along with all unbound virions) and fresh media was added. 96 h post-transduction, cells were analyzed by flow cytometry for GFP positivity. The number of GFP positive cells when transducing particles were not removed was set to 100% to calculate the percentage of control values. Data represent the means and standard errors of the means from three independent experiments performed in triplicate.
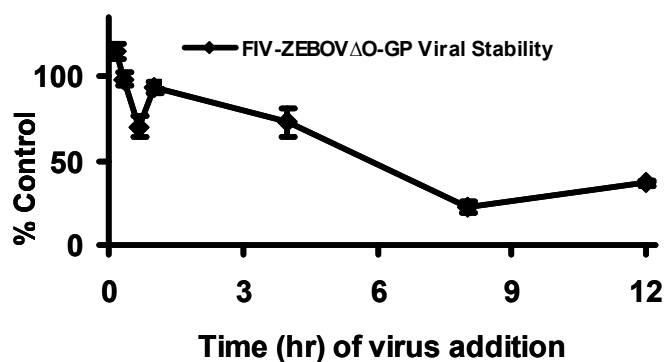
Figure 8. The filoviral-GP on retroviral pseudovirions remain capable of facilitating productive pseudovirion entry into permissive cells for extended time periods. FIV pseudotyped virions bearing ZEBOVΔO-GP were incubated in media alone for the indicated amount of time. At the time points, virus was added to fresh cells SNB19 cells. 96 h post-transduction, cells were fixed and stained for β-gal activity. The number of β-gal positive cells when transducing particles were added at time zero was set to 100% to calculate the percentage of control values. Data represent the means and standard errors of the means from three independent experiments performed in triplicate.
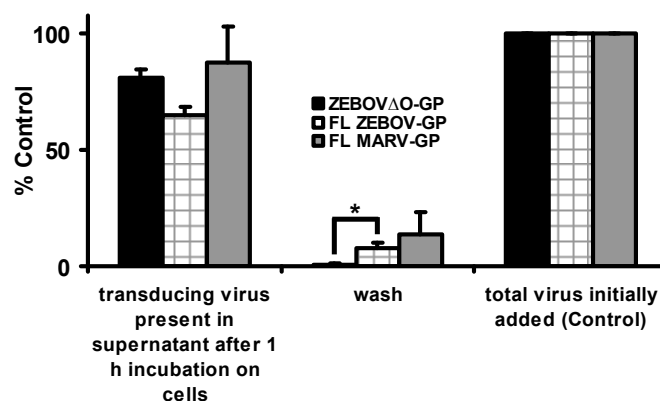
Figure 9. Filoviral-GP-dependent binding to permissive cells at 4°C is inefficient.
Full length (FL) MARV, ZEBOV-GP- and mucin domain deleted (ΔO) ZEBOV-GP-
mediated binding to SNB19s at 4°C was measured after one hour. FIV pseudotyped
virions were applied to 3 x 10⁴ adherent SNB19 cells in a 48-well plate. The plates
were incubated at 4°C for one hour, at which time, the media was removed (along with
all unbound virions). The media containing unbound virions was applied to fresh
SNB19 cells also in a 48-well format. This process was repeated, and 96 h post-
transduction, all cells were fixed and stained for β-galactosidase (β-gal) activity. The
number of β-gal positive cells when transducing particles were not removed was set to
100% to calculate the "% Control" value. Data represent the means and standard
errors of the means from three independent experiments performed in triplicate. *, *P*
<0.05.
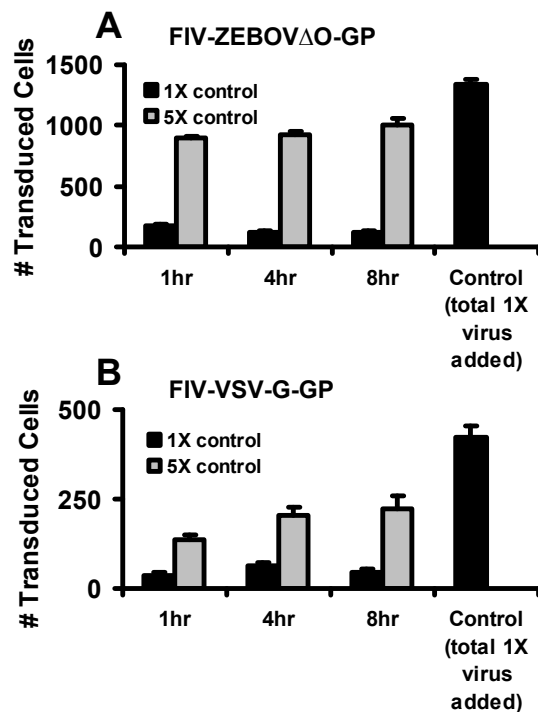
Figure 10. Binding of filoviral-GP expressing pseudovirions to the surface of permissive cells is not limited by the amount of available attachment factor(s)/receptor(s). FIV pseudotyped virions bearing ZEBOVΔO-GP (A) or VSV-G-GP (B) were applied to 3×10^4 adherent SNB19 cells in a 48-well plate at a 1X or 5X concentrations. The plates were incubated at 4°C until the indicated time points, at which time, the media was removed (along with all unbound virions), and fresh media added. After 8 h, cells were incubated at 37°C for the remainder of the experiment. 96 h post-transduction, all cells were fixed and stained for β-gal activity. The number of β-gal positive cells when the 1X concentration of transducing particles were not removed was set to 100% to calculate the percentage of control values. Data represent the means and standard errors of the means from three independent experiments performed in triplicate.
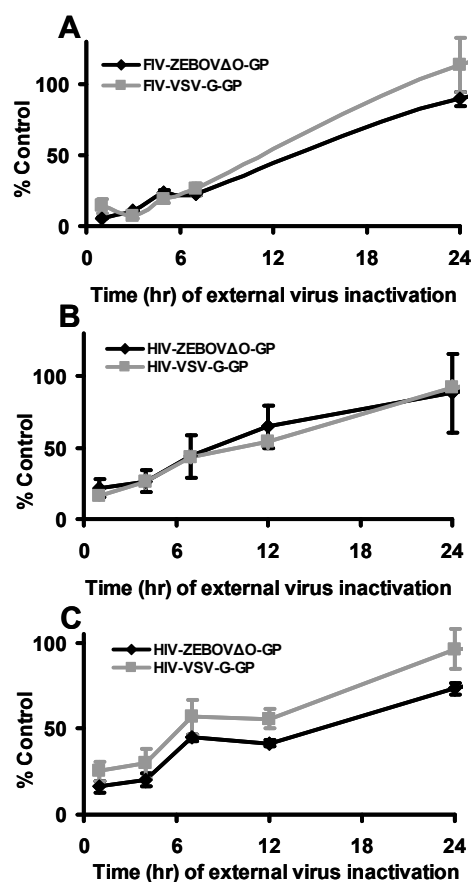
Figure 11. Retroviral based pseudovirions bearing ZEBOVΔO-GP mediate internalization into permissive cells slowly. Pseudotyped virions bearing ZEBOVΔO-GP or VSV-G-GP were applied to 3 x 10^4 adherent SNB19 cells **(A-B)** or 786-0 cells **(C)** in a 48-well plate. The plates were incubated at 4ºC for one hour at which time, the media was removed (along with all unbound virions), and fresh media added. The cells were then incubated at 37ºC until the indicated time point. At the indicated time points, cells were treated for 30 seconds with citric acid buffer to inactivate all non-internalized viral particles. The cells were then washed to return the pH to normal, and fresh media was added to the cells. 96 h post initial transduction, all cells were either fixed and stained for β-gal activity or analyzed for GFP positivity. The number of β-gal or GFP positive cells when transducing particles were bound to the cells for one hour but not inactivated was set to 100% to calculate the percentage of control values. Data represent the means and standard errors of the means from three independent experiments performed in triplicate.
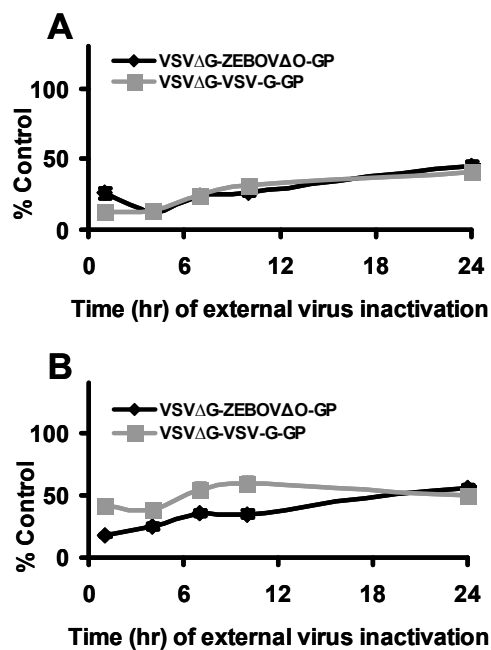
Figure 12. Internalization of rhabdovirus based pseudovirions bearing ZEBOVΔO-GP stalls shortly after initial virion internalization flux. Pseudotyped virions bearing ZEBOVΔO-GP or VSV-G-GP were applied to 3 x 10^4 adherent SNB19 cells **(A)** or Vero cells **(B)** in a 48-well plate. The plates were incubated at 4ºC for one hour at which time, the media was removed (along with all unbound virions), and fresh media added. The cells were then incubated at 37ºC until the indicated time point. At the indicated time points, cells were treated for 30 seconds with citric acid buffer to inactivate all non-internalized viral particles. The cells were then washed to return the pH to normal, and fresh media was added to the cells. 96 h post initial transduction, cells were analyzed for GFP positivity. The number of GFP positive cells when transducing particles were bound to the cells for one hour but not inactivated was set to 100% to calculate the percentage of control values. Data represent the means and standard errors of the means from three independent experiments performed in triplicate.

Figure 13. The full-length forms of the filoviral-GPs also mediate virion internalization into SNB19 cells slowly. FIV pseudotyped virions bearing full length ZEBOV-GP or full length MARV-GP were applied to 3×10^4 adherent SNB19 cells in a 48-well plate. The plates were incubated at 4ºC for one hour at which time, the media was removed (along with all unbound virions), and fresh media added. The cells were then incubated at 37ºC until the indicated time point. At the indicated time points, cells were treated for 30 seconds with citric acid buffer to inactivate all non-internalized viral particles. The cells were then washed to return the pH to normal, and fresh media was added to the cells. 96 h post initial transduction, all cells were fixed and stained for β-gal activity. The number of β-gal positive cells when transducing particles were bound to the cells for one hour but not inactivated was set to 100% to calculate the percentage of control values. Data represent the means and standard errors of the means from three independent experiments performed in triplicate.

Figure 14. Following filoviral-GP-mediated internalization into an endosome, the virus remains there for an extended period of time. FIV pseudotyped virions bearing full length ZEBOV-GP were applied to 3 x 10^{4} adherent SNB19 cells in a 48-well plate. The plates were incubated at 37ºC until the indicated time point. At the indicated time point, ammonium chloride or media containing carrier (DMSO) alone was added to the cells. 24 hours post-transduction media was refreshed on all wells to remove ammonium chloride and DMSO. 96 h post initial transduction, all cells were fixed and stained for β-gal activity. The number of β-gal positive cells when transducing particles were applied to the cells for and then not removed was set to 100% to calculate the percentage of control values. Data represent the means and standard errors of the means from three independent experiments performed in triplicate. *, P <0.05.
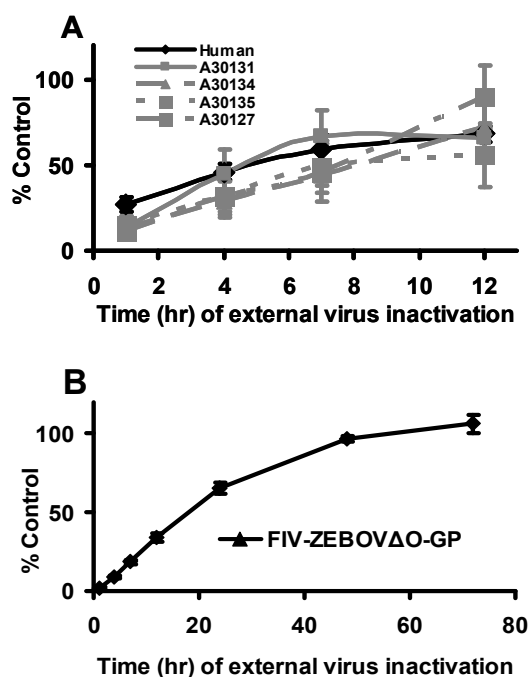
Figure 15. Filoviral-GP-mediated internalization into primary human and reservoir cell populations is slow. VSV pseudovirions (A) or FIV pseudovirions (B) bearing ZEBOVΔO-GP were applied to 3 x 10^4 adherent Hff cells **(A**; black lines**)**, fruit bat cells **(A**; gray lines**)** or HuVEC cells **(B)** in a 48-well plate. The plates were incubated at 4°C for one hour at which time, the media was removed (along with all unbound virions), and fresh media added. The cells were then incubated at 37°C until the indicated time point. At the indicated time points, cells were treated for 30 seconds with citric acid buffer to inactivate all non-internalized viral particles. The cells were then washed to return the pH to normal, and fresh media was added to the cells. 96 h post initial transduction, all cells were analyzed for GFP positivity or fixed and stained for β-gal activity. The number of GFP or β-gal positive cells when transducing particles were bound to the cells for one hour but not inactivated was set to 100% to calculate the percentage of control values. Data represent the means and standard errors of the means from three independent experiments performed in triplicate.

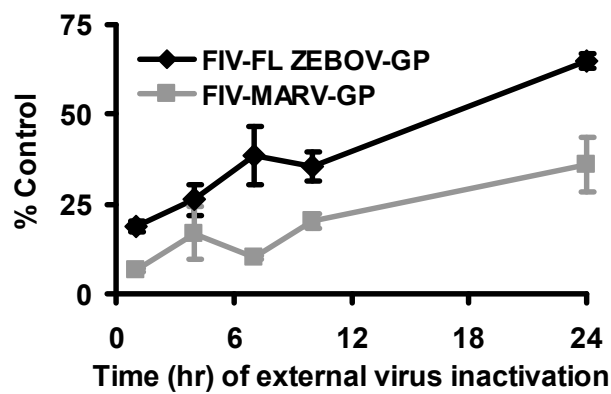# CHAPTER THREE: IMPORTANCE OF GLYCOSYLATION PATTERNS ON HOST PLASMA MEMBRANE PROTEINS IN FILOVIRAL ENTRY

Abstract

To determine the impact of specific carbohydrate linkages on host cell plasma membrane proteins involved in filoviral entry, we have used a series of Chinese hamster ovary (CHO) cell lines that are deficient in one or more enzymes that are required for N- and O- linked glycosylation. The LdlD cell mutant line that expresses normal surface N-linked glycans but has abbreviated O-linked surface glycans showed a 50% reduction in transduction by both ZEBOV and Lake Victoria MARV-GP pseudotyped particles as compared to the control wild type parental CHO cell line (Pro5). Use of the novel O-linked inhibitor drug 1-68A allowed us to confirm the necessity of O-linked glycans in efficient ZEBOV entry into additional permissive cells types. Interestingly, loss of terminal sialic acids (Lec2 cells) or galactose (Lec8 cells) on both N- and O- linked sugars resulted in a 2-fold enhancement of filoviral GP mediated entry compared to control. However, Lec1 cells that have wild type O-linked glycans but highly abbreviated N-linked glycans had similar levels of transduction to control Pro5 cells. Further studies indicated that binding of ZEBOV to Pro5 and all mutant CHO cells was equal, indicating that a post-binding defect or enhancement in ZEBOV internalization may be occurring. These data identify the importance of host cell O linked glycosylation during the initial steps in filovirus infection.

Introduction

Although the specific host proteins involved in filoviral-GP-mediated entry remain poorly characterized, assessment of the importance of the carbohydrate linkages for EBOV-GP-dependent entry may provide insights into cell surface events that mediate filovirion uptake. Indeed, it has been suggested through the use of tunicamycin that N-

linked glycosylation of surface membrane proteins is important for EBOV-GP-dependent entry [95]. However, little else is known concerning filoviral dependence upon host-plasma membrane protein glycosylation during infection and the role of O-linked glycosylation in entry mediated by filoviral-GPs has not been investigated.

Through the use of Chinese hamster ovary (CHO) cells that contain one or more mutations in the pathways involved in N- and O-linked glycosylation, we sought to determine specific sugar linkages that are important for efficient filoviral-GP-mediated transduction of the CHO cells. The five CHO cell lines that we will be using are only a few from a much larger collection of glycan mutants. The parental CHO cell line that our mutants were created from are all haploid, and therefore express only one copy of each gene within their chromosome, making it much easier to create single, double or even triple mutations within these cells [140]. For our purposes, the large collection of CHO cell mutants that exists makes it possible to test the necessity of specific sugars in viral entry without the need for highly cytotoxic biochemicals.

The CHO cell lines utilized are listed in **Table 2** and include the wild type (parental) Pro5 line that will be used as a reference strain during our studies. Each line used has been previously characterized and verified to lack the specified sugars on it N- and/or O-linked glycans. The Lec1 CHO cell line lacks *N*-acetylglucosamine on it N-linked glycans but has wild type O-linked glycans [141]. The Lec2 CHO cell line lacks sialic acid on both its N- and O-linked glycans [142]. The Lec8 CHO cell line lacks galactose on both its N- and O-linked glycans [143]. The final CHO cell line, LdlD, will be of particular interest to this study, as it lacks virtually all O-glycan linkages, but has intact N-linked glycans [144].

Here, we show that lack of O-linked glycans reduces filoviral-GP pseudovirion transduction by approximately 50%, whereas lack of either sialic acid or galactose on N- and O-linked glycans increased transduction approximately 2-3 fold. The necessity for O-linked glycosylation in filoviral-GP-mediated entry was confirmed using a novel O-

linked biochemical inhibitor. Interestingly, the lack of N-acetylglucosamine on N- and O-linked glycans had no effect on filoviral-GP-mediated entry. Pseudovirions bearing filoviral-GPs bound to all of the CHO cells, including the wild type cell line, equally well, indicating that an event post-binding, such as internalization, was enhanced or was decreased in cells expressing altered surface glycosylation. Together, these data represent the first time carbohydrate linkages on host plasma membrane proteins have been shown to modulate filoviral-GP-mediated entry events.

Materials and methods

Cells lines

Human embryonic kidney cells 293T (CRL-11268; ATCC), a human glioblastoma line, SNB19 (NCI 0502596) and an African green monkey kidney cell line, Vero (CCL-81; ATCC) were maintained in high-glucose Dulbecco's modified Eagle's medium (DMEM) (Invitrogen) supplemented with 100 units/ml of penicillin and 100 μg/ml streptomycin (1% P/S) and 10% fetal calf serum (FBS) (HyClone). Chinese hamster ovary cells (CHO) cells were maintained in F-12 media (Invitrogen) supplemented with 100 units/ml of penicillin and 100 μg/ml streptomycin (1% P/S) and 10% FBS. CHO cell lines used included the wild type Pro5 line (CRL-1781; ATCC), the Lec1 line (CRL-1735; ATCC), the Lec2 line (CRL-1736; ATCC), the Lec8 line (CRL-1737; ATCC) and the LdlD line (kindly provided by Dr. Kevin Campbell, University of Iowa, Department of Physiology).

Plasmids used

All plasmids used to generate feline immunodeficiency virus (FIV) core pseudovirions have been previously described [121, 125].

Production of ZEBOV-GP pseudotyped
FIV-β-galactosidase particles

FIV virions were generated as previously described [121]. Virus was produced by transfection of three plasmids into 80% confluent HEK 293T cells in a total of 75 μg of

plasmid DNA. The transfected plasmids consisted of the following at a ratio of 1:2:3, respectively: pCMV/EBOVΔO that expresses Zaire (ZEBOV-GP) with a deletion of the mucin domain, pCMV/FIVΔΔ that expresses FIV gag-pol, and pFIVΨβgal. Full length forms of the ZEBOV-GP and MARV-GP were also used in place of the pCMV/EBOVΔ O expression plasmid. The DNA was transfected into 15-cm diameter dishes of 293T cells using calcium phosphate transfection [127]. After 12 h the cells were washed, and fresh medium was added (DMEM, 2% [vol/vol] FBS, 1% [vol/vol] Pen-Strep). Supernatants were collected at 24, 36, 48, 60, and 72 h post-transfection and frozen at – 80°C. The supernatants were thawed, filtered through a 0.45-μm-pore-size filter, and pelleted by a 16-h centrifugation step (7,700 x g at 4°C in a Sorvall GSA rotor). The viral pellet was resuspended in DMEM for an approximate 200-fold concentration, and the virus was either used immediately for infection or stored at –80°C until use.

Detection of β-galactosidase based
pseudovirion entry

FIV transduction studies were performed in a 48 well format using a MOI of ~0.005 (resulting in approximately 200 β-gal positive cells/40,000 cells/well in control wells). FIV pseudovirion transduction was detected by fixing cells in 3.7% formalin and evaluating for β-gal activity using the substrate 5-bromo-4-chloro-3-indolyl-β-D-galactopyranoside. All FIV transduction evaluation was done 48 h after initial FIV pseudovirion addition to cells. The number of β-gal-positive cells was enumerated by microscopic visual inspection.

Chemical reagents

The novel O-linked glycan inhibitor 1-68A was kindly provided by Dr. Carolyn Bertozzi at the University of California, Berkeley, Department of Biochemistry. The drug was resuspended in DMSO at a concentration of 10 mM and, in all experiments where 1-68A was used, negative control wells contained equivalent concentrations of DMSO as the experimental wells.

1-68A drug studies

Drug was applied to 3 x 10^4 cells per well in a 48-well format. Cells were incubated with 1-68A for 8 h before the addition of virions. Media containing the drug was removed and FIV-ZEBOVΔO-GP pseudovirions (MOI=0.005) were added to wells for an additional 16 h in fresh media lacking FBS. 24 h after the initiation of the experiment, media was refreshed on the cells, and cells were fixed and stained for β-gal activity 48 h after transduction initiation.

Virion transduction studies

All transduction studies were preformed in a 48-well format using ~3 x 10^4 cells per well. Pseudovirions were applied to cells at time zero and incubated with the cells at 37ºC to allow virion entry into the cells. Cells were analyzed for pseudovirion transduction 48 hours post-transduction.

Virion binding studies (protein based)

FIV-ZEBOVΔO-GP pseudovirions were applied for 1 h at 4ºC to CHO cells in a 96-well format. After one hour, media was aspirated from the cells, the cells were washed 3X in PBS, and the cells were lysed in 1% SDS, and proteins separated using SDS-PAGE and transferred to a nitrocellulose membrane as described previously [121]. FIV Capsid was analyzed by incubating feline anti-FIV sera (1:5,000) overnight at room temperature followed by incubation with appropriate secondary peroxidase-conjugated antisera (1:20,000; Sigma). Actin was detected by incubating primary peroxidase-conjugated antibody (1:10,000) for 3 h at room temperature. Blots were developed with enhanced chemiluminescence (ECL; Pierce Biotechnology, Rockford, IL), read on a low-light digital camera (LAS-1000; Fujifilm Medical Systems USA, Stamford, CT), and quantified using Image Gauge (Fujifilm).

Cell viability assay

At the time of pseudovirion transduction evaluation, cell viability was monitored in an ATP-Lite assay (Packard Biosciences) as per the manufacturer's instructions.

Statistical analysis

Statistical analyses were conducted by Student's *t* test, utilizing the two-tailed distribution and two-sample equal-variance conditions. *P* values were assessed by comparing the level of transduction with treatment to the level of cytotoxicity observed with that specific treatment. A significant difference was determined by a *P* value of <0.05. If the *P* value was >0.05, the data were not considered significant.

Results

O-linked glycosylation of host plasma membrane

proteins is important for efficient

ZEBOVΔO-GP-mediated entry into CHO cells

To gain a general understanding of the involvement of specific glycan linkages in filoviral-GP-mediated transduction of permissive cells, we first assessed the transduction levels of pseudovirions bearing ZEBOVΔO-GP. Transduction levels of the pseudovirions were compared to the transduction levels of the wild type Pro5 CHO cell line. The LdlD cell mutant line that lacks UDP-Gal/Glc-4 epimerase and that expresses normal surface N-linked glycans but has abbreviated O-linked surface glycans showed a 30% reduction in transduction by ZEBOVΔO-GP pseudotyped particles as compared to the Pro5 control cell line (**Fig. 16**). Interestingly, loss of terminal sialic acids on both N- and O- linked sugars (Lec2 cells) resulted in an almost 3-fold enhancement of filoviral GP mediated entry compared to control (**Fig. 16**). Lec8 cells that lack terminal sialic acid, N-acetyl glucosamine and galactose residues on both N- and O-linkages also showed enhanced transduction of approximately 3.25 fold (**Fig. 16**). However, Lec1 cells that have wild type O-linked glycans, highly abbreviated N-linked glycans had similar levels of transduction to control Pro5 cells (**Fig. 16**). Together, these studies indicate a necessity for intact O-linked glycans for efficient filoviral-GP-mediated entry into CHO cells; however, the changes in N-linked glycans that were examined had no deleterious effect on EBOV transduction. Interestingly, we also found that loss of either

sialic acid or galactose on N- and O-linked glycans allowed for more efficient

ZEBOVΔO-GP-mediated entry into CHO cells.

The necessity for O-linked glycosylation for
efficient viral entry into CHO cells is specific
to filoviral-GPs

To determine if the necessity for O-linked glycans for efficient pseudovirion entry

was specific to ZEBOV-GP, we first assessed the transduction ability of pseudovirions

bearing two other viral-GPs. We tested the ability of pseudovirions bearing vesicular

stomatitis virus GP (VSV-G-GP) or the baculovirus GP (GP64) to transduce the LdlD

CHO cells compared to the Pro5 CHO cells (**Fig. 17**). In these studies, we confirmed that

the loss of O-linked glycans on CHO cells decreased the transduction of pseudovirions

bearing ZEBOVΔO-GP by approximately 30%, but found that the loss of O-linked

glycans did not inhibit transduction of pseudovirions bearing either VSV-G-GP or GP64

(**Fig. 17**). These findings indicated that the effect of O-linked glycan loss on transduction

ability was specific to ZEBOVΔO-GP, and not other viral GPs from two unrelated

viruses.

In these initial studies, we utilized the mucin-domain deleted form of the

ZEBOV-GP to test the necessity of various host plasma membrane glycan linkages for

filoviral-GP-dependent entry. Next, we sought to determine if transduction of full length

forms of ZEBOV-GP as well as the glycoprotein from the related Marburgvirus, MARV-

GP, were also sensitive to loss of O linked glycosylation. We therefore tested the

transduction ability of pseudovirions bearing ZEBOVΔO-GP, full length ZEBOV-GP and

full length MARV-GP in the different CHO cell lines. Not surprisingly, we found that

transduction of the full-length forms of the filoviral-GPs had similar trends to that

observed with the mucin domain deleted form of ZEBOV-GP (**Fig. 18**). The loss of O-

linked glycans inhibited transduction of all of the filoviral-GPs by approximately 50%,

whereas loss of either sialic acid or galactose from the surface of plasma membrane

proteins increased filoviral-GP-dependent transduction (**Fig. 18**). The lack of N-acetylglucosamine from both N- and O-linked glycans had no effect on filoviral-GP transduction (**Fig. 18**). These results led us to next confirm the necessity for O-linked glycans in efficient filoviral-GP-mediated entry into permissive cells using an independent approach.

<div align="center">

O-linked glycosylation is important for

efficient filoviral-GP-mediated entry into

CHO cells

</div>

To confirm the importance of O-linked glycans in efficient ZEBOVΔO-GP-mediated transduction, we assessed the effect of a novel O-linked glycan inhibitor, 1-68A, on ZEBOVΔO-GP-mediated transduction of the Pro5 CHO cells as well as two additional filoviral permissive cell populations. This compound that has been shown to block the synthesis of new O linked glycans [145] was applied to the Pro5 cells, as well as the highly filoviral permissive human glioblastoma cell line SNB19 and to the filoviral permissive African green monkey kidney cell line, Vero. The inhibitor was applied to these cells for 8 hours prior to the addition of pseudovirions bearing ZEBOVΔO-GP, allowing the cells to metabolize the drug and inhibit the addition of O-linked glycans on newly synthesized plasma membrane proteins. Under these conditions, the cytotoxicity of I-68A was modest with only detectable toxicity at the higher concentrations. The resulting host plasma membrane surface glycans should therefore not contain any O-linked glycans [145]. Through the use of the O-linked inhibitor in SNB19 (**Fig. 19***A*) and Vero cells (**Fig. 19***B*), we were able to confirm that ZEBOVΔO-GP-dependent entry does require O-linked glycans on the surface of permissive cells. Unfortunately, the cytotoxicity curve was nearly the same as the transduction curve in Pro5 cells and did not allow us to conclude anything from this cell population (**Fig. 19***C*). However, these data independently verify that O-linked glycans are important for efficient entry mediated by ZEBOVΔO-GP into permissive cells of multiple mammalian species.

O-linked glycans, sialic acid and galactose

impact ZEBOVΔO-GP-dependent entry

post-binding to CHO cells

To assess EBOV pseudovirion binding to the CHO cells lines, direct pseudovirion binding studies were performed. We bound FIV-ZEBOVΔO-GP expressing pseudovirions to the different CHO cells for one hour at 4°C or 37°C in a 96-well format. Unbound virions were removed, cells were washed three times in PBS and cells with bound virus were lysed in 1% SDS. The proteins present in cell lysates were separated using SDS-PAGE and transferred to a nitrocellulose membrane and probed with antibodies against FIV antigens and antisera binding was quantified by chemiluminescence detection using a low-light digital camera and the Image Gauge protein quantification program. FIV capsid binding was normalized for cell numbers using an actin antibody that was directly conjugated to HRP. Surprisingly, we observed no difference in the amount of virions bound to each of the CHO cell lines, including the Pro5 (wild-type) cells (**Fig. 20**). We also observed that the binding appeared to be temperature independent. In these assays, approximately 20-25% of the input amount of virions bound to the CHO cell lines (**Fig. 20**). Thus, direct assessment of virion binding indicated that ZEBOVΔO-GP bearing pseudovirion binding to the CHO cells was not dependent on N- or O-linked glycosylation. Combined these last pieces of data suggest that a step post-binding is altered or affected in the Lce2, Lec8 and LdlD mutant cell lines. We are currently investigating the rates of virion internalization into these mutant CHO cells lines.

<u>Discussion</u>

The study of the glycosylation patterns of host plasma membrane proteins and their role in viral entry is often accomplished through the use of biochemical inhibitors [146-151]. However, significant cytotoxicity associated with these drugs along with the absence of specificity prevents analysis of specific N- or O-linked alterations. To

circumvent these problems, we have primarily used mutant Chinese hamster ovary (CHO) cells. Each of these lines contains a characterized mutation in their glycosylation pathway, thereby exhibiting altered glycosylation patterns on plasma membrane proteins. Because the filoviral-GP can enter virtually all mammalian cells [100, 128, 152-154], the CHO collection of cells was ideal for this study.
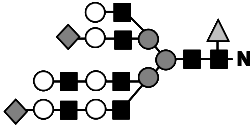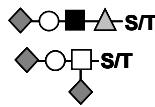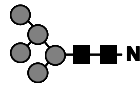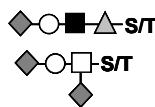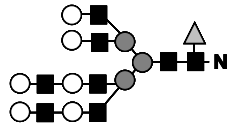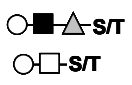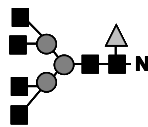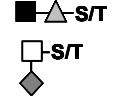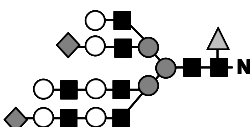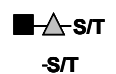
The data generated from this study is the first analysis of the role of multiple, specific N- and O-linked glycans in filoviral-GP-dependent binding and entry into permissive cell populations. We have identified a role for O-linked glycans in facilitating efficient filoviral-GP-dependent pseudovirion transduction. Without O-linked glycans present on the plasma membrane surface, entry of filoviral-GP expressing pseudovirions, but not pseudovirions expressing GPs from other viral families, is decreased by approximately 30% (**Fig. 16 and Fig. 17**). We utilized a novel O-linked biochemical inhibitor to confirm the necessity of O-linked glycans for filoviral-GP-dependent entry into permissive cells (**Fig. 18**). The drug inhibits the family of UDP-GalNAc:polypeptide N-acetylgalactosaminyltransferases (ppGaNTases) that are responsible for initiating mucin-type O-linked glycosylation in higher eukaryotes [145]. This is the first time that this inhibitor has been used to assess entry of a virus. Although we were unable to determine the ability of the inhibitor to reduce filoviral-GP-mediated entry into the parental Pro5 CHO cell line due to the cytotoxicity of the drug (**Fig. 19***C*), we were clearly able to show that the drug significantly diminished entry into two other permissive mammalian cell populations (**Fig. 19***A* **and 19***B*). This data confirms the importance of O-linked glycans in filoviral-GP-mediated entry, and also shows the feasibility of using this novel O-linked glycosylation inhibitor to study the importance of O-linked glycans in the entry of other viruses.

Interestingly, we have also identified a role for sialic acid and galactose on both N- and O-linked glycans in filoviral-GP-dependent entry. Loss of these glycans on the plasma membrane allows for a 2-3 fold increase in filoviral-GP-dependent pseudovirion

transduction (**Fig. 16**). We then determined that this increase was not due to an increase in virion binding, as equal amounts of virions bound to each of the CHO cell lines tested, including the parental cell (**Fig. 20**). This led us to conclude that a defect is likely present in the LdlD cells that impacts the efficient entry of filoviral-GP bearing virions after they are bound to the cells. These results also indicate that in the Lec2 and Lec8 cell populations, an enhancement in transduction of virions post-binding may be occurring. We are currently studying the internalization rates of filoviral-GP expressing pseudovirions and virus like particles into these CHO cell mutants.

Although specific glycans involved in specific steps during filoviral entry have never been appreciated before, many other viruses recognize one or more carbohydrate structures on the surface of host cells. The viral recognition of and subsequent interaction with different carbohydrate structures on viral attachment factors, receptors, or both are often necessary for productive viral entry. Viruses including polyomaviruses, coronaviruses, influenza virus, HIV-1 and adenoviruses all require the correct expression of specific glycans on plasma membrane proteins to mediate attachment and internalization [147, 155-159]. Knowledge of the specific glycans involved in viral engagement of attachment factors and receptors is key to the development of novel carbohydrate-based treatments that can be used to potentially block viral attachment and entry. This information could be especially useful for the filovirus family, for which no treatments are currently available to reduce viral loads of infected individuals.

Table 2. Glycosylation defects in lectin-resistant CHO mutants.

CHO line	Biochemical change	Genetic change	Predicted *N*-glycans	Predicted *O*-glycans
Pro5 (parent)	↓ Gal on *N*-glycans	No expression of *B4galt6*		
Lec1	↓ GlcNAc-TI	Insertion/deletion in *Mgat1* ORF		
Lec2	↓ CMP-sialic acid Golgi transproter	Mutation in *Slc35a1* ORF		
Lec8	↓ UDP-Gal Golgi transporter	Mutation in *Slc35a2* ORF		
LdlD	↓ UDP-Gal/Glc-4-epimerase	?		

Note: Sugar symbols: gray triangle, fucose; gray circle, mannose; white circle, galactose; black square, *N*-acetylglucosamine; white square, *N*-acetylgalactosamine; gray trapezoid, sialic acid.
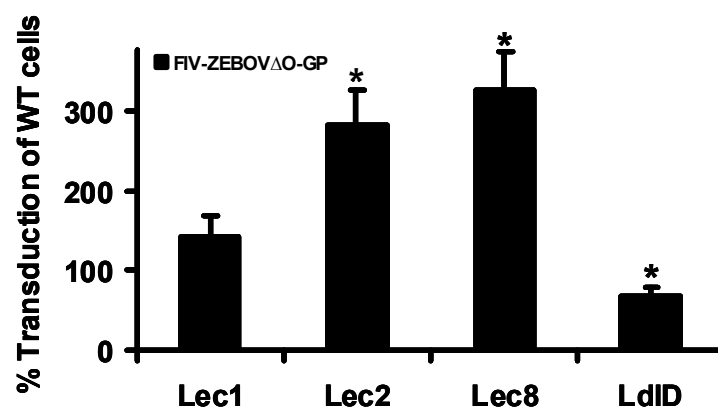
Figure 16. O-linked glycosylation of host plasma membrane proteins is important for efficient ZEBOVΔO-GP-mediated entry into CHO cells. Cells (3 x 10^4) were transduced with FIV pseudotyped virus at time zero. All cells were fixed and stained for β-gal activity 48 h post-transduction. The number of transduced cells in the parental CHO cells (Pro5) was set to 100% for percentage of control calculations. Data represent the means and standard errors of the means from three independent experiments performed in triplicate. *, $p<0.05$.
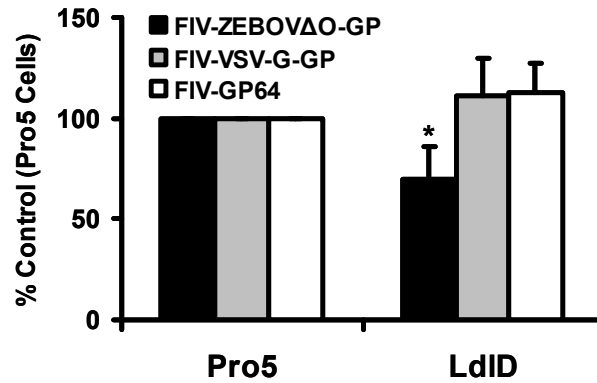
Figure 17. The necessity for O-linked glycosylation for efficient viral entry into CHO cells is specific to ZEBOVΔO-GPs. Cells (3 x 10^4) were transduced with FIV pseudotyped virus at time zero. Glycoproteins used in addition to ZEBOVΔO-GP include the vesicular stomatitis virus (VSV-G-GP) and the baculovirus GP64 GP. All cells were fixed and stained for β-gal activity 48 h post-transduction. The number of transduced cells in the parental CHO cells (Pro5) was set to 100% for the percentage of control calculation. Data represent the means and standard errors of the means from three independent experiments performed in triplicate. *, $p<0.05$.
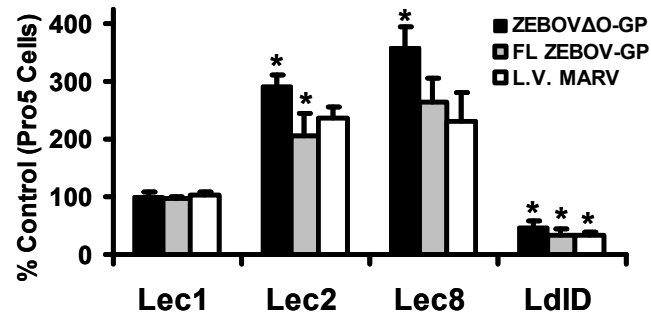
Figure 18. O-linked glycosylation is important for efficient filoviral-GP-mediated entry into CHO cells. Cells (3 X 10⁴) were transduced with FIV pseudotyped virus at time zero. All cells were fixed and stained for β-gal activity 48 h post-transduction. The number of transduced cells in the parental CHO cells (Pro5) was set to 100% for percentage of control calculations. Data represent the means and standard errors of the means from three independent experiments performed in triplicate. *, $p<0.05$.
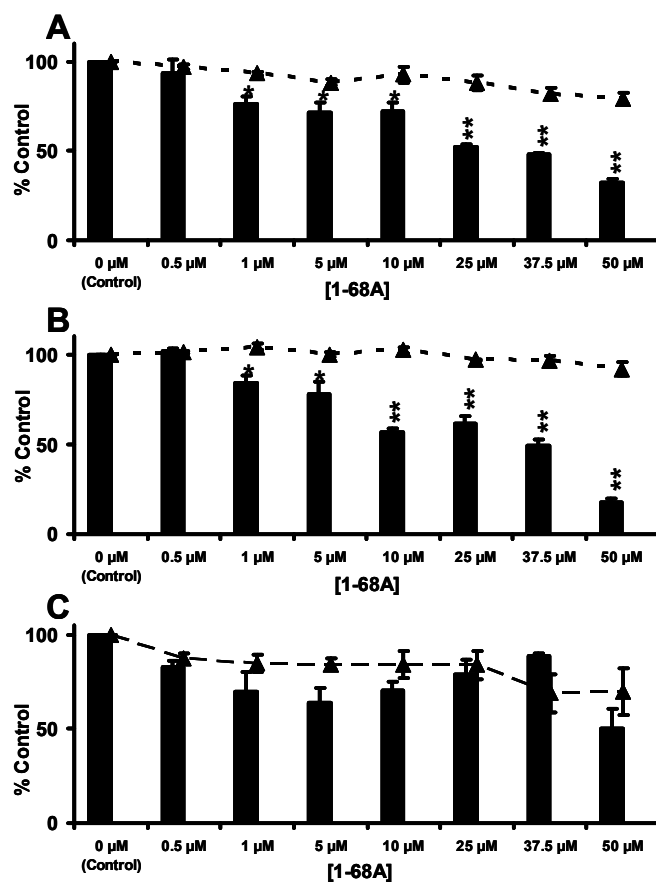
Figure 19. The necessity for O-linked glycosylation for efficient ZEBOVΔO-GP-dependent viral entry into filoviral permissive mammalian cells. A) SNB19 cells, **B)** Vero cells and **C)** Pro5 cells (3 x 10⁴) were treated for 8 h with the indicated concentration of 1-68A. The drug was removed and cells were then transduced with FIV-ZEBOVΔO-GP pseudotyped virus for an additional 16 h after which time, the media was refreshed. All cells were fixed and stained for β-gal activity 48 h post-transduction. Dashed line represents viability. Data represent the means and standard errors of the means from three independent experiments performed in triplicate. *, $p<0.05$; **, $p=0.005$.
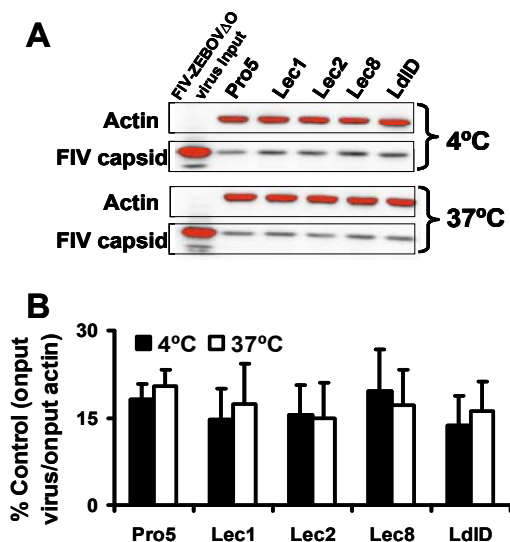
Figure 20. ZEBOVΔO-GP-dependent binding to wild type and mutant CHO cells is equal at 4°C and 37°C. FIV-ZEBOVΔO-GP pseudovirions were applied for 1 h at 4°C or 1 h at 37°C to CHO cells in a 96-well format. After one hour, media was aspirated from the cells, the cells were washed 3X in PBS, and the cells were lysed in 1% SDS, and proteins separated using SDS-PAGE and transferred to a nitrocellulose membrane. FIV capsid was analyzed by incubating sera (1:5,000) from an FIV positive feline overnight at room temperature followed by incubation with appropriate secondary peroxidase-conjugated antisera (1:20,000; Sigma). Actin was detected by incubating primary peroxidase-conjugated antibody (1:10,000) for 3 h at room temperature. Blots were developed with enhanced chemiluminescence, read on a low-light digital camera, and quantified using Image Gauge. The immunoblot shown is representative of all immunoblots assessed during the experiment. Data represent the means and standard errors of the means format least three independent experiments performed in triplicate.

CHAPTER FOUR: ENDOCYTIC MECHANISM(S)
OF ZEBOV-GP-MEDIATED ENTRY INTO
CELLS THAT REQUIRE AXL FOR
OPTIMAL ENTRY

Abstract

The plasma membrane associated Tyro3 receptor kinase family member Axl is necessary for optimal ZEBOV-GP-dependent entry into some permissive cells but not others. The focus of this study was to characterize ZEBOV pseudovirion entry pathways that are used in cells that require Axl for optimal transduction (Axl-dependent cells). Through the use of biochemical inhibitors, RNAi, and dominant-negative constructs, we demonstrate that ZEBOV-GP-dependent entry into Axl-dependent cell populations requires the expression of Axl and occurs through multiple pathways including both clathrin-dependent and caveolae/lipid raft-mediated endocytosis. Surprisingly, both dynamin-dependent and -independent fluid-phase uptake (FPU) pathways mediated ZEBOV-GP entry into the Axl-dependent cells. These data represent the first time a filovirus has been shown to utilize FPU pathways to gain entry into a permissive cell population.

Introduction

To enter cells, EBOV must bind to target cells and internalize into endocytic vesicles [53-55, 100]. Within the endosome, low pH-dependent proteolysis of the viral surface GP (GP1) is required for virion fusion with cellular membranes [54, 55].

The mechanism(s) that mediate filovirus uptake into the endosomal compartment remain controversial. Early reports indicated that the caveolae vesicular system and/or lipid raft domains were important for EBOV-GP-mediated entry [91, 95]. However, another study demonstrated that overexpression of Caveolin 1 in the poorly permissive lymphocytic cell line CEM did not enhance levels of EBOV-GP-dependent transduction suggesting that caveolae may not play a role in filovirus entry [114]. Sanchez reported in a

preliminary study that EBOV enters endosomes through a variety of different uptake mechanisms including caveolae, clathrin-coated pits and through actin- and microtubule-dependent pathways in VeroE6 cells [90]. Recently, a study confirmed that clathrin-mediated endocytosis is indeed utilized by EBOV to gain entry into VeroE6 cells [94].

While the receptor(s) used by filoviruses for productive binding and entry into cells remains to be identified, several proteins have been shown to enhance filoviral entry into cells. One of these proteins is the Tyro3 receptor kinase family member Axl. Axl is important for filoviral transduction of some highly permissive cells such as HeLa cells, but not others such as VeroE6 [115, 160]. Because no direct interaction between Axl and a filoviral GP has been shown, a role for Axl in filoviral entry remains to be elucidated. Recent observations that multiple uptake mechanisms facilitate filoviral entry into the Axl-independent VeroE6 cells led us to explore if multiple mechanisms were also being used by EBOV-GP to enter Axl-dependent cells, including mechanisms such as macropinocytosis and fluid-phase uptake (FPU) which are dependent on actin.

Materials and Methods

Cells lines and antibodies

A human embryonic kidney cell line, 293T (CRL-11268; ATCC), a human glioblastoma line, SNB19 (NCI 0502596) and a human cervical cancer cell line, HeLa (CCL-2; ATCC) were maintained in high-glucose Dulbecco's modified Eagle's medium (DMEM) (Invitrogen) supplemented with 100 units/ml of penicillin and 100 μg/ml streptomycin (1% P/S) and 10% fetal calf serum (FBS) (HyClone). Primary human foreskin fibroblasts (Hffs) isolated from fresh penile foreskin were maintained in DMEM supplemented with 100 units/ml of penicillin and 100 μg/ml streptomycin (1% P/S) and 15% FBS. Primary human umbilical vein macrovascular endothelial cells (HuVECs) isolated from a fresh umbilical cord were maintained in Endothelial Cell Basal Medium (EBM) supplemented with bovine brain extract, hEGF, hydrocortisone, gentamicin, amphotericin B and 5% fetal calf serum (Lonza/Cambrex). All cells were maintained at

37ºC with 5% CO_2. Antibodies used included anti-human Caveolin1 (Cav1) (AbCam), anti-human Caveolin2 (Cav2) (BD Biosciences) and anti-human actin (AbCam).

Plasmids used

Plasmids used to generate the FIV-ZEBOVΔO (Zaire species; mucin domain deleted) and FIV-VSV-G (wild type; Indiana strain) viral particles have been previously described [99, 121]. DN Eps15 expression plasmid was used to disrupt clathrin-mediated endocytosis, whereas a Wt Eps15 expression plasmid served as a control for these studies as previously described [93]. Plasmid encoding ZEBOV matrix protein (VP40) (Entrez gene#NC002549) was kindly provided by Dr. Ronald Harty (University of Pennsylvania). Plasmid encoding the firefly luciferase gene driven by the Rous sarcoma virus promoter [125] has been previously described. Plasmids encoding the full length ZEBOV-GP [99] and the full length Lake Victoria MARV-GP (Musoke variant) [161] have also been described previously.

Drugs and drug studies

All drugs were obtained from Sigma (St. Louis, MO) unless noted. All studies were performed in a 48-well format. Concentrations of drugs are noted in figures. The no-drug control contained the appropriate dilution of vehicle. All cells were fixed and stained for β-gal activity 48 hours after the initial addition of pseudovirions to the cells. The findings are shown as the ratio of the number of transduced cells in the presence of inhibitor divided by the number of transduced cells when no inhibitor was added (% control). In all inhibitor studies, the ability of the inhibitors to decrease pseudovirion transduction was adjusted for cytotoxicity associated with the inhibitor when statistics were calculated.

Chlorpromazine. Chlorpromazine (CPZ) was resuspended in ethanol at 1 mg/ml. CPZ was diluted into the medium (containing FBS) and pre-incubated with cells for 1 hour. Cells were transduced in the presence of the drug, the CPZ-containing inoculum was

removed 6 hours after transduction, and replaced with fresh, chlorpromazine-free medium (DMEM containing 10% FCS and 1% P/S).

Filipin. Filipin (FIL) was resuspended in methanol at 5 mg/ml. Filipin was diluted into DMEM (without FBS) and pre-incubated with cells for 1 hour. The filipin-containing medium was removed and replaced with fresh media (without FBS or filipin) containing ZEBOVΔO-GP or VSV-G-GP pseudotyped pseudovirions. The media was then refreshed with medium 24 hours after the initial addition of pseudovirions.

Blebbistatin. Blebbistatin (BLB) was resuspended in DMSO at 100 mM. BLB was diluted into the medium (containing FBS) and pre-incubated with cells for 1 hour. Cells were transduced in the presence of the drug, and the blebbistatin-containing inoculum was removed 5 hours after ZEBOVΔO-GP or VSV-G-GP pseudotyped FIV transduction, and replaced with fresh medium that did not contain inhibitor.

5-(N-Ethyl-N-isopropyl)amiloride. 5-(N-Ethyl-N-isopropyl)amiloride (EIPA) was resuspended in dimethylsulfoxide (DMSO) at 200 mM. EIPA was diluted into the medium (containing FBS) and pre-incubated with cells for 1 h. Cells were transduced in the presence of the drug, and the EIPA-containing inoculum was removed 5 h after ZEBOVΔO-GP or VSV-G-GP pseudotyped FIV transduction, and refreshed with fresh medium not containing inhibitor.

Cytochalasin B and cytochalasin D. Cytochalasin B (CYTO-B) and cytochalasin D (CYTO-D) were obtained from Calbiochem (EMD) and were each resuspended in DMSO at 25 mM. CYTO-B or CYTO-D was diluted in medium and incubated with cells for 1 h. Cells were transduced in the presence of the drug, and the drug-containing inoculum was removed 5 h after ZEBOVΔO-GP or VSV-G-GP pseudotyped FIV transduction, and refreshed with medium not containing inhibitor.

Dynasore. Dynasore was resuspended at 100 mM in DMSO. The drug was diluted in medium and incubated with cells for 1 h. Cells were transduced in the presence of the drug, and the drug-containing inoculum was removed 5 h after ZEBOVΔO-GP or VSV-

G-GP pseudotyped FIV transduction, and refreshed with medium not containing inhibitor.

<u>Filipin and cytochalasin B.</u> Cells were first treated with FIL (1μg/ml) diluted into medium (without FBS) for 1 hour. The FIL-containing medium was removed and replaced with fresh media (without FBS) (for FIL treated cells) or with media without FBS but containing CYTO-B (1μM) (for FIL/CYTO-B treated cells). All cells were transduced (in the presence of the drug if applicable) for 5 h. All media on all cells containing inoculum was removed 5 h after transduction, and replaced with media lacking FBS. 24 h after the initial addition of pseudovirions, the media was replaced with fresh media (DMEM++).

Detection and analysis of labeled conjugate uptake

All conjugates were purchased from Invitrogen. Dextran (70 kDa conjugated to FITC) and dextran (2,000 kDa conjugated to Cy5) were resuspended in sterile H_2O at 10 mg/ml. Human transferrin (Tfn) and cholera toxin subunit B (CTb) conjugated to AlexaFluor 647 were resuspended in sterile H_2O at a concentration of 5 mg/ml and 1 mg/ml, respectively. For drug studies with dextran, Tfr or CTb, cells were pretreated with drug alone for 1 h followed by addition of the labeled conjugate for an additional hour in the presence of drug. Cells were washed 3X in sterile PBS and lifted with Accumax (Fisher) for analysis by flow cytometry on a FACScan cytometer (BD Biosciences) using FL-1 (dextrans) or FL-4 (Tfr and CTb) channels.

Detection and analysis of surface Axl

10^6 cells were lifted using 5 mM EDTA. Cells were washed three times in PBS with 5% FBS before a 1 h incubation with a 1:100 dilution of goat sera or a 1:100 dilution of goat anti-human Axl antibodies. Cells were then washed 3 times in PBS with 5% FBS and a 1:50 dilution of Cy5-labeled donkey anti-goat secondary was incubated with the cells for 15 min. The cells were then washed 3 times again in PBS with 5% FBS and analyzed by flow cytometry for expression in the FL-4 channel.

Axl antibody entry inhibition studies

These studies were performed in a 48-well format using 4×10^4 cells per well. A 1:50 dilution of goat anti-human Axl antisera or normal goat sera was incubated in DMEM with 10% FBS and 1% P/S for 1 hour at 4ºC with cells. After 1 hour, VSVΔG pseudovirions bearing either ZEBOVΔO-GP, full length ZEBOV-GP or Lake Victoria MARV-GP were added to the cells in the presence of antisera. The cells were then shifted to 37ºC with 5% CO_2 for an additional 23 hours at which time they were lifted in Accumax and analyzed with a FACScan cytometer (BD Biosciences) for FL-1 intensity.

Immunoblotting

Cells were lysed and proteins separated using SDS-PAGE as described previously [121]. Cav1, Cav2 and Axl were detected by incubating with primary antibodies (1:1000, 1:250 and 1:4,000, respectively) overnight at 4ºC followed by incubation with appropriate secondary peroxidase-conjugated antisera (1:20,000; Sigma). Actin was detected by incubating primary peroxidase-conjugated antibody (1:10,000) for 3 h at room temperature. Membranes were visualized by the chemiluminescence method according to the manufacturer's protocol (Pierce).

Generation of and detection of pseudovirions

and virus like particles (VLPs)

FIV pseudovirions were generated in 293T cells as previously described [113, 121, 162]. All pseudovirions were concentrated using a 16-h centrifugation step at 7,000 rpm at 4°C in a Sorvall GSA rotor. The viral pellet was resuspended in 250 µl DMEM for an approximately 200-fold concentration prior to use. All FIV pseudovirions expressed the reporter β-galactosidase (β-gal) upon delivery into the recipient cell. FIV transduction studies were performed in a 48 well format using a MOI of ~0.005 (resulting in approximately 200 β-gal positive cells/40,000 cells/well in control wells). FIV pseudovirion transduction was detected by fixing cells in 3.7% formalin and evaluating for β-gal activity using the substrate 5-bromo-4-chloro-3-indolyl-β-D-galactopyranoside.

All FIV transduction evaluation was done 48 h after initial FIV pseudovirion addition to cells. The number of β-gal-positive cells was enumerated by microscopic visual inspection.

VSVΔG/EGFP pseudovirions (a kind gift of Michael Whitt, University of Tennessee Health Sciences) bearing ZEBOVΔO-GP or VSV-G (wild type; Indiana strain) were generated in 293T cells as previously described [124]. For detection of VSVΔG/EGFP pseudovirion transduction, 24 h following transduction, cells were lifted in Accumax (Fisher) and analyzed with a FACScan cytometer (BD Biosciences) for FL-1 intensity. VSVΔG pseudovirions were applied to cells to yield approximately 1,000 GFP positive cells for every 20,000 cells analyzed by flow cytometry. This gives an MOI of approximately 0.05 for all studies using the VSVΔG system.

ZEBOV-VLPs were generated in 293T cells by transfection of 75 μg total of a 1:1:1 ratio of ZEBOVΔO-GP, ZEBOV VP-40 and firefly luciferase expressing plasmids using a standard calcium phosphate transfection protocol. The luciferase protein expressed in the transfected cell was non-specifically incorporated into VLPs. VLPs in the cell supernatant were collected every 12 h from 36 to 72 hours. VLPs were concentrated as stated above for FIV pseudovirion particles. Equivalent amounts of VLPs were added to all virus treated cells in each experiment. Seven hours following infection, cells were washed to remove unbound particles and lysed in equal parts sterile PBS and SteadyGlo (Promega), and assayed for luminescence per the manufacturer's protocol.

Because there is some variation in absolute numbers of on-put virions used between different experiments and all experiments shown are a compilation of at least three different experiments, the control findings were set to 100% and the results shown are represented as % control rather than absolute transduction values.

RNAi

0.75 x 10^6 SNB19s were transfected with 200 pmol of a mixture of small interfering RNA (siRNA) against Cav1 (Invitrogen #15299372), Cav2 (Invitrogen #16495103) in a 6 well format. 2 x 10^6 SNB19 cells were transfected with 500 pmol of human Axl (two Axl validated RNAi constructs; Invitrogen) in a T25 tissue culture flask. Appropriate concentrations of control fluorescently labeled nonspecific siRNA (Block-It; Invitrogen) were transfected as a control. All transfection were performed using the Lipofectamine 2000 (Invitrogen) protocol. Transfected cell populations were plated in a 48-well format at 24 h post RNAi transfection. At 48 h following transfection, cells were transduced with FIV pseudovirions, used for dextran uptake studies or harvested for immunoblotting analysis.

Infectious ZEBOV studies

Twenty-four hours after siRNA transfection, cells were split into a 96-well plate at a concentration of 10^4 cells per well. Twenty-four hours later, cells were pretreated with EIPA, CYTO-B or DMSO control at indicated concentration. After 1 hour, Zaire ebolavirus encoding GFP (kind gift of Dr. J. Towner, CDC) was added to cells at an MOI of 0.25. After 18 hours, the culture medium was replaced with fresh medium without drugs. After an additional 6 hours the media was removed and cells were fixed in formalin for 48 hours. Infected cells were then analyzed for GFP positivity (compared to number of cell nuclei stained with DAPI) to generate a "proportion of infected cells" calculation. All experiments with ZEBOV were performed under biosafety level 4 conditions in the Robert E. Shope BSL-4 Laboratory, UTMB.

Cell transfection with Eps15 constructs

10^6 SNB19s were transfected with 5μg of either wtEps15 or DNEps15 expression plasmids using 100μl Amaxa solution T and program L-029 on the Amaxa nucleotransfection device. Transfected cells were distributed into 12 wells of a 48-well

plate. Cells were transduced with FIV-ZEBOV or FIV-VSV-G pseudovirions 24 h after plasmid transfection.

Adenovirus DN dynamin studies

3×10^4 SNB19s were plated in a 48-well format. Ad vectors expressing GFP or DN dyn 2 (K44A) (a gift from Jeff Pessin, SUNY-Stony Brook) were incubated with the cells for 24 h [163]. Ad vector transduction efficiency was determined by the percentage of cells expressing GFP, which was greater than 95%. Cells were transduced with FIV-ZEBOV or FIV-VSV-G 24 h after Ad transduction.

Cell viability assay

At the time of FIV pseudovirion transduction evaluation, cell viability was monitored in an ATP-Lite assay (Packard Biosciences) as per the manufacturer's instructions.

Statistical analysis

Statistical analyses were conducted by Student's t test, utilizing the two-tailed distribution and two-sample equal-variance conditions. P values were assessed by comparing the level of transduction with treatment to the level of cytotoxicity observed with that specific treatment. A significant difference was determined by a P value of <0.05. If the P value was >0.05, the data were not considered significant.

Results

Axl is crucial for efficient infectious Zaire ebolavirus (ZEBOV) and ZEBOV-GP-dependent pseudovirion entry into some cells

We first determined the necessity of Axl expression for ZEBOV infection into the highly permissive human glioblastoma cell line, SNB19 cells. SNB19 cells served as a principal model cell line for these studies because these neuroblastoma cells were found to be the most highly ZEBOV-GP pseudovirion transducible line from the NCI-60 panel of human tumor lines. Further, these cells expressed large quantities of Axl on their

surface (**Fig. 21**) and the cells were readily transfectable. These cells were transfected

with 200 pmol of non-specific RNAi or RNAi specific for Axl. Cell lysates were

assessed by western blot for Axl expression demonstrating efficient knock down of Axl

by Axl RNAi, but not by an irrelevant RNAi (**Fig. 22*B***). At 48 hours following

transfection, these RNAi-transfected cells were infected with ZEBOV expressing EGPF

(**Fig. 22*A***). The loss of Axl reduced ZEBOV infectivity by 80% demonstrating for the

first time the importance of endogenous Axl expression for filovirus infection. We also

observed that mucin domain deleted ZEBOV-GP pseudotyped FIV (FIV-ZEBOVΔO)

transduction was decreased into SNB19 cells (**Fig. 22*C***) when cells were treated with Axl

RNAi (**Fig. 22*D***). These latter findings indicate that our FIV-ZEBOV transduction

studies can serve to model ZEBOV infection mechanisms in a BSL2 setting. To further

validate our ZEBOV pseudovirion transduction system, we tested the ability of

polyclonal anti-Axl antisera to block entry of mucin domain-containing ZEBOV-GP and

Lake Victoria MARV-GP pseudotyped vesicular stomatitis virus (VSV-ZEBOV or VSV-

MARV) pseudovirions into SNB19 cells (**Fig. 23*A***). The Axl antibody was able to

significantly reduce transduction of these viral particles as well as VSV-ZEBOVΔO entry

in HeLa cells (**Fig. 23*B***), a cell line previously shown to be Axl-dependent for filoviral

entry [115]. Two additional cell populations were identified to express abundant levels of

Axl on their plasma membranes (**Fig. 21**). FIV-ZEBOVΔO transduction of both of the

primary human cell populations, foreskin fibroblasts (Hffs) and umbilical vein

endothelial cells (HuVECs), was found to be Axl-dependent,[160]. In total, these data

clearly demonstrate a significant role for Axl during filoviral infection of these cells, and

indicate that the pseudovirion transduction system can serve to model infectious ZEBOV

entry events.

Clathrin-mediated endocytosis is utilized
by ZEBOV-GP pseudovirions for entry
into Axl-dependent cells

The current body of evidence suggests that both clathrin and caveolae/lipid raft-dependent endocytosis mediate ZEBOV-GP entry into cells. However, mechanism-of-entry studies have only been performed in cell populations that do not require the tyrosine kinase receptor Axl for efficient transduction [90]. As Axl-dependent cells include some clinically relevant, primary endothelial human cells (Hffs and HuVECs) and a number of cell lines that are routinely used in EBOV-GP studies (SNB19 and HeLa cells) [115, 116, 160], we sought to fill this knowledge gap. Two cell populations (SNB19 and primary Hffs), that are both easily transducible with ZEBOV-GP pseudovirions were used in this study.

To determine if clathrin coated pits mediated ZEBOV-GP entry in Axl-dependent cells, SNB19s were treated with increasing concentrations of chlorpromazine (CPZ). CPZ has been used extensively to evaluate the role of clathrin coated pits in receptor-mediated uptake as it prevents clathrin-mediated endocytosis by redirecting clathrin adapter proteins from plasma membrane proteins to internal membranes [164]. Treated and untreated cells were transduced with FIV particles pseudotyped with either ZEBOV-GP (FIV-ZEBOVΔO-GP) or the vesicular stomatitis G (FIV-VSV-G-GP). The effect of CPZ (and all treatments used in these studies) on cell viability was evaluated in parallel. FIV-ZEBOVΔO-GP transduction was inhibited in a dose dependent manner by CPZ with little detectable toxicity (**Fig. 24A**). Because VSV-G-dependent transduction of other cell lines has been reported to be clathrin-dependent [129, 165, 166], FIV-VSV-G-GP was used as a control for this experiment. As expected, FIV-VSV-G-GP was also inhibited by 5µg/ml of CPZ. The FIV pseudovirion transduction studies in the presence of CPZ were also carried out in Hffs with similar findings **(Fig. 26A).** Uptake of fluorescent transferrin (Tfr) and cholera toxin subunit B (CTb) were also evaluated in these studies as Tfr is a marker of uptake via clathrin coated pits, whereas CTb is commonly used as a marker of

uptake via caveolin/lipid raft mediated endocytosis [167]. CPZ did not affect uptake of CTb, but decreased uptake of Tfr, indicating that CPZ was indeed affecting clathrin-mediated endocytic events (**Fig. 24***A*). These initial studies suggested that clathrin-dependent mechanisms are important for ZEBOV-GP-mediated entry into Axl-dependent SNB19 and Hff cells.

The biochemical finding that ZEBOV-GP-dependent entry into SNB19s was blocked by inhibition of clathrin coated pit formation was independently verified via ectopic expression of the dominant negative (DN) form of the clathrin-associated protein Eps15. Eps15 serves as a protein bridge between the cargo being internalized and the clathrin coat [167]. pDN-Eps15Δ95-295-GFP (DNEps15) inhibits clathrin-mediated uptake because it lacks the Eps homology domains necessary for clathrin coated pit targeting, whereas pEps15Δ3Δ2-GFP expresses wild type Eps15 (wtEps15) [93]. Transfected cells were transduced 24 h later with FIV-ZEBOV or FIV-VSV-G. Both FIV-ZEBOVΔO-GP and FIV-VSV-G-GP transduction was decreased by 40-60% of control levels in cell populations expressing the DNEps15 construct, but not by expression of wtEps15 (**Fig. 24***B*). SNB19s expressing the DNEps15 construct also showed a significant decreased ability to take up Tfr, but not CTb, indicating that the expression of DNEps15 was specifically inhibiting clathrin-mediated endocytosis in these cells. These results support our findings with CPZ that ZEBOV-GP-dependent entry utilizes clathrin-mediated endocytosis as a mechanism of entry into SNB19s.

Cholesterol is important for efficient
ZEBOV-GP pseudovirion entry into
Axl-dependent cells

Cholesterol is a principal component of plasma membrane lipid rafts [168]. While lipid raft-associated endocytosis has been primarily linked to caveolae-dependent uptake [168], recent studies have found that clathrin-dependent endocytosis can also be associated with lipid rafts [100]. To determine the role of host plasma membrane cholesterol in

ZEBOV-GP-mediated entry, cells were treated with the drug filipin (FIL) to bind to cholesterol and disrupt lipid rafts [169]. FIL treatment did not inhibit the entry of FIV-VSV-G-GP but decreased transduction of FIV-ZEBOVΔO-GP by ~40% (**Fig. 25***A*). A similar partial reduction in ZEBOV-GP-mediated entry in the presence of FIL was also seen in Hffs (**Fig. 26***B*). FIL inhibited CTb uptake, but not Tfr uptake, indicating that the FIL drug was specifically acting on an endocytic pathway involving membrane cholesterol and lipid rafts (**Fig. 25***A*). Our findings are consistent with recently published results demonstrating that ZEBOV-GP-dependent entry is blocked by treatment of SNB19s with the cholesterol sequestering drug methyl-beta-cyclodextrin [93]. These results indicate that plasma membrane cholesterol and lipid rafts are important for efficient ZEBOV-GP-mediated entry into these cells.

Caveolin is involved in ZEBOV-GP pseudovirion
entry into Axl-dependent cells

The inhibition of ZEBOV-GP-mediated entry by loss of plasma membrane cholesterol suggested that caveolae might be involved in ZEBOV-GP entry into Axl-dependent cells. Caveolae dependence of ZEBOV-GP-mediated uptake has been previously proposed [91, 95], but also refuted [114]. To directly test the role of caveolae in ZEBOV-GP-mediated entry, a combination of RNAi specific for human Caveolin1 (Cav1) and Caveolin2 (Cav2) or a non-specific RNAi control (Block-It) were transfected into SNB19s. 48 h after transfection, the efficacy of the RNAi-specific Cav1/2 protein knockdown was determined in a portion of the cells (**Fig. 25***C*), and the remaining cells were transduced with FIV-ZEBOVΔO-GP or FIV-VSV-G-GP. The decrease in Cav1/2 had no effect on VSV-G-GP-dependent transduction, but significantly reduced FIV-ZEBOVΔO-GP transduction by ~50% (**Fig. 25***B*). These results were confirmed in Hffs (**Fig. 26***C* **and 26***D*). Taken together, these findings implicate the use of both clathrin and caveolin pathways by ZEBOV-GP for entry into the Axl-dependent cells.

Dynamin is necessary for efficient ZEBOV-GP

pseudovirion entry into Axl-dependent cells

Because both clathrin and lipid raft/caveolin endocytic vesicles require the host cell GTPase dynamin, we sought to confirm that dynamin was indeed needed for FIV-ZEBOVΔO-GP entry into Axl-dependent cells. SNB19s were transduced with adenovirus (Ad) particles that express GFP or a dominant-negative form of dynamin 2 (DNdyn2 (K44A)), as dynamin 2 is ubiquitously expressed in cells [170]. At 24 h following Ad transduction, cells were transduced with FIV-ZEBOVΔO-GP or FIV-VSV-G-GP. VSV-G-GP-dependent entry has been shown to be dynamin-dependent into numerous cell types [129, 165, 166]. ZEBOVΔO-GP- and VSV-G-GP-mediated entry in SNB19s was inhibited by expression of DNdyn2 with a loss of 90-95% of transduction (**Fig. 27A**). These results were confirmed in Hffs (**Fig. 28A**) and another Axl-dependent cell population, primary HuVECs (**Fig. 28B**). The pan-dynamin inhibitor Dynasore was also evaluated to verify the importance of dynamin for ZEBOVΔO-GP transduction. This inhibitor significantly reduced both ZEBOVΔO-GP and VSV-G-GP-mediated entry into SNB19s at all concentrations tested (**Fig. 27B**). As a control, treatment of cells with Dynasore also significantly reduced the uptake of labeled Tfr, indicating the involvement of host dynamins in receptor-mediated endocytic events (**Fig. 27B**).

Dynamin 2 has been reported to not only be involved in receptor-mediated endocytosis, but to be necessary for micropinocytosis [88]. Micropinocytosis in one of a number of fluid-phase uptake (FPU) mechanisms that have been characterized [167], but is the only FPU pathway that has been described to require dynamin [88]. To investigate the role of dynamin-dependent FPU of Axl-dependent SNB19s, we analyzed uptake of FITC-labeled dextran in our untreated cells or cells transduced with either a GFP-expressing or DNdyn2-expressing Ad vector. Dextran uptake has been used extensively to study FPU pathways including micro- and macropinocytosis [171]. We observed that uptake of dextran was decreased by 20 to 40% in the presence of DNdyn or Dynasore suggesting that a

portion of FPU in SNB19s was indeed dynamin dependent (**Fig. 27A and 27B**). These results were confirmed in Hffs (**Fig. 28C**) using two high molecular weight dextrans and suggest that micropinocytosis is active in the Axl-dependent cells tested. To test if ZEBOVΔO-GP-mediated entry could be occurring by micropinocytosis, or other mechanisms of FPU, such as macropinocytosis, we tested if FPU was utilized by ZEBOVΔO-GP as a route of entry into Axl-dependent cells.

Inhibitors of FPU decrease ZEBOV-GP
pseudovirion and infectious ZEBOV uptake
into Axl-dependent cells

Initial studies to evaluate the role of FPU pathways in ZEBOV-GP-dependent entry investigated FIV-ZEBOVΔO-GP transduction in the presence of various drugs that inhibit FPU. The amiloride analog EIPA inhibits the Na+/H+ exchanger that in turn prevents the normal cellular trafficking of endosomal vesicles related to fluid phase uptake. EIPA thus blocks the formation of macropinosomes but does not affect other endocytic pathways [171]. BLB has also been shown to indirectly inhibit the formation of myosin II independent processes such as macropinocytosis and has been used extensively as an inhibitor of FPU pathways [171]. CYTO-B and CYTO-D inhibit microfilament formation as well as actin polymerization [172]. As active actin polymerization is required for FPU [171], these inhibitors block FPU. We first confirmed the ability of these drugs to inhibit FPU in Axl-dependent cells, by determining the ability of the drugs to decrease uptake of dextran. As expected, each drug significantly reduced dextran uptake in SNB19s (**Fig. 29**). As a negative control, the uptake of Tfr and CTb in the presence of the FPU inhibitors was also assessed and found to not be significantly increased or decreased by the drugs tested (**Fig. 29**), demonstrating the specificity of these inhibitors for FPU.

We next evaluated if the drugs inhibited ZEBOVΔO-GP-mediated transduction in Axl-dependent cells. Because VSV-G-GP-mediated entry has only been shown to occur

via clathrin-mediated endocytosis, it was used as a negative control in these studies. Despite the cytotoxicity associated with CYTO-D, all FPU inhibitors tested significantly decreased FIV-ZEBOVΔO-GP but not FIV-VSV-G-GP transduction in SNB19s (**Fig. 30A-D**) and Hffs (**Fig. 31A-C**) in a dose dependent manner when adjusted for inhibitor-associated cytotoxicity. We also confirmed the ability of CYTO-B and EIPA to inhibit entry of VSVΔG pseudovirions bearing ZEBOVΔO-GP in another Axl-dependent cell population, HeLa cells (**Fig. 31D**). We then went on to test the ability of the FPU inhibitors to decrease entry of FIV pseudovirions bearing full length filoviral-GPs in SNB19 cells. As expected, we observed a significant decrease in full length filoviral-GP-mediated entry with all of the FPU inhibitors tested (**Fig. 31E**). These levels of pseudovirion entry inhibition observed with the full-length filoviral-GPs were similar to those observed for FIV-ZEBOVΔO-GP pseudovirions, confirming our previous findings.

To confirm that the FPU inhibitors were blocking filovirus entry events, we tested the ability of these drugs to inhibit entry of infectious ZEBOV. We confirmed the reduction in ZEBOV-GP-mediated entry in SNB19s by the two FPU inhibitors most effective at decreasing FIV-ZEBOV-GP (**Fig. 32A-B**). Together, these data strongly indicate that the FPU inhibitors affect ZEBOV-GP-mediated cell entry rather subsequent steps such as intracellular trafficking and confirm that ZEBOV entry can be mediated through one or more FPU mechanisms into Axl-dependent cells.

Finally, we tested the ability of FPU inhibitors to inhibit ZEBOVΔO VLP entry into SNB19 cells. VLPs composed of ZEBOV VP40 and GP have the same size and morphology as wild-type (infectious) filoviruses [100]. Our VLPs nonspecifically contained luciferase that was expressed in the producer cell line and incorporated into the VLPs. In the target cell, fusion of VLP membranes with endocytic membranes released luciferase allowing detection of this reporter protein following membrane fusion events [173]. Three out of four of the FPU inhibitors significantly decreased luciferase activity following

addition of VLPs to SNB19 cells (**Fig. 32*C***), confirming that FPU is involved in early filoviral-GP-mediated entry events in Axl-dependent cells.

<div align="center">

Simultaneous disruption of membrane cholesterol

and restriction of the actin cytoskeleton additively

disrupt ZEBOV-GP mediated entry into

Axl-dependent cells

</div>

From our studies thus far using inhibitors that target different uptake pathways, we concluded that multiple mechanisms of uptake are used by ZEBOV to enter these cells. To determine if mechanisms of FPU were truly independent of the receptor mediated mechanism, we assessed a combination of a FPU inhibitor with either an inhibitor of clathrin dependent or lipid raft dependent endocytosis. In these studies, concentrations of drugs used gave 20 to 40% since we wanted to assess if the combinations provided additional inhibition.

A combination of FIL and CYTO-D treatments were evaluated on both FIV-ZEBOVΔO-GP and FIV-VSV-G-GP-mediated entry**.**   The disruption of membrane cholesterol and the simultaneous disruption of the actin cytoskeleton in SNB19 cells (**Fig. 33*A***) and Hffs (**Fig. 33*B***) reduced ZEBOVΔO-GP-mediated entry in what appeared to be an additive manner, although the reduction was not statistically significant in Hffs. This finding suggests that EBOV-GP uptake mechanisms involving membrane cholesterol and actin polymerization are independent of each other and can act concurrently to reduce ZEBOVΔO-GP pseudotyped virion uptake.

VSV-G-GP-mediated entry in SNB19s was not significantly affected by the addition of the concentrations of FIL and CYTO-D alone used in this portion of the study. However, FIL and CYTO-D together were able to reduce VSV-G-GP-mediated entry into Hffs. These effects were additive, and the addition of FIL and CYTO-D significantly reduced VSV-G-GP-dependent entry compared to either drug alone (**Fig. 33*B***).

Discussion

These studies were initiated to identify uptake pathway(s) used by ZEBOV for entry into Axl-dependent cells. We demonstrate that ZEBOV entry occurs through multiple mechanisms including clathrin-and caveolae-mediated endocytosis as well as FPU pathways. Previous studies in cells that do not require Axl for optimal EBOV transduction have shown that both clathrin-and caveolae-mediated endocytosis are used for filovirus entry [72, 90, 91, 94]. However, a preliminary report in Vero cells suggested that a FPU inhibitor had no effect on ZEBOV infectivity providing evidence that FPU may not be important for EBOV entry into Axl-independent cell lines [90]. As this study clearly demonstrates that FPU is important for EBOV transduction into the Axl-dependent cells that were tested, this finding suggests the intriguing possibility that FPU mechanisms may only be important for EBOV entry in Axl-dependent cells.

Many of the inhibitors tested partially inhibited ZEBOV entry, reducing virus uptake by 25-75%. Incomplete abrogation of ZEBOV entry with any single inhibitor suggests that multiple, independent mechanisms of uptake are used by ZEBOV-GP. Additionally, previous studies have demonstrated that inhibition of one uptake pathway enhances uptake activity through other pathways [174]. This compensation mechanism is likely occurring and can help explain the moderate levels of inhibition observed in many of these studies.

While this study focuses on entry events associated with filoviral-GPs, parallel studies were performed using VSV-G-GP pseudovirions to allow comparison. VSV-G-GP dependent entry mechanisms have been previously investigated and it is widely accepted that VSV-G-GP-mediates entry into a variety of cells via clathrin-mediated endocytic pathways [129, 165, 166]. Pseudovirions bearing VSV-G-GP behaved as expected during clathrin-mediated endocytic inhibition experiments in SNB19s (**Fig. 24**). However, VSV-G-GP-mediated entry into the Axl-dependent primary cell population Hffs was completely unaffected by CPZ, a common and potent inhibitor of clathrin-

mediated endocytic events (**Fig. 26***A*). Interestingly, the expression of a dominant-negative form of the small GTPase dynamin2 in Hffs also had no effect on VSV-G-GP-mediated entry (**Fig. 28***A*). Because clathrin-mediated endocytosis as well as other receptor-mediated endocytic events and micropinocytosis are dependent upon dynamin2, this data suggests, that in Hffs, VSV-G-GP-mediated entry occurs through a clathrin and dynamin 2 independent pathway, such as macropinocytosis. Consistent with our findings, Bhattacharyya et al recently demonstrated in HOS cells that VSV-G-GP dependent entry was independent of clathrin coated pits [94]. While only one of our FPU inhibiting drugs had a significant disruptive effect on VSV-G-GP-mediated entry into Hffs (BLB; **Fig. 31***B*), it has been suggested that VSV-G-GP is capable of mediating entry into other cells via macropinocytosis [124].

It is widely accepted that filoviruses likely rely on specific receptor binding to facilitate entry via endocytosis to enter permissive cells [100]. Although it has not yet been determined if Axl serves as a receptor for EBOV-GP [115, 116, 160], or if Axl and EBOV-GP directly interact, it does appear that receptor-mediated endocytosis is at least partially responsible for EBOV-GP mediated entry in Axl-dependent cells. However, EBOV-GP is clearly capable of facilitating entry through a non-receptor mediated (and arguably less specific) endocytic pathway. Therefore, it is possible in Axl-dependent cells that Axl is not acting as a receptor (binding to and mediating endocytosis of an EBOV-GP bearing virion), but is instead acting as a signaling molecule within these cells.

Receptor-mediated clathrin and caveolae endocytic events are generally thought to be limited, in part, by the size of their respective endocytic vesicles, as clathrin vesicles have an average diameter of ~120 nm and caveolae vesicles have a diameter of ~60-80 nm [87]. The length of filoviral particles (800-1400nm) could potentially hinder ZEBOV from utilizing these uptake mechanisms. However, others have shown that both of these pathways are important for ZEBOV infection of Vero cells [90, 94]. In addition, size constraint of the cargo is not an issue for many FPU pathways. For instance,

macropinocytosis can facilitate uptake of particles larger than 1µm in size [53]. Vesicles generated by these uptake pathways also have the ability to become acidified and interact with endocytic vesicles [74] and therefore could fulfill the requirement of a low pH step that is essential for filovirus entry. To date, several other viruses have been shown to utilize FPU mechanisms to enter host cells, including vaccinia virus and HIV-1 [171]. The evidence presented here in Axl dependent cells allows the addition of ZEBOV to that list.
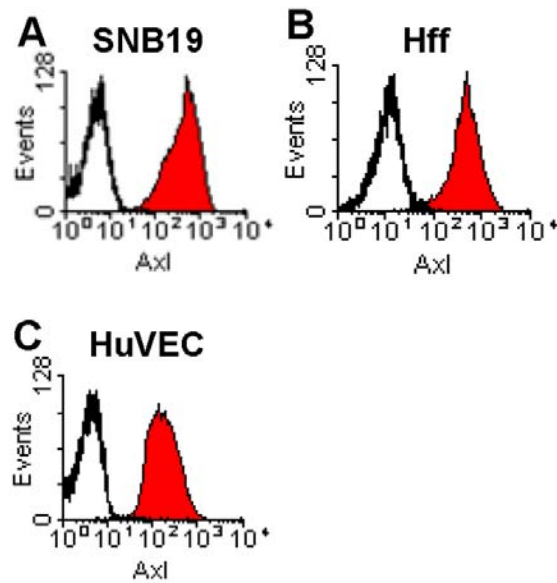
Figure 21. Axl surface expression profiles. A) SNB19s, **B)** Hffs and **C)** HuVECs were lifted and incubated with a 1:50 dilution of normal goat sera or goat anti-human Axl antisera at 4°C followed by a 1:100 dilution of Cy5-donkey anti-goat secondary. Cells were analyzed by flow cytometry in the FL-4 channel. Open histograms show staining with normal goat sera and shaded histograms represent staining with Axl antisera. The profiles shown are representative of three experiments preformed independently.
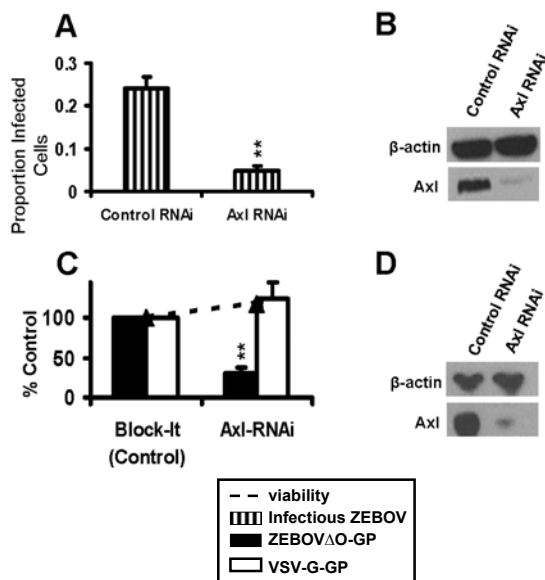
Figure 22. Axl is necessary for efficient infectious Zaire ebolavirus infection and FIV-ZEBOV-GP-dependent transduction into Axl-dependent cells. A and C) Effect of Axl RNAi on ZEBOV infection or transduction. SNB19s were transfected with 200 pmol of a non-specific luciferase siRNA control (A), 200 pmol of a non-specific siRNA control (Block-it) (C), or 200 pmol of a human Axl-specific siRNA (A and C). At 48 h following RNAi transfection, cells were infected with ZEBOV (A; MOI=0.25) for 24 hours or transduced with FIV pseudovirions for 48 hours (C; MOI=0.005). At 24 hours following infection, cells were fixed and analyzed by microscopy for GFP positivity relative to the number of cells for each condition (A), or at 48 h following transduction, cells were fixed and stained for β-gal activity (C). **B and D)** Knock down of Axl by RNAi. 48 h after RNAi transfection, a portion of the transfected cells were lysed and proteins were separated using SDS-PAGE and Axl was detected on the nitrocellulose membrane with primary antibody (1:4,000) overnight at 4ºC. The signal was detected by incubating with secondary horseradish peroxidase (HRP)-conjugated antiserum (1:20,000) for 1 h at room temperature followed by visualization by chemiluminescence. Actin was detected by incubating primary HRP-conjugated antibody. The immunoblots shown are representative of three experiments performed independently. Data represent the averages and standard errors of three experiments performed in triplicate. **, *P* <0.001.
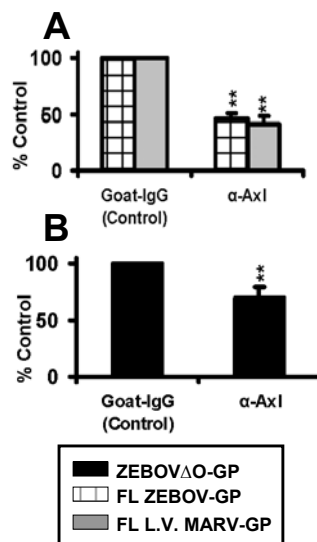
Figure 23. Axl is necessary for efficient filoviral-GP-dependent transduction of Axl-dependent cells. Ability of Axl antisera to block transduction of FIV-ZEBOV-GP (full length and ΔO form) or FIV-Lake Victoria MARV-GP. **A)** A 1:50 dilution of anti-human Axl antisera or normal goat sera was incubated with SNB19 cells for 1 hour at 4ºC. VSVΔG pseudovirions (MOI=0.05) bearing full length ZEBOV-GP or Lake Victoria MARV-GP were applied in the presence of antisera and incubated for an additional 23 hours. Cells were lifted and analyzed by flow cytometry for GFP positivity, indicating viral transduction. **B)** HeLa cells were treated for 1 h at 4ºC with a 1:50 dilution of anti-human Axl antisera or a 1:50 dilution of goat-IgG control sera. After 1 h, VSVΔG pseudovirions bearing ZEBOVΔO-GP were added to the cells in the presence of antisera. Pseudovirion transduction was assessed 23 h later by lifting the cells with Accumax and analyzing EGFP by flow cytometry. Data represent the averages and standard errors of three experiments performed in triplicate. ******, *P* <0.001.
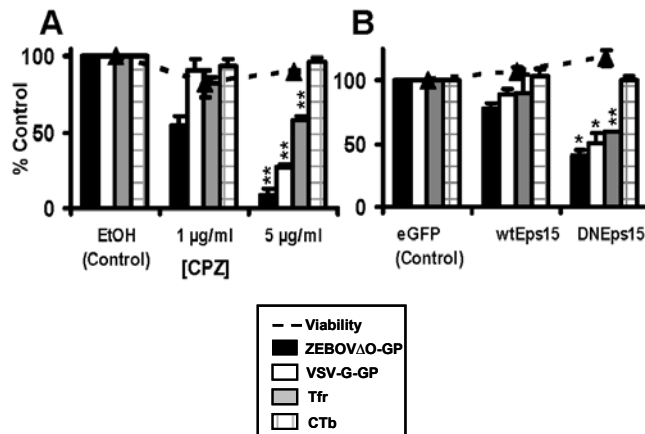
Figure 24. Clathrin-mediated endocytic pathways facilitate FIV-ZEBOV transduction of Axl-dependent cells. A) Ability of CPZ to inhibit FIV-ZEBOV transduction. SNB19 cells were pretreated with the indicated amount of CPZ for 1h. Treated cells were incubated with Cy5-Tfr (20μg/ml final), Cy5-CTb (10 μg/ml final) or FIV pseudovirions (MOI=0.005) in the continued presence of CPZ. Tfr or CTb treated cells were washed after 1 h and analyzed by flow cytometry for uptake of Tfr or CTb. The media on cells transduced with FIV-ZEBOV or FIV-VSV-G was refreshed after 6 h with media not containing CPZ and transduced cells were fixed and stained for β-gal activity 48 h following transduction. **B)** Ability of DN Eps15 to inhibit FIV-ZEBOVΔO transduction. SNB19s were transfected with plasmid DNA expressing EGFP, wild type Eps15-GFP (wtEps15) or dominant-negative Eps-GFP (DNEps15). The transfection efficiency of SNB19s was evaluated at 24 hours by analyzing GFP expression in the cells by flow cytometry, and was found to be between 50 and 60%. Transfected cells were transduced with FIV pseudovirions (MOI=0.005) at 24 h following transfection and maintained in media. After 48 h, cells were fixed and stained for β-gal activity. Alternatively, transfected cells were incubated for 1 h with Cy5-labeled Tfr or CTb, washed and cells were analyzed by flow cytometry for uptake of Tfr and CTb. Data represent the averages and standard errors of three experiments performed in triplicate. *, $P <0.05$; **, $P <0.001$.
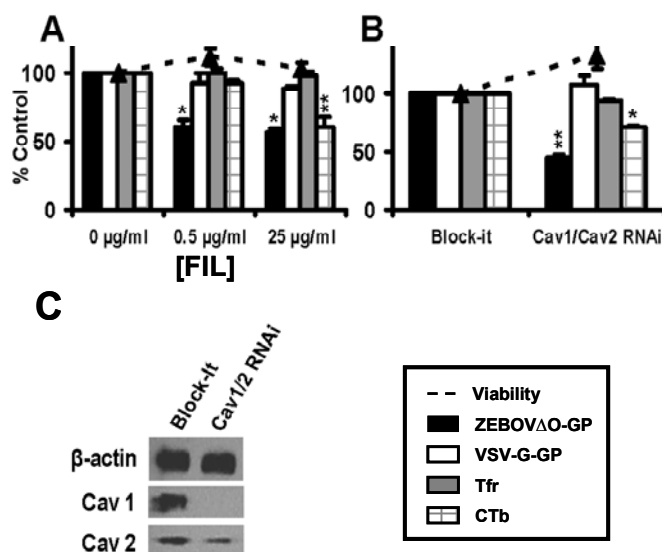
Figure 25. Caveolin/cholesterol-mediated endocytic pathways facilitate FIV-ZEBOV transduction of Axl-dependent cells. A) Ability of FIL to inhibit ZEBOVΔO transduction. Cells were pretreated with the indicated amount of FIL for 1 h. After 1 h, cells were incubated with Cy5-labeled Tfr, CTb or FIV pseudovirions (MOI=0.005) in media without serum but containing drug. Tfr or CTb treated cells were washed after 1 h and analyzed by flow cytometry for uptake of Tfr or CTb. The media on cells transduced with FIV-ZEBOVΔO-GP or FIV-VSV-G-GP was refreshed after 6 h with media containing serum without FIL, and transduced cells were fixed and stained for β-gal activity 48 h following transduction. **B)** Ability of knock down of Cav 1/2 to inhibit FIV-ZEBOV transduction. 0.75×10^6 SNB19s were transfected with 200 pmol of a non-specific siRNA control (Block-it) or 200 pmol of a mixture of Cav1 and Cav 2 human specific siRNA. 48 h after transfection, cells were either transduced with FIV pseudovirions for an additional 48 h or incubated for 1 h with Tfr or CTb. After 1 h, cells were analyzed by flow cytometry for uptake of Tfr and CTb. 48 h following transduction, transduced cells were fixed and stained for β-gal activity. **C)** Knock down of Cav 1/2 by RNAi. 48 h after transfection, a portion of the cells were lysed and proteins were separated using SDS-PAGE. Cav1 and Cav2 were detected on the nitrocellulose membrane with primary antibodies (1:1000 and 1:250, respectively) incubated overnight at 4ºC followed by incubation with HRP-conjugated secondary antiserum (1:20,000) for 1 h at room temperature. The blot was visualized by chemiluminescence. Actin was detected by incubating primary HRP-conjugated antibody (1:10,000). Data represent the averages and standard errors of three experiments performed in triplicate. *, $P < 0.05$; **, $P < 0.001$.
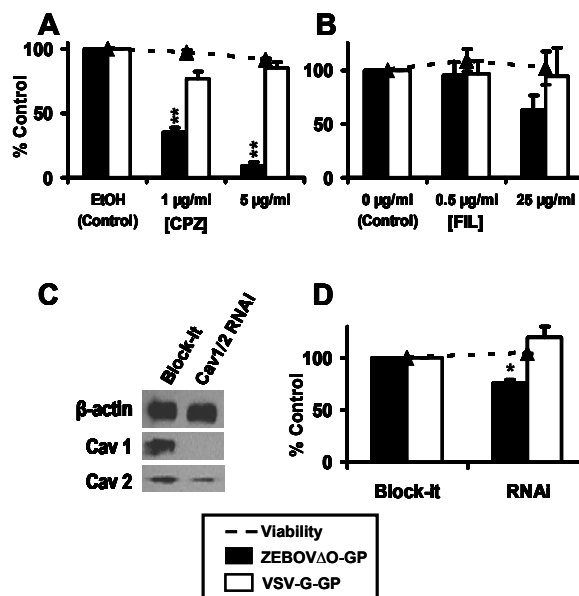
Figure 26. Receptor mediated endocytosis pathways are important for ZEBOVΔO-GP-mediated transduction of Axl-dependent cells, Hffs. A and B) Hffs were pretreated with the indicated amount of CPZ (A) or FIL (B) for 1h. Cells were then incubated with FIV pseudovirions (MOI=0.005) in the continued presence of drug. The media on the transduced cells was refreshed after 6 h with media not containing drug and transduced cells were fixed and stained for β-gal activity 48 h following transduction. **C)** Hffs were transfected with 200pmol of a non-specific siRNA control (Block-it) or 200pmol of a mixture of Cav1 and Cav2 human specific siRNA. 48 h after transfection, cells were lysed and proteins were separated using SDS-PAGE. Cav1 and Cav2 were detected by incubating the nitrocellulose membrane with primary antibodies (1:1000 and 1:250, respectively) overnight at 4ºC and washed 3 times in PBS with 0.0015% Tween and 10% milk (blotto). Secondary peroxidase-conjugated antiserum (1:20,000) was applied to the blot for 1 h at room temperature, the blot was washed 3 times in blotto, and the membranes were visualized by the chemiluminescence method. Actin was detected by incubating primary peroxidase-conjugated antibody (1:10,000) for 3 h at room temperature, and washing 3 times with blotto before visualizing the membranes by the chemiluminescence method. **D)** Hffs transfected with a non-specific siRNA control (Block-it) or Cav1/2 human specific siRNA were transduced with FIV pseudovirions 48 h after transfection. 48 h following pseudovirion transduction (MOI=0.005), cells were fixed and stained for β-gal activity. Data represent the averages and standard errors of three experiments performed in triplicate. The immunoblots shown is representative of three experiments performed independently. *, *P* <0.05; **, *P* <0.001.
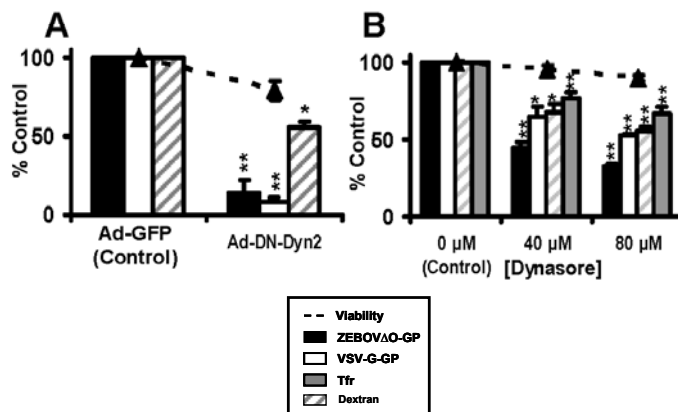
Figure 27. Receptor-mediated and non-receptor-mediated endocytic pathways facilitate FIV-ZEBOV transduction of Axl-dependent cells. A) Ability of DN dynamin to inhibit FIV-ZEBOV transduction. SNB19s were transduced with adenoviral vectors encoding GFP (Ad-GFP) or a dominant-negative form of dynamin 2 (Ad-DN-dyn2) at an MOI of 30. 18 h following adenoviral transduction, the cells were incubated with FITC-labeled dextran (0.5 mg/ml final) for 1 h or transduced with FIV pseudovirions for 48 h. Cells were analyzed by flow cytometry for uptake of dextran after 1 h or transduced cells were fixed and stained for β-gal activity after 48 h. **B)** Ability of Dynasore to inhibit FIV-ZEBOV transduction. SNB19s were treated for 1 h with the indicated amount of Dynasore. Treated cells were incubated with dextran or Tfr for one hour, or with FIV pseudovirions (MOI=0.005) for an additional 6 h in the presence of the drug. After 1 h, cells were analyzed by flow cytometry for uptake of dextran and Tfr. The media on cells transduced with FIV-ZEBOVΔO or FIV-VSV-G was refreshed after 6 h with media not containing drug and transduced cells were fixed and stained for β-gal activity 48 h following transduction. Data represent the averages and standard errors of three experiments performed in triplicate. *, $P <0.05$; **, $P <0.001$.
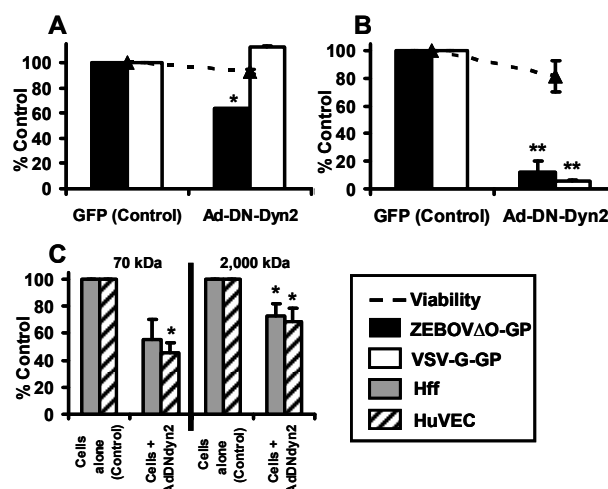
Figure 28. Receptor-mediated and non-receptor-mediated endocytic pathways are utilized during ZEBOV-GP-dependent transduction of two primary human cell populations. A and B) Ability of DN dynamin-Ad virus to inhibit FIV-ZEBOV transduction into Hffs (A) and HuVECs (B). Cells were transduced with adenoviral vectors encoding GFP (Ad-GFP) or dominant-negative dynamin 2 (Ad-DN-Dyn2) at an MOI of 90. After 18 h, cells were transduced with FIV-ZEBOVΔO (MOI=0.005) for 48 h. Cells were then stained for β-gal activity. **C)** Ability of dynamin2 to facilitate non-receptor-mediated FPU. Hff and HuVEC cells were transduced with adenoviral vectors encoding GFP (Ad-GFP) or dominant-negative dynamin 2 (Ad-DN-Dyn2) at an MOI of 90. After 18 h, cells were incubated with FITC-labeled dextran (70 kDa or 2,000 kDa; 0.5 mg/ml final) for 1 h. After 1 h, cells were analyzed by flow cytometry for uptake of dextran. Data represent the averages and standard errors of three experiments performed in triplicate. *, $P < 0.05$; **, $P < 0.001$.

Figure 29. Inhibitors of FPU decrease uptake of dextran but not uptake of Tfr or CTb in Axl-dependent cells. Ability of FPU inhibitors to inhibit dextran, Tfr and CTb uptake. SNB19s were treated for 1h with the indicated amount of FPU inhibitors. After 1 h, Cy5-Tfr, Cy5-CTb or FITC-labeled dextran was added to the cells in the presence of drug for an additional 1 h. The cells were then analyzed by flow cytometry for uptake of the labeled conjugates. Data represent the averages and standard errors of three experiments performed in triplicate. *, $P < 0.05$; **, $P < 0.001$.
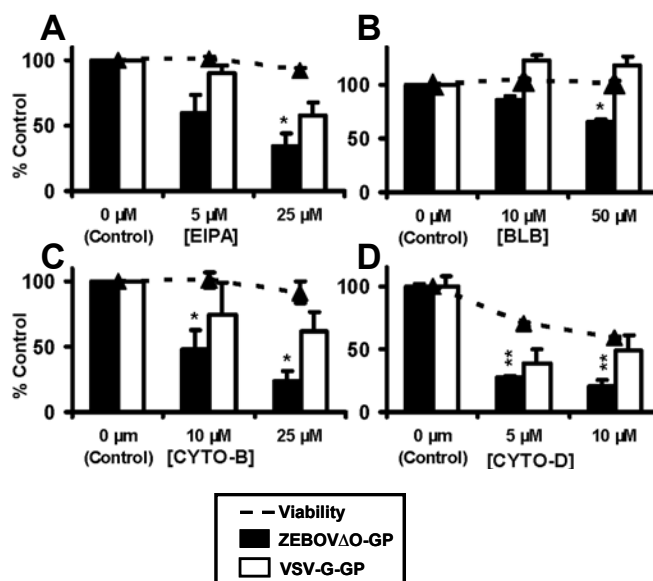
**Figure 30. Inhibitors of FPU decrease infectious ZEBOV and ZEBOV-GP pseudovirion uptake in Axl-dependent cells. A-D)** Ability of FPU inhibitors to inhibit FIV-ZEBOV transduction. SNB19s were incubated for 1 h with the indicated concentration of FPU inhibitor. After 1 h, the cells were transduced with FIV pseudovirions (MOI=0.005) in the presence of the drug for an additional 6 h. Media was refreshed without drug and cells were incubated for 48 h. After 48 h, cells were fixed and stained for β-gal activity. Data represent the averages and standard errors of three experiments performed in triplicate. *, $P < 0.05$; **, $P < 0.001$.
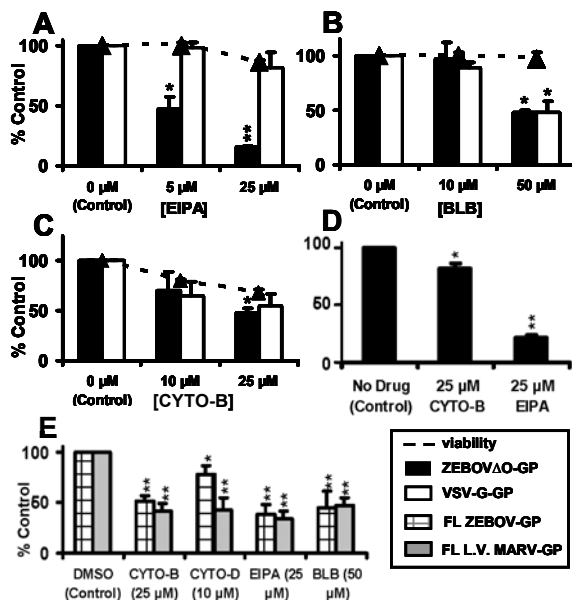
Figure 31. Inhibitors of FPU decrease filoviral-GP pseudovirion entry in Axl-dependent cells. Ability of FPU inhibitors to inhibit filoviral-GP-mediated entry into Axl-dependent cells. **A-C, E)** Hff cells were incubated for 1 h with the indicated concentration of FPU inhibitor. After 1 h, the cells were transduced with FIV pseudovirions (MOI=0.005) in the presence of the drug for an additional 6 h. Media was refreshed without drug and cells were incubated for 48 h. After 48 h, cells were fixed and stained for β-gal activity. **D)** HeLa cells were incubated for 1 h with the indicated concentration of FPU inhibitor. After 1 h, the cells were transduced with VSV pseudovirions (MOI=0.05) in the presence of the drug for an additional 6 h. Media was refreshed without drug and cells were incubated for 18 h. 24 h after initial transduction, cells were lifted with accumax and assessed for GFP activity using flow cytometry. Data represent the averages and standard errors of three experiments performed in triplicate. *, $P < 0.05$; **, $P < 0.001$.

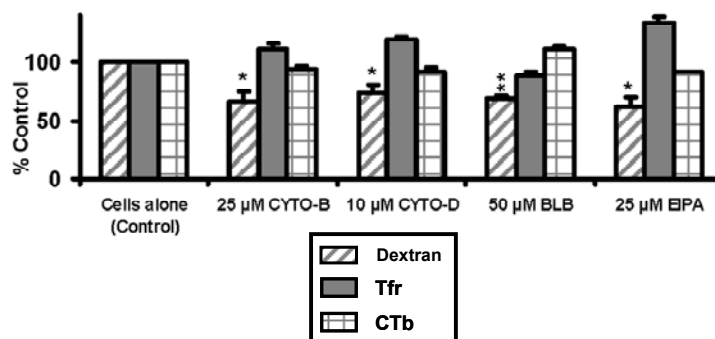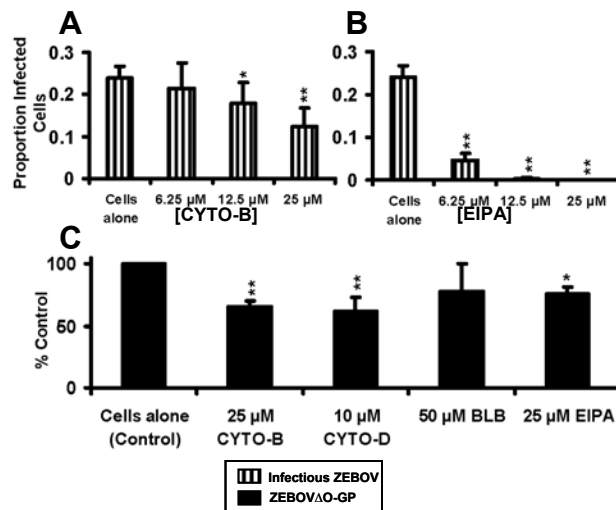**Figure 32. Inhibitors of FPU decrease ZEBOV-GP pseudovirion and infectious ZEBOV uptake in Axl-dependent cells. A-B)** Ability of FPU inhibits to decrease ZEBOV infection. SNB19 cells were incubated with the indicated concentration of drug for 1 h. Infectious ZEBOV (MOI=0.25) was then added in the presence of the drug for an additional 17 h. 17 h following ZEBOV infection, the media was changed on the cells, and 6 h after that, cells were fixed and assessed by microscopy for GFP positivity relative to the number of cells present for each condition. **C)** Ability of FPU inhibitors to inhibit ZEBOV VLP entry into SNB19s. SNB19s were treated for 1h with the indicated amount of FPU inhibitors. After 1 h, filoviral-like particles (VLPs) were added to cells in the presence of drug for an additional 6 h. Non-associated VLPs were then removed and cells were lysed and analyzed for luciferase activity. Data represent the averages and standard errors of three experiments performed in triplicate. *, P <0.05; **, P <0.001.
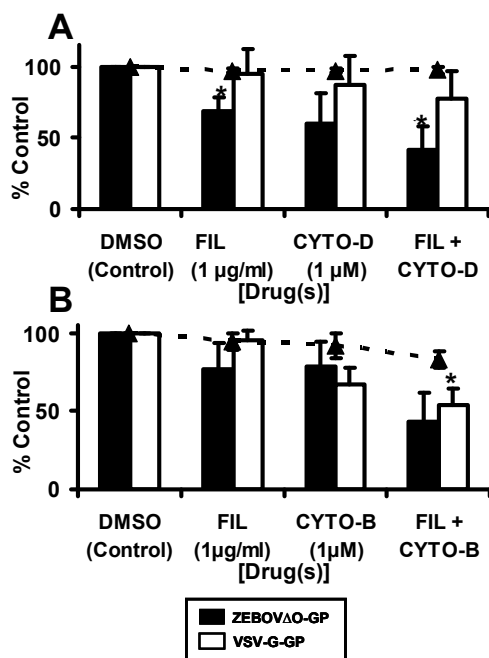
Figure 33. Simultaneous disruption of membrane cholesterol and restriction of the actin cytoskeleton additively disrupt ZEBOVΔO-GP mediated entry. A) SNB19s and **B)** Hff cells were treated for 1h with the indicated amount of drug alone or in combination at the indicated concentrations. After 1 h, cells were transduced with FIV-ZEBOVΔO-GP or FIV-VSV-G-GP (MOI=0.005) in the presence of drug for an additional 5 h. Media was then replaced on the cells, and the cells were fixed and stained for β-gal activity 48 h after initial transduction. Data represent the averages and standard errors of three experiments performed in triplicate. *, $P < 0.05$.

CHAPTER FIVE: ROLE OF AXL IN

FILOVIRUS ENTRY

Abstract

The role of the TAM family member Axl in filoviral entry is unknown. ZEBOV gains entry into cells by multiple uptake mechanisms, including clathrin and caveolae-dependent pathways. Surprisingly, we also found that a major route of entry into Axl-dependent cells was through non-receptor mediated fluid-phase-uptake (FPU). The goal of this study was to determine if Axl is involved in these endocytic processes. Axl-specific RNAi was used in combination with multiple drugs to inhibit endocytotic pathways. We observed that a reduction in Axl expression by RNAi treatment resulted in abrogation of ZEBOV entry by FPU-dependent pathways, but the knock down of Axl had no effect on receptor-mediated endocytosis mechanisms. Additionally, through the use biochemical inhibitors that target specific signaling pathways we demonstrated that phospholipase C (PLC) dependent pathways were important for ZEBOV transduction in Axl-dependent cells, but that phosphoinositol 3 kinase (PI3K) dependent pathways were required for ZEBOV transduction of Axl-independent cells. Our findings demonstrate for the first time that Axl modulates FPU, thereby increasing productive ZEBOV entry. Furthermore, our signaling studies suggest that activation of PLC downstream of Axl activation may lead to enhanced FPU leading to increased ZEBOV entry.

Introduction

Our laboratory is particularly interested in understanding how the Tyro3 receptor kinase member, Axl, mediates increased filovirus entry. A previous study identified a number of cell lines that require Axl for optimal filovirus transduction [115]. These lines include human HT1080 cells, human HeLa cells, human lung carcinoma A549 cells, African green monkey kidney COS-7 cells and human embryonic kidney 293 cells [115]. Studies within the laboratory have identified additional cell populations that express endogenous Axl and have dependence upon Axl expression for maximal levels of

ZEBOV transduction. These additional cell populations include Hff cells, HuVEC cells and SNB19 cells [160]. We used these cell populations to uncover a role for Axl in the filovirus entry process.

To identify a role of Axl in entry mediated by the filoviral-GP in Axl-dependent cell populations, we utilized a multi-faceted approach. By using biochemical inhibitors of signaling molecules that are downstream of Axl we were able to determine that different signaling molecules are important for filoviral-GP-dependent entry into Axl-dependent and Axl-independent cell populations. Through the use of Axl-specific RNAi alone and in combination with endocytic inhibitors we were able to determine that Axl is directly involved in enhancing FPU of extracellular cargo including filoviral-GP bearing pseudovirions. We showed that in Axl-dependent cells the loss of Axl expression through the use of Axl-specific RNAi significantly decreased the rate of filoviral-GP-mediated internalization, indicating that Axl is involved in early entry events mediated by the filoviral-GP. Together, these data represent the first time that a host protein has been shown to be involved in the internalization process mediated by a filoviral-GP.

Materials and methods

Cells lines and antibodies

Human embryonic kidney cells 293T (CRL-11268; ATCC), a human glioblastoma line, SNB19 (NCI 0502596), a human cervical cancer cell line, HeLa (CCL-2; ATCC) and an African green monkey kidney cell line, Vero (CCL-81; ATCC) were maintained in high-glucose Dulbecco's modified Eagle's medium (DMEM) (Invitrogen) supplemented with 100 units/ml of penicillin and 100 μg/ml streptomycin (1% P/S) and 10% fetal calf serum (FBS) (HyClone). Primary human foreskin fibroblasts (Hffs) isolated from fresh penile foreskin were maintained in DMEM supplemented with 100 units/ml of penicillin and 100 μg/ml streptomycin (1% P/S) and 15% FBS. The human renal cancer cell line SN12C (NCI0502585) was maintained in Roswell Park Memorial Institute media 1640 (RPMI) with 100 units/ml of penicillin and 100 μg/ml streptomycin

(1% P/S) and 5% FBS. Cells were maintained at 37ºC with 5% CO_2. Antibodies used included anti-human Axl (R&D Systems) and anti-human actin (AbCam).

Plasmids used

Plasmids used to generate the FIV-ZEBOV (Zaire species; mucin domain deleted) and FIV-VSV-G (wild type; Indiana strain) particles have been previously described [113, 162]. Plasmids encoding the full length ZEBOV-GP [99] and the full length Lake Victoria MARV-GP (Musoke variant) [161] have also been described previously.

Generation of and detection of pseudovirions

FIV pseudovirions were generated in 293T cells as previously described [113, 121, 162]. All pseudovirions were concentrated using a 16-h centrifugation step at 7,000 rpm at 4°C in a Sorvall GSA rotor. The viral pellet was resuspended in 250 µl DMEM for an approximately 200-fold concentration prior to use. All FIV pseudovirions expressed the reporter β-galactosidase (β-gal) upon delivery into the recipient cell. FIV transduction studies were performed in a 48 well format using a MOI of ~0.005 (resulting in approximately 200 β-gal positive cells/40,000 cells/well in control wells). FIV pseudovirion transduction was detected by fixing cells in 3.7% formalin and evaluating for β-gal activity using the substrate 5-bromo-4-chloro-3-indolyl-β-D-galactopyranoside. All FIV transduction evaluation was done 48 h after initial FIV pseudovirion addition to cells. The number of β-gal-positive cells was enumerated by microscopic visual inspection.

VSVΔG/EGFP pseudovirions (a kind gift of Michael Whitt, University of Tennessee Health Sciences) bearing ZEBOVΔO-GP or VSV-G (wild type; Indiana strain) were generated in 293T cells as previously described [124]. For detection of VSVΔG/EGFP pseudovirion transduction, 24 h following transduction, cells were lifted in Accumax (Fisher) and analyzed with a FACScan cytometer (BD Biosciences) for FL-1 intensity. VSVΔG pseudovirions were applied to cells to yield approximately 1,000 GFP

positive cells for every 20,000 cells analyzed by flow cytometry. This gives an MOI of approximately 0.05 for all studies using the VSVΔG system.

Because there is some variation in absolute numbers of on-put virions used in different experiments and all experiments shown are a compilation of at least three different experiments, the control findings were set to 100% and the results shown are represented as % control rather than absolute transduction values.

Drug studies

All drugs were obtained from Sigma (St. Louis, MO, USA) unless otherwise noted. All studies were performed in a 48-well format. Concentrations of drugs are noted in figures. The no-drug control contained the appropriate dilution of vehicle. All cells were fixed and stained for β-gal activity 48 hours after the initial addition of pseudovirions to the cells. The findings are shown as the ratio of the number of transduced cells in the presence of inhibitor divided by the number of transduced cells when no inhibitor was added (% control). In all inhibitor studies, the ability of the inhibitors to decrease pseudovirion transduction was adjusted for cytotoxicity associated with the inhibitor.

Blebbistatin. Blebbistatin (BLB) was resuspended in DMSO at 100 mM. BLB was diluted into the medium (containing FBS) and pre-incubated with cells for 1 hour. Cells were transduced in the presence of the drug, and the blebbistatin-containing inoculum was removed 5 hours after ZEBOV-GP or VSV-G pseudotyped FIV transduction, and replaced with fresh medium that did not contain inhibitor.

5-(N-Ethyl-N-isopropyl)amiloride. 5-(N-Ethyl-N-isopropyl)amiloride (EIPA) was resuspended in dimethylsulfoxide (DMSO) at 200 mM. EIPA was diluted into the medium (containing FBS) and pre-incubated with cells for 1 h. Cells were transduced in the presence of the drug, and the EIPA-containing inoculum was removed 5 h after ZEBOV-GP or VSV-G pseudotyped FIV transduction, and refreshed with fresh medium not containing inhibitor.

Cytochalasin B and cytochalasin D. Cytochalasin B (CYTO-B) and cytochalasin D (CYTO-D) were obtained from Calbiochem (EMD) and were each resuspended in DMSO at 25 mM. CYTO-B or CYTO-D was diluted in medium and incubated with cells for 1 h. Cells were transduced in the presence of the drug, and the drug-containing inoculum was removed 5 h after ZEBOV-GP or VSV-G pseudotyped FIV transduction, and refreshed with medium not containing inhibitor.

4-Amino-5-(4-chlorophenyl)-7-(t-butyl)pyrazolo[3,4-d]pyrimidine. The *src* family kinase inhibitor 4-Amino-5-(4-chlorophenyl)-7-(*t*-butyl)pyrazolo[3,4-d]pyrimidine (PP2) PP2 was obtained from Calbiochem (USA) and was resuspended in DMSO at a concentration of 100 mM. PP2 was diluted into the medium and pre incubated with cells for 1 hour. Cells were transduced in the presence of the drug, and the PP2-containing inoculum was removed 5 hours after transduction, and replaced with fresh medium that did not contain inhibitor.

1-[6-((17-beta-3-Methoxyestra-1,3,5(10)-trien-17-yl)amino)hexyl]-1H-pyrrole-2,5-dione. The phospholipase C (PLC) inhibitor 1-[6-((17-beta-3-Methoxyestra-1,3,5(10)-trien-17-yl)amino)hexyl]-1H-pyrrole-2,5-dione (U-73122) was obtained from Calbiochem/EMD and was resuspended in MeOH at a concentration of 100 mM. U-73122 was diluted into the medium and pre-incubated with cells for 1 hour. Cells were transduced in the presence of the drug, and the U73122-containing inoculum was removed 5 hours after transduction, and replaced with fresh medium that did not contain inhibitor.

2-(4-Morpholinyl)-8-phenyl-1(4H)-benzopyran-4-one hydrochloride. The phosphatidylinositol 3-kinase inhibitor (PI3K) inhibitor 2-(4-Morpholinyl)-8-phenyl-1(4H)-benzopyran-4-one hydrochloride (LY-294, 002) was resuspended in DMSO at a concentration of 500 mM. LY-294, 002 was diluted into the medium and pre-incubated with cells for 1 hour. Cells were transduced in the presence of the drug, and the LY-294,

002-containing inoculum was removed 5 hours after transduction, and replaced with fresh medium that did not contain inhibitor.

1-O-Octadecyl-2-O-methyl-rac-glycero-3-phosphorylcholine and tricyclodecan-9-yl-xanthogenate, K. The PLC inhibitors 1-O-Octadecyl-2-O-methyl-*rac*-glycero-3-phosphorylcholine (ET-18-OCH$_3$) and tricyclodecan-9-yl-xanthogenate, K (D609, potassium salt) were both purchased from Calbiochem and were each resuspended at 50 mM in sterile ddH$_2$O. Each drug was diluted into the medium and pre-incubated with cells for 1 hour. Cells were transduced in the presence of the drug, and the drug-containing inoculum was removed 5 hours after transduction, and replaced with fresh medium that did not contain inhibitor.

Detection and analysis of labeled conjugate uptake

Dextran (70 kDa conjugated to FITC) was resuspended in sterile H$_2$O at 10 mg/ml. Human transferrin (Tfn) and cholera toxin subunit B (CTb) conjugated to AlexaFluor 647 were obtained from Invitrogen and resuspended in sterile H$_2$O at a concentration of 5 mg/ml and 1 mg/ml, respectively. For drug studies with dextran, Tfr or CTb, cells were pretreated with drug alone for 1 h followed by addition of the labeled conjugate for an additional hour in the presence of drug. Cells were washed 3X in sterile PBS and lifted with accumax (Fisher) for analysis by flow cytometry on a FACScan cytometer (BD Biosciences) using FL-1 (dextran) or FL-4 (Tfr and CTb) channels.

RNAi

SNB19s were transfected with 200 pmol of a mixture of small interfering RNA (siRNA) against human Axl (two Axl validated RNAi constructs; Invitrogen) or 200 pmol of control nonspecific luciferase RNAi (Invitrogen) using the Lipofectamine 2000 (Invitrogen) protocol. Transfected cell populations were plated in a 48-well format at 24 h post RNAi transfection and transduced with FIV pseudovirions or harvested for immunoblotting analysis at 48 h post transfection. Drug and dextran studies on Axl

RNAi treated cells were conducted as described above in cells transfected for 48 h with RNAi.

Immunoblotting

Cells were lysed and proteins separated using SDS-PAGE as described previously [121]. Axl was detected by incubating the nitrocellulose with primary antibody (1:4,000) overnight at 4ºC and with appropriate secondary peroxidase-conjugated antiserum (1:20,000; Sigma). Actin was detected by incubating primary peroxidase-conjugated antibody (1:10,000) for 3 h at room temperature. Membrane was visualized by the chemiluminescence method according to the manufacturer's protocol (Pierce).

Far Western Blot

10 μl of concentrated FIV pseudovirions bearing either the mucin-domain deleted form of ZEBOV-GP or no viral envelope protein were applied to a dry nitrocellulose membrane and allowed to dry. 10 μl of liposomes reconstituted with PS were also applied and dried to the nitrocellulose. The membrane was blocked for one hour in 10% milk. 300 ng/ml of recombinant human Gas6 (R&D systems) was then incubated overnight at 4°C with the membrane. A 1:20,000 dilution of appropriate HRP-conjugated secondary antibody was then used to determine binding of Gas6. Membrane was visualized by the chemiluminescence method according to the manufacturer's protocol.

Cell viability assay

At the time of pseudovirion transduction evaluation, cell viability was monitored in an ATP-Lite assay (Packard Biosciences) as per the manufacturer's instructions.

Statistical analysis

Statistical analyses were conducted by Student's t test, utilizing the two-tailed distribution and two-sample equal-variance conditions. P values were assessed by comparing the level of transduction with treatment to the level of cytotoxicity observed

with that specific treatment. A significant difference was determined by a *P* value of <0.05. If the *P* value was >0.05, the data were not considered significant.

Results

Axl facilitates FPU of ZEBOV-GP pseudovirions

and infectious ZEBOV

To determine if one or more of the ZEBOV-GP entry pathways was altered by the loss of Axl expression, Axl was knocked down in SNB19s (**Fig. 34**) and the impact on FPU pathways as well as the receptor mediated endocytosis pathways was evaluated using the following well established, pathway-specific cargo: 1) dextran that serves as cargo for FPU, 2) transferrin (Tfr) that enters cells through clathrin coated pits and 3) cholera toxin b (CTb) that is internalized through caveolae. Reduction of Axl in SNB19s significantly reduced uptake of dextran but not Tfr or CTb suggesting that Axl is specifically modulating FPU within this cell population (**Fig. 34**).

To confirm that loss of Axl was affecting FPU dependent FIV-ZEBOV transduction, we evaluated FIV-ZEBOV transduction in the presence of both FPU inhibitors and Axl RNAi anticipating that loss of Axl expression would lead to an abrogation of FPU inhibitor effects. Indeed, while we observed that Axl RNAi treatment inhibited ~75% of ZEBOV-GP transduction, the addition of CYTO-B, CYTO-D and BLB to Axl RNAi-treated cells no longer decreased ZEBOV-GP-mediated transduction indicating that Axl is responsible for ZEBOV-GP-mediated entry via FPU pathways within SNB19s (**Fig. 35***A*). Interestingly, although its ability to inhibit ZEBOV-GP entry was drastically reduced, EIPA was still able to reduce ZEBOV-GP entry by more than 50% in Axl RNAi-treated cells (**Fig. 35***A*). This suggests that in addition to inhibiting FPU pathways, EIPA may also be acting to partially inhibit one or more other endocytic pathways independently of Axl. As expected, FIV-VSV-G entry was unaffected by a combination of Axl RNAi and FPU inhibitors since neither Axl RNAi nor the FPU

inhibitors alone affected VSV-G-dependent transduction (**Fig. 35***B*) relative to the cytotoxicity associated with the drugs alone (data not shown).

Finally, if FPU mediated entry of ZEBOV was dependent upon Axl, we predicted that FPU inhibitors would not inhibit ZEBOV entry into Axl-independent Vero cells. As anticipated, FIV and VSV based pseudovirion ZEBOV-GP-dependent entry was unaffected by the inhibitors (**Fig. 36**). Together, these data provide strong evidence that Axl enhances ZEBOV entry through one or more FPU pathways in Axl-dependent cells but not Axl-independent cells.

Axl is required for efficient FIV-ZEBOV pseudovirion internalization into SNB19 cells

Previously published data [115] and our findings shown in **Fig. 22 and Fig. 23 of Chapter 4** demonstrate that Axl antisera and Axl RNAi inhibited FIV-ZEBOV transduction and entry of infectious ZEBOV. Because multiple steps are involved in filoviral-GP-dependent entry including binding and internalization, we tested the ability of Axl RNAi to interfere with FIV-ZEBOVΔO-GP pseudovirion binding and subsequent internalization. SNB19 cells were treated with Axl RNAi for 48 hours prior to addition of ZEBOVΔO-GP pseudotyped FIV for 1h at 4°C. Cells were washed to remove unbound particles and warm media was added and the cells were incubated at 37°C for the times indicated. At each time point, the cells were trypsinized to remove any non-internalized virus that was still bound to the cell surface. The cells were then washed to remove the trypsin and lysed in 1% SDS, and the amount of internalized virus was evaluated by immunoblotting for FIV capsid. The amount of FIV capsid internalized was quantified following normalization of cell equivalents by quantitatively immunoblotting the cell lysates for actin (**Fig. 37**). In cells transduced with FIV-ZEBOVΔO-GP pseudovirions, the quantity of capsids internalized at each time point was significantly

reduced by treatment with RNAi against Axl. These findings suggest that Axl is needed for optimal internalization of FIV-ZEBOVΔO-GP pseudovirions.

<div align="center">

Signaling pathways required for FIV-

ZEBOV pseudovirion transduction differ in

Axl-dependent cells and Axl-independent cells

</div>

Recent studies have demonstrated that in addition to inhibiting the formation of clathrin coated vesicles, the drug CPZ has broader inhibitory activities, interfering with the generation of vesicles such as phagosomes and macropinosomes within cells [164]. The mechanism of this activity is believed to be due to CPZ inhibition of one or more isoforms of phospholipase C (PLC) [175]. PLC is an important regulator of actin dynamics and inhibition of PLC activation leads to inhibition of FPU [85]. A previous study have shown that PLC interacts with phosphorylated tyrosines on the cytoplasmic tail of activated Axl suggesting that PLC signaling may be a downstream event of Axl activation [117]. We therefore investigated the role of CPZ in FPU inhibition as well as the role of PLC in ZEBOVΔO-GP-mediated entry into Axl-dependent cells. We observed that CPZ modestly, but significantly inhibited the uptake of dextran (**Fig. 38A**), indicating that in addition to inhibiting clathrin-mediated endocytosis, CPZ also inhibits FPU activity in SNB19s. The ability of the pan PLC inhibitor U-73122 to inhibit FIV-ZEBOVΔO-GP transduction into Axl-dependent and -independent cells was also evaluated. This inhibitor diminished FIV-ZEBOVΔO-GP entry into SNB19s (**Fig. 38D**) and Hffs (**Fig. 38E**), but not Axl-independent Vero cells (**Fig. 38G**) or an additional Axl-independent cell line, SN12C (**Fig. 38F**). Only FIV-VSV-G-GP entry into Hff cells was significantly affected by treatment with U-73122 (**Fig. 38E**).

The importance of PLC activity in ZEBOVΔO-GP-mediated entry was confirmed in SNB19 cells using two additional PLC inhibitors, ET-18-OCH$_3$ and D609, potassium salt (**Fig. 38B and 38C**). Both drugs significantly inhibited FIV-ZEBOVΔO-GP transduction in SNB19 cells at the IC$_{50}$ of each drug (~15 μM) [176] and at a higher

concentration, 50μM (**Fig. 38*B* and 38*C***). Together, these results clearly show a significant involvement of PLC during ZEBOV-GP-mediated entry into Axl-dependent cells, but not in the Axl-independent cells that were studied.

Axl signaling has been shown to be mediated through phosphoinositide 3-kinase (PI3K) pathways [117]. In addition, ZEBOV entry into the Axl-independent VeroE6 cells requires PI3K activity [173]. Consequently, in parallel with our PLC studies, we evaluated whether FIV-ZEBOVΔO transduction was decreased in the presence of the PI3K inhibitor LY-294,002. LY-294,002 had no effect on ZEBOVΔO-GP-mediated entry into SNB19s (**Fig. 39*A***) or Hffs (**Fig. 39*B***), but decreased FIV-ZEBOVΔO transduction into Axl-independent Vero (**Fig. 39*D***) and SN12C cells (**Fig. 39*C***). VSV-G-GP-dependent entry into all of the cells tested was unaffected by LY-294,002, except in Vero cells, where VSV-G-GP-dependent entry was significantly decreased, but only at the highest concentration of drug tested (**Fig. 39*D***).

The Src pathway has been reported to also be downstream of Axl signaling [117]. Consequently, a Src family inhibitor, PP2, was tested for its effect on FIV-ZEBOVΔO-GP and FIV-VSV-G-GP pseudovirion transduction. In contrast to the PI3K and PLCγ inhibitors, the Src inhibitor PP2 inhibited FIV-ZEBOVΔO-GP pseudovirion transduction of both Axl-dependent and Axl-independent lines implicating Src-dependent signaling events are needed for ZEBOVΔO-GP-mediated transduction in Axl-dependent and Axl-independent cells (**Fig. 40*A*-40*D***). PP2 only decreased VSV-G-GP pseudovirion transduction in Vero cells (**Fig. 40*D***). In total, our findings indicate that signaling through PLC and Src, but not PI3K is necessary for optimal ZEBOVΔO-GP-mediated entry into Axl-dependent cells. In contrast, as others have shown [173], PI3K activity is needed for ZEBOVΔO-GP entry into Axl-independent cells. Additionally, Src activity is also needed for optimal ZEBOVΔO-GP entry into Axl-independent cells.

The Axl ligand Gas6 binds to ZEBOV-GP

containing pseudovirions

Previous studies in the laboratory had attempted to detect direct interactions between the ectodomain of Axl and ZEBOV pseudovirions to no avail. However, it is possible that an indirect interaction between these two molecules may occur. In an attempt to determine a mechanism by which the filoviral-GP uses Axl to gain entry into an Axl-dependent cell, we decided to take a closer look at the natural ligand of the TAM family of tyrosine kinase receptors, the molecule Gas6. The C-terminal portion of Gas6 is capable of binding to the Axl receptor, whereas the N-terminal region is capable of binding to lipid membranes that contain the lipid phosphatidylserine (PS). Recently, it has been shown that viral-GPs are located with PS on the outer leaflet of the host plasma membrane before budding of the respective virus [81] and work by others in the laboratory have demonstrated that ZEBOV GP pseudotyped FIV particles contain PS on the outer leaflet of their viral envelope (data not shown). To test if a filoviral-GP bearing pseudovirion could interact with Gas6, we took FIV-ZEBOVΔO-GP pseudovirions and determined if they bound to exogenous Gas6 by utilizing a "far-western blot" technique. We tested Gas6 binding to FIV pseudovirions expressing ZEBOVΔO-GP or no viral envelope (negative control). We also tested the ability of Gas6 to bind to liposomes containing PS as a positive control.

The pseudovirions or the liposomes were first applied to dry nitrocellulose and allowed to dry. The nitrocellulose was then blocked in milk and incubated with recombinant Gas6 for one hour. The blot was then washed, and incubated with the appropriate secondary antibody to detect bound Gas6. Gas6 bound strongly to both FIV-ZEBOVΔO-GP virions and PS-containing liposomes (**Fig. 41**). Gas6 did not bind strongly to the FIV pseudovirions without a viral envelope, indicating that Gas6 is capable of binding to FIV pseudovirions expressing ZEBOVΔO-GP. This indicates that

Gas6 has the potential to bridge an interaction between the filoviral-GP and membrane bound Axl.

Discussion

Here, for the first time, we have shown that the Tyro3 receptor kinase receptor Axl is capable of enhancing entry of infectious ZEBOV as well as pseudovirions bearing filoviral-GP into certain cell populations by fluid phase endocytic pathways. Although Axl does not appear to interact directly with any form of any of the filoviral-GPs, we have identified preliminary evidence suggesting a possible mechanism by which this can indirectly occur. The interaction of exogenous Gas6 with PS on the surface of pseudovirions expressing ZEBOVΔO-GP may allow indirect binding between the filoviral-GP and membrane bound Axl. The exact nature of these interactions is currently under study.

Interestingly, one of the FPU inhibiting drugs tested (EIPA) retained a partial ability to decrease ZEBOV entry in the Axl-dependent SNB19 cells even in the presence of Axl RNAi treatment (**Fig. 35***A*). This indicates that EIPA may also be inhibiting an endocytic pathway or pathways other than those involved in FPU. Evidence does exist showing that inhibition of the Na+/H+ exchanger by EIPA or another amiloride inhibits the uptake of albumin [177, 178]. Because uptake of albumin requires a receptor-mediated event (clathrin or caveolin involvement), it is possible that EIPA is affecting endocytic pathways other than and including FPU. Therefore, the involvement of FPU in addition to one or more other receptor-mediated endocytic events within the same Axl-dependent cell population is consistent with our current findings.

While FPU pathways are not implicated in ZEBOV entry in Axl-independent cells (**Fig. 36**), we demonstrate a role for FPU in ZEBOV transduction of Axl-dependent cells (**Fig. 35***A*). Decreased Axl expression in SNB19s by RNAi led to reduced dextran uptake as well as ZEBOV entry, but did not alter uptake of Tfn, CTb or FIV-VSV-G-GP pseudovirions. Peptides from the Axl cytoplasmic tail containing phosphorylated Y821

or Y866 serve as docking sites for PLCγ [117]. Consequently, it is tempting to speculate that direct Axl/PLC interactions lead to signaling events that result in enhanced FPU. This idea is also supported by evidence showing that signaling through Axl/Mer/Tyro3 receptors in professional phagocytic cells is crucial for phagocytosis and clearance of apoptotic cells [179]. To date, a role for any TAM family member in signal-induced FPU within a non-professional phagocytic cell population has not been shown.

As Axl signaling has been predicted to activate PLC, which in turn enhances FPU [85], we evaluated if ZEBOV entry was inhibited by a pan-PLC inhibitor. Indeed, we observed a reduction in ZEBOV entry in the presence of U-73122 (as well as two additional PLC inhibitors) implicating PLC signaling in ZEBOV transduction. We also show that a portion of the CPZ dependent inhibition of ZEBOV entry is due to FPU pathways that are likely being mediated through PLC [175]. We therefore postulate that Axl expression enhances ZEBOV entry into SNB19s through PLC signaling, thereby identifying a mechanistic role for Axl in filovirus entry for the first time.

We also confirm recent findings that the PI3K/Akt signaling is important for ZEBOV entry into Vero cells [173], but did not observe a role for PI3K/Akt signaling in the Axl-dependent cells tested. Signaling through PI3Ks in Axl-independent cells may represent a function analogous to Axl signaling in Axl-dependent cells. Supporting this idea is data showing that class 1 PI3Ks that indirectly regulate host cell actin mediated cell functions via regulation of Rac1 that are necessary for efficient ZEBOV entry into other Axl-independent cells [173].

Not only does Axl enhance FPU-mediated ZEBOV entry, over expression of RhoB or RhoC is also capable of enhancing FPU leading to increased FIV-ZEBOV transduction [124]. In the case of RhoB or C, enhancement is not specific for ZEBOV since VSV-G pseudotyped transduction and VSV infection are also dramatically increased. In contrast, we observed specific enhancement of ZEBOV entry by Axl. Thus, it is likely

that Axl-dependent enhancement and Rho-dependent enhancement of FPU result from activation of different signaling pathways.

We have also identified signaling pathways that are important for efficient VSV-G-GP-mediated pathways. These signaling events have not previously been appreciated or reported during VSV-G-GP-mediated entry into any cell population. We have found that PLC activity is important for VSV-G-GP dependent entry into Hff cells, but not SNB19, Vero or SN12C cells (**Fig. 38***E*). We have also found that PI3K as well as Src kinases are necessary for efficient VSV-G-GP-dependent entry into Vero cells (**Fig. 39***D* **and 40***D*). As these are novel findings, and the receptor for VSV-G is unknown, it is unclear what protein or proteins VSV-G-GP is signaling through. It also remains to be determined if any of these signaling events are mediated through a potential VSV-G receptor or attachment factor.
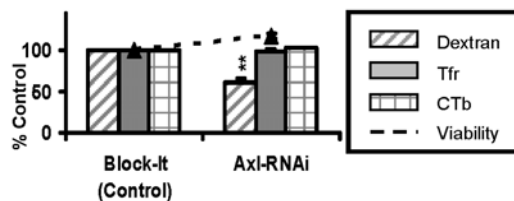
Figure 34. Knockdown of Axl protein specifically decreases FPU in Axl-dependent cells. Ability of Axl RNAi to inhibit dextran, Tfr and CTb uptake. 0.75 x 10^6 SNB19s were transfected with 200 pmol of a non-specific siRNA control (Block-it) or 200 pmol of a human Axl-specific siRNA. At 48 h following RNAi transfection, cells were incubated for 1 h with Cy5-Tfr or Cy5-CTb or FITC-dextran. After 1 h, cells were analyzed by flow cytometry for uptake of labeled conjugates. Data represent the averages and standard errors of three experiments performed in triplicate. **, $P < 0.001$.
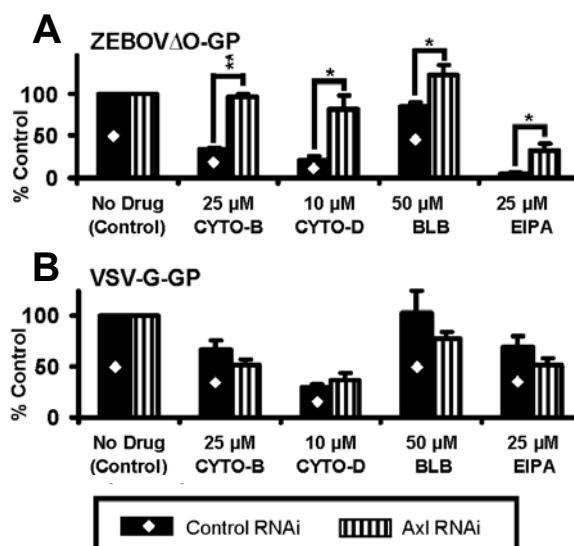
Figure 35. Axl facilitates FPU of ZEBOVΔO-GP pseudovirions. A) FPU inhibitors do not inhibit FIV-ZEBOVΔO-GP transduction when Axl is knocked down by RNAi in SNB19 cells. SNB19s were transfected with Axl siRNA or control siRNA (Block-It). At 48 h post transfection, cells were treated for 1 h with the indicated amount of FPU inhibitors. Cells were then transduced with FIV-ZEBOVΔO-GP (MOI=0.005) for an additional 6 h in the presence of the drugs. The media was refreshed after 6 h with media not containing drug, and transduced cells were fixed and stained for β-gal activity at 48 h following transduction. As shown in Figure 1, panel A, ZEBOVΔO-GP-mediated transduction of cells transfected with an irrelevant RNAi was about 4 fold higher than that observed in the presence of Axl RNAi. Each of these transduction values was set to 100% (No Drug control values) and we assessed the effect of FPU inhibitors on ZEBOVΔO-GP pseudovirion transduction in the presence or absence of Axl expression relative to these controls. **B)** FPU inhibitors have no effect on FIV-VSV-G-GP transduction in the presence or absence of Axl in SNB19 cells. Studies were performed as in (A) but FIV-VSV-G-GP (MOI=0.005) was transduced. Data represent the averages and standard errors of three experiments performed in triplicate. *, $P < 0.05$; **, $P < 0.001$.
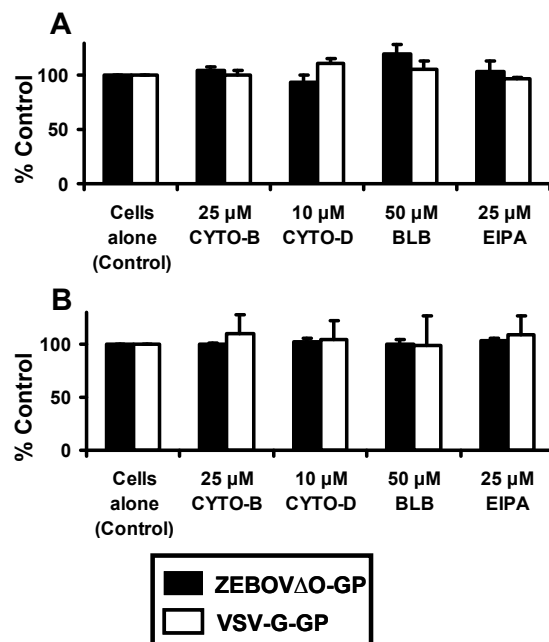
Figure 36. Axl does not facilitate FPU of ZEBOV-GP pseudovirions in Axl-independent cells. FPU inhibitors have no impact on EBOV-GP-mediated entry into Vero cells. Vero cells were incubated for 1 h with the indicated concentration of FPU inhibitor. After 1 h, FIV pseudovirions (MOI=0.005; **A)** or VSV pseudovirions (MOI=0.05; **B)** were added to cells in the presence of the drug for an additional 6 h. Media was then changed and transduced cells were fixed and stained for β-gal activity at 48 h following transduction. Data represent the averages and standard errors of three experiments performed in triplicate.
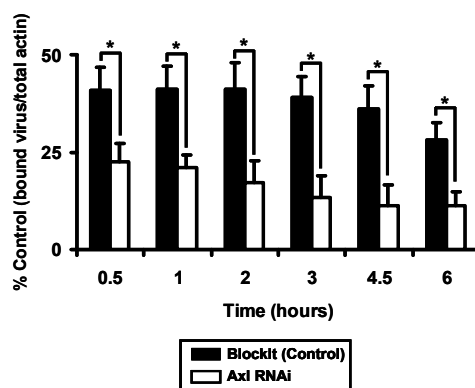
Figure 37. Axl is required for optimal ZEBOVΔO-GP-dependent internalization into Axl-dependent cells. Early internalization kinetics of ZEBOVΔO-GP pseudotyped FIV particles in SNB19 cells treated with Axl siRNA or an irrelevant siRNA. SNB19s were transfected with 200 pmol of a non-specific siRNA control (BlockIt) or 200 pmol of a human Axl-specific siRNA. At 48 h following RNAi transfection, FIV-ZEBOVΔO-GP (MOI=0.05) was applied to the cells for 1 h at 4ºC. Non-bound virus was removed, and cell were incubated for the indicated amount of time at 37ºC. At the indicated time point, cells were trypsinized to remove all non-internalized virus. Cells were then pelleted, and washed 3 times in PBS. Cells were then lysed in 1% SDS and proteins were separated using SDS-PAGE and FIV capsid was detected on the nitrocellulose membrane with primary antibody (1:5,000) overnight at 4ºC. The signal was detected by incubating with secondary horseradish peroxidase (HRP)-conjugated antiserum (1:20,000) for 1 h at room temperature. Blots were read on a low-light digital camera and quantified using Image Gauge. Actin was detected by incubating primary HRP-conjugated antibody. The immunoblots were then quantified as described above for FIV capsid. The total amount of virus internalized at each time point was divided by the total actin signal at each time point. Data represent the averages and standard errors of three experiments performed in triplicate. *, *P* <0.05.
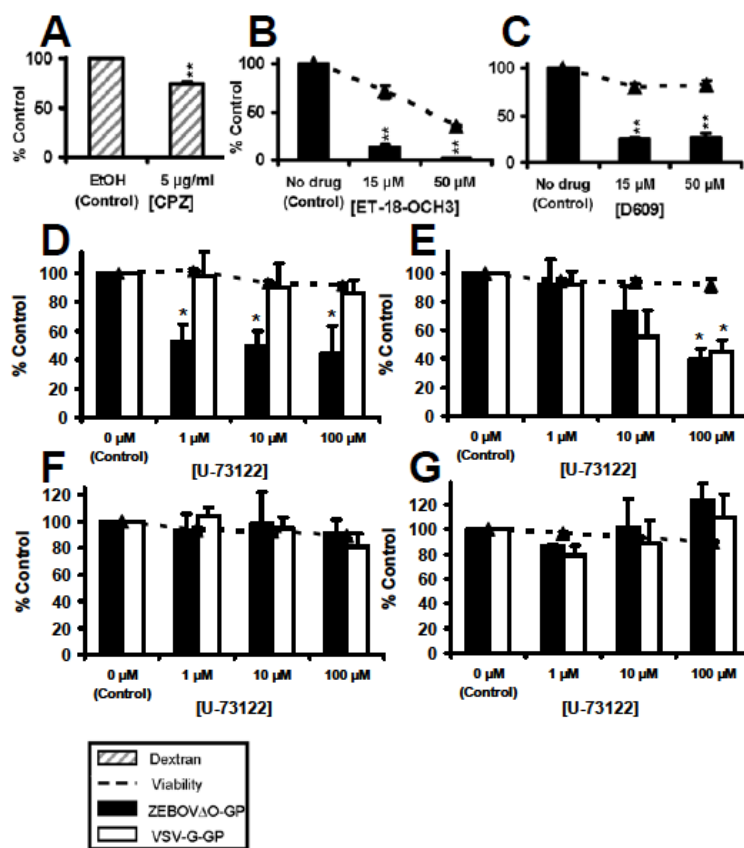
Figure 38. PLC is necessary for efficient ZEBOVΔO-GP mediated entry into Axl-dependent cells, but not Axl-independent cells. A) Ability of CPZ to inhibit dextran uptake. SNB19s were incubated with the indicated amount of CPZ for 1 h. After 1 h, FITC-labeled dextran was added in the presence of the drug. Dextran treated cells were washed after 1 h and analyzed by flow cytometry for uptake of dextran. **B-G)** Ability of PLC inhibitors to inhibit FIV-ZEBOVΔO-GP transduction in Axl-dependent and Axl-independent cells. SNB19 cells (B-D), Hff cells (E), SN12C cells (F) and Vero cells (G) were treated for one hour with the indicated amount of drug. Cells were then transduced with FIV pseudovirions bearing ZEBOVΔO-GP or VSV-G-GP for an additional 5 h in the presence of the drug. 48 h after initial transduction, cells were fixed and stained for β-gal activity. Data represent the averages and standard errors of three experiments performed in triplicate. *, $P <0.05$; **, $P <0.005$.
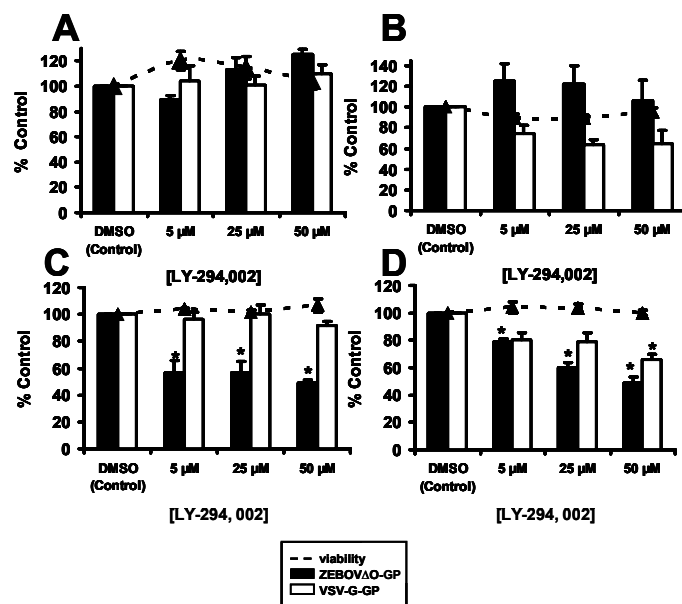
Figure 39. Analysis of the role of PI3K in ZEBOVΔO-GP mediated entry into Axl-independent and Axl-dependent cells. SNB-19 **(A, E)**, Hff **(B,F)**, SN12C **(C)** or Vero **(D)** cells were treated with the indicated amount of drug for 1 h. Cells were then transduced with FIV pseudovirions bearing ZEBOVΔO-GP or VSV-G-GP for an additional 5 h in the presence of the drug. 48 h after initial transduction, cells were fixed and stained for β-gal activity. Data represent the averages and standard errors of three experiments performed in triplicate. *, $P < 0.05$.
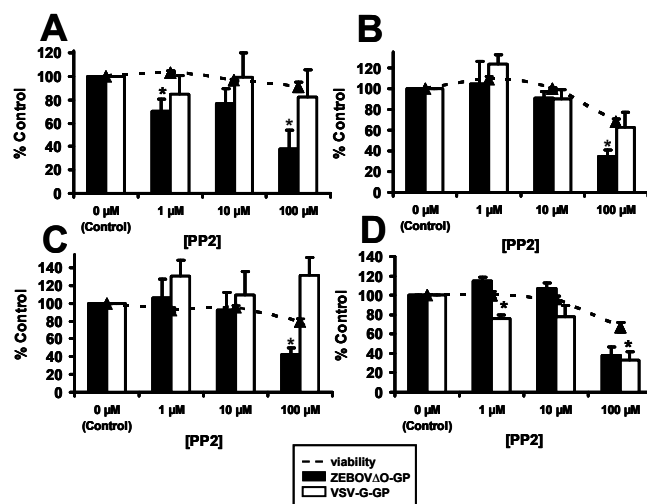
Figure 40. Src family kinases are necessary for efficient ZEBOVΔO-GP mediated entry into both Axl-dependent and Axl-independent cells. SNB19 **(A)**, Hff **(B)**, SN12C **(C)** or Vero **(D)** cells were treated for 1 h with the indicated amount of PP2. Cells were then transduced with FIV pseudovirions bearing ZEBOVΔO-GP or VSV-G-GP for an additional 5 h in the presence of the drug. 48 h after initial transduction, cells were fixed and stained for β-gal activity. Data represent the averages and standard errors of three experiments performed in triplicate. *, P <0.05.
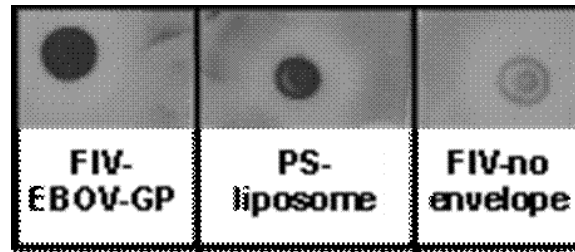
Fig. 41. FIV-ZEBOVΔO-GP bearing pseudovirions interact with Gas6. Far western blot showing the interaction between FIV-ZEBOVΔO-GP bearing pseudovirions and Gas6. Concentrated EBOVΔO-GP pseudotyped FIV, FIV lacking a viral GP or liposomes bearing PS were applied to nitrocellulose, blocked overnight, and then incubated with Gas6. Membranes were immunoblotted with anti-Gas6 antisera.

CHAPTER SIX: DISCUSSION

The filoviruses Ebola (EBOV) and Marburg (MARV) are responsible for devastating hemorrhagic fever outbreaks and are thus listed by the Centers for Disease Control as Class A Priority Pathogens. No vaccines or therapies are currently available against these viruses and the mechanism(s) of entry of filovirus is poorly understood. This general lack of understanding led us to more thoroughly characterize filoviral entry, including the kinetics of entry, the importance of glycans on host plasma membrane proteins for entry, as well as the entry mechanism(s) that were being used to enter cells. We also set out to determine what role the protein Axl, a member of the Tyro3 family of receptor kinases, was playing in filoviral entry. Our studies primarily involved the use of surrogate systems to assess the properties of entry associated with the filoviral-GP. This system provided valuable, novel information about the initial steps in filoviral-GP-mediated entry events.

The kinetics of filoviral-GP-mediated entry

Before undertaking these studies, little was known concerning the timing of entry events involved in early filoviral infection. Earlier studies provided an incomplete picture of filovirus uptake since those studies had only explored entry for 2 or 6 hours [72, 91]. By evaluating virus entry for long time periods, we have been able to determine that the entry kinetics mediated by the filoviral-GP are actually much different than previously thought. This work led to a more thorough understanding and appreciation of the kinetics associated with filoviral-GP-mediated entry, and how different pseudotyped systems and cell types affect these kinetics.

Retroviral based filoviral-GP pseudovirion properties

We were surprised to learn that retroviral based pseudovirions bearing filoviral-GPs bound poorly to permissive SNB19 cells (**Fig. 10**), and that once bound, internalization of the pseudovirions was a slow process but occurred in a linear fashion over time. All cell populations tested showed slow internalization kinetics of filoviral-

GP retrovirions, including cells from the filoviral reservoir organism, the fruit bat. We were able to determine that the filoviral-GP retroviral particles remained quite stable over time (**Fig. 11**), indicating that they could potentially mediate entry into cells for extended periods of time. This idea was supported by the slow, but steadily increasing, linear kinetics of retroviral based pseudovirion entry and internalization.

The fact that retrovirion based filoviral-GP-mediated binding is so inefficient and entry/internalization are so slow in the cell populations tested seems at odds with the ability of the wild type infectious virus to cause lethal infection in some hosts in less than two weeks [53]. One possible reason for this paradox may be that even small amounts of the virus can elicit high morbidity or mortality within the host. If this were true, the virus would not need to undergo multiple rounds of replication over the course of the infection. However, this does not seem to be true, as high loads of filoviral RNA in the blood of infected individuals is often used as a diagnosis tool [180]. Additionally, early onset of high-level viremia has been noted in infected individuals and is often associated with poor clinical outcomes for those individuals [180].

If correct, the slow entry seen with the retrovirion based system could reflect the initial incubation period that is seen in filoviral infected individuals before the onset of notable/visible infection. It is also possible that filoviral binding and entry into certain cell types, like the fibroblastic and endothelial cells tested in our studies is different from that observed with other cell types, such as dendritic cells (DCs) or macrophages (MΦs). Fibroblastic reticular cells (like Hffs) [181] as well as DCs and MΦs [53] are known to be early targets of filoviral infection. Because DCs and MΦs are professional phagocytic cells, they may facilitate filovirion entry much more efficiently and quickly than non-professional phagocytic cells. Additionally, it is possible that the kinetics observed with our surrogate system are not indicative of true filoviral infection. The analysis of the entry kinetics associated with infections EBOV and MARV will allow us to determine this.

Rhabdoviral based filoviral-GP pseudovirion

properties

Assessment of the entry and internalization kinetics of rhabdoviral based filoviral-GP pseudovirions did not show the same linear kinetics associated with the entry and internalization using the retroviral system. In fact, pre binding of virions to cells at 4ºC for one hour resulted in internalization of about 50% of virions. However, internalization kinetics appeared to stall shortly thereafter, leading to transduction of only about half of the virions. This finding led us to speculate that the rhabdoviral system may be much less stable that the retroviral system. This possibility is consistent with non-linear kinetics observed with the rhabdoviral system. These potential differences in viral stability between viral cores could have a large impact on the usage of these surrogate systems for applications such as gene therapy, where vector longevity may be an issue. More work is needed to determine if retroviral and rhabdoviral pseudovirion systems have different virion stability. Additional work will also help determine if other properties such as virion density, virion shape or GP distribution and/or abundancy impact the observed entry kinetics. Finally, it will be interesting to see if the presentation of the filoviral-GPs using a rhabdovirion background will also affect the length of time that the pseudovirion remains in an endosome, and if triggering of the filoviral-GP for fusion is potentially altered.

Retroviral and Rhabdoviral based

VSV-G-GP pseudovirion properties

Our work studying viral-GP-mediated entry events has also allowed us to appreciate the kinetics involved in VSV-G-GP entry. We observed that retrovirions pseudotyped with VSV-G-GP entered/internalized into all but one of the cell populations tested with kinetics nearly identical to those observed for retrovirions bearing the filoviral-GP. This data was unanticipated, as VSV-G-GP-mediated entry was meant to serve as a control. Entry kinetics associated with VSV-G-GP have been reported to be very fast, with 100%

entry of wild type VSV occurring within 2.5-3 minutes in HeLa cells [129]. Our studies have shown that using the retroviral system, VSV-G-GP-mediated entry and internalization is also linear over a 24 h time period. Additionally, VSV-G-GP-mediated internalization is slow (**Fig. 11**). In all of the cells tested, retrovirion based-VSV-G-GP-mediated entry and internalization was very similar to that observed with the filoviral-GPs. We were only able to observe a major difference in the uptake kinetics between the filovirus-GP and VSV-G-GP bearing retroviral pseudovirions in one cell line, HT1080s. However, VSV-G-GP-mediated entry in HT1080s was still very slow in comparison to the reported VSV-G entry kinetics in HeLa cells [129]. We are currently in the process of testing the timing of events associated with infectious VSV entry in the cell populations used previously in our pseudovirion studies.

It is currently unclear why the VSV-G-GP would mediate faster entry into the HT1080 cell line. We can only speculate that there may be more VSV-G-GP-specific attachment factors or receptors on the surface of this cell line that are available to mediated VSV-G-GP specific uptake. It is also possible that the VSV-G-GP may be endocytosed by a different mechanism or mechanisms in the HT1080 cells, and that once endocytosed, the VSV-G-GP is triggered for fusion more quickly than in other cell populations. Because the VSV-G-GP receptor(s) are currently unknown, it is difficult to test some of these hypotheses at this time. However, it should be noted that although the rhabdoviral VSV-G-GP-mediated entry and internalization kinetics in HT1080s are the fastest we have observed in this laboratory to date, the kinetics are still much slower than those already reported for VSV-G [129]. The analysis of infectious VSV entry into this cell population will determine whether our findings presented here are correct or artifacts associated with the retroviral pseudovirion system used.

As observed with the rhabdoviral pseudovirion system and filoviral-GP-mediated entry and internalization, rhabdoviral pseudovirions bearing their native VSV-G-GP entry and internalization was not linear and stalled at later time points (**Fig. 12**). At this time,

we are unsure why this is occurring, but may be due to instability of the rhabdoviral core, as discussed above. Combined our kinetic data allows us to conclude that the pseudoviral background as well as the cell population tested can each affect the kinetics of entry and internalization.

<div align="center">

Viral-GP-mediated access of attachment

factors versus receptor(s)

</div>

The data presented here indicate that the internalization step is a limiting step during both filoviral-GP- and VSV-G-GP-mediated retroviral system based entry (**Fig. 8-10**). For virus internalization via either of these glycoproteins, the viral GP must bind to its receptor or receptors that facilitate endocytosis. Additionally, the viral-GP may first bind to one or more attachment factors prior to interaction with its actual receptor(s). It is unclear at this point if the slow internalization kinetics observed with retroviral pseudovirions bearing filoviral-GPs and VSV-G-GPs could be the result of viral-GP binding to an attachment factor or factors first, and then binding to a receptor(s) after that. This "two-step" attachment factor then receptor usage mechanism has been proposed for HIV-1 as well as HSV type-1 and type-2 during infection, and thus may be a plausible means of entry by other DNA and RNA viruses as well [157, 159, 182]. Although this could explain the results seen with the retroviral based system background, it does not explain the results observed with the rhabdoviral system.

<div align="center">

Filoviral-GP-mediated endosome stay

</div>

In addition to the slow kinetics involved in filoviral-GP-mediated internalization, we have also determined that once internalized, the virus remains sensitive to ammonium chloride for an extended period of time (**Fig. 14**). We know from our data obtained in **Fig. 14** that it takes approximately 11 hours for 20 transducible virions to become insensitive to the ammonium chloride treatment. Although we cannot absolutely determine that these virions are inside of an endosome during this time period, the fact that they are sensitive to the drug means that they are dependent upon an acidified

environment during this time period. Because the filoviral-GP needs to be present within an acidified endosome with host cysteine cathepsins to promote viral and host membrane fusion, it is a possibility that the virions are remaining within and endosomal vesicle for this time period [54, 55].

The filoviral-GP is "trimmed" multiple times by at least three cathepsins, including cathepsins B and L to yield an approximate 17-18 kDa GP that is activated for fusion [54, 55]. These cathepsins are active at a pH range of 4.5-5.5, which is readily achievable during normal cell endocytic trafficking and within the late endosome [57]. Entry through some endocytic mechanisms, including clathrin-mediated endocytosis, allows progression to a low pH endosomal environment within minutes after cargo internalization [57]. From these studies, it is unclear why the filoviral-GP would need to stay in an endosome for a prolonged period of time. It also remains to be determined whether any filoviral proteins are responsible for this prolonged endosomal stay.

Cell type and surrogate system influence
on entry and internalization

These kinetic studies have also allowed us to appreciate that different cell populations may exhibit different viral-GP-mediated entry and internalization kinetics. It is not clear why certain cell types may be better or worse at endocytosis of external material, such as viral particles. Some cell lineages may have better endocytic capacities than others. Alternatively, certain cell populations may lack or overexpress attachment factors which could impact viral-GP access to receptor(s). Lastly, the signaling capacities of attachment factors and receptors on the different cell populations tested may also vary greatly, which could also affect virion-GP-dependent entry.

We also determined that the pseudovirion system used has an impact on viral-GP-mediated entry and internalization. This was surprising, since entry and internalization of the pseudovirion is supposed to be reliant on the viral-GP it is pseudotyped with, and not other factors associated with the surrogate system. In the future, it will be interesting to

see if the entry kinetics associated with infectious filovirus are also dependent upon cell type, and if the kinetics most closely mimic those associated with the rhabdoviral or the retroviral systems.

<div align="center">

The role of host plasma membrane protein

glycans in filoviral-GP-mediated entry

</div>

This work has also shown the necessity for O-linked glycans for efficient filoviral-GP-dependent entry into permissive cells. We demonstrated this in two independent ways, first, by using a mutant cell population expressing severely trimmed O-linked glycans (LdlD cells; **Fig. 16**), and secondly, by using a novel biochemical inhibitor (**Fig. 19**). This is the first demonstration that this O-linked glycan inhibitor 1-68A decreases viral entry into a cell population. The reduced susceptibility to EBOV transduction in cells with trimmed O-linked glycans may be due directly to a requirement for the trimmed sugar moiety or due to a decreased stability of attachment proteins and/or receptor(s), leading to decreased abundance of the protein(s) on the cellular surface. The total protein from membrane fractions of the Pro5 parental cell line could be compared to those in the LdlD cell line using a silver stain or a Coomassie stain. This would provide a general idea if gross differences in membrane associated protein content occur between the two CHO cell lines. Additional analysis of specific proteins, such as DC-SIGN, L-SIGN, Axl or other known proteins associated with filoviral entry could then be assessed in the cell lines by immunoblot or flow cytometry. A technical problem with CHO cells that has prevented this analysis to date is that these cells are hamster cells. Numerous antibodies directed against human proteins have been found to be non-reactive with the hamster homolog in these lines.

The use of the O-linked inhibitor drug, 1-68A allowed us to confirm our findings biochemically. The drug exhibited surprisingly low cytotoxicity in two of the three cell lines that were tested, and we were therefore able to determine that efficient filoviral-GP-mediated entry into permissive cells does require O-linked glycans.   Although it has

been previously suggested that N-linked glycans are important for filoviral entry [95], we were unable to provide data supporting this. In fact, we showed in Lec1 cells that exhibit severely trimmed N-linked glycans, but intact O-linked glycans, filoviral-GP-dependent entry was unaffected (**Fig. 16**).

We were also surprised to learn that the loss of either sialic acid or galactose on both N- and O-linked glycans enhanced filoviral-GP-dependent entry into Lec2 and Lec8 cells, respectively (**Fig. 16**). Because binding of the filoviral-GP expressing pseudovirions to all of the CHO cell lines was indistinguishable (**Fig. 20**), it is likely that an event post-binding such as viral internalization or fusion is being enhanced by the loss of surface sialic acid and galactose glycans and decreased by the loss of O-linked glycans. We are currently testing the internalization rates of filoviral virus like particles (VLPs) that contain luciferase protein. This system will also allow us to determine if the internalization rate and fusion rate of the VLPs into the mutant CHO lines is altered. All of the current findings as well as those derived using the filoviral VLPs will then need to be confirmed using infectious virus.

<div align="center">

Role of glycosylation of the TIM family

of potential filoviral receptors

</div>

It should be noted that our laboratory has recently identified members of the TIM family of proteins that interact directly with filoviral-GPs and appear to mediate filoviral entry into Vero cells and other epithelial cells [183]. Ard5, an antibody specific to one of these family members, blocks greater than 95% of infectious filoviral entry into Vero cells, indicating that the TIM family of molecules may indeed be a receptor for the filovirus family [183]. Unfortunately, we were unable to detect the presence of any of the TIM family or Axl family members on the surface of any of the CHO cell lines used in our studies. It is not clear if these proteins are absent from the surface of these cells, or if our current antibodies are unable to detect these proteins. More work will need to be done to determine if the TIM or Axl molecules are responsible for filoviral entry into the

CHO cells, and whether the glycosylation state of those proteins is altered in those cell lines.

The mechanisms of filoviral entry
into Axl-dependent cells

In vivo, filoviruses infect most major organ systems, including the liver, kidney, spleen, adrenal gland and brain during human, murine, guinea-pig and non-human primate infection [184-187]. The wide tropism exhibited by the filoviruses results from the ability of the filoviral GP to bind and enter into many different cell types. The literature concerning filoviral entry into cells has been contradictory, indicating either caveolin/lipid rafts [91], clathrin [94], or both [90] are important for filoviral entry. In this body of work, we have shown that ZEBOV-GP mediated entry occurs through both caveolin/lipid rafts and clathrin in ZEBOV-GP entry in Axl-dependent cells (**Fig. 24-26**). These findings are consistent with those previously reported in Axl-independent VeroE6 cells and indicate that filoviruses use these mechanisms for entry into a broad variety of different cells, and not just Axl-dependent cells [90].

We also show that ZEBOV-GP-mediated entry occurs through fluid-phase uptake (FPU) in Axl-dependent cells (**Fig. 30-32**). We demonstrated this using both infectious ZEBOV and pseudovirions bearing ZEBOV-GP. In his work, Sanchez has provided evidence that the FPU inhibitor amiloride had no effect on ZEBOV infection in Axl-independent cells [90]. Our study was able to confirm that FPU inhibitors indeed do not affect ZEBOV entry into Vero cells (**Fig. 34**). Therefore, our data suggests that FPU might only be used in certain cell populations and not others and indicates that FPU is not an important route of entry into Axl-independent cells. Interestingly, as Vero cells express cell surface Axl, this would suggest that pathways connecting Axl to FPU may be disrupted in this cell line.

The data presented also indicate that filoviral-GP-mediated entry is occurring via receptor-mediated and non-receptor-mediated endocytosis within the same cell

population. Our work therefore supports the hypothesis that filoviruses may be using more than one receptor to enter permissive cells [100]. The use of multiple receptors as well as multiple routes of entry by a filovirus would also help explain the broad tropism exhibited by these viruses. Our mechanism of entry studies are summarized in **Fig. 42**.

The role of Axl in filoviral entry

Knock down of Axl expression in the Axl-dependent cell line SNB19 abrogated greater than 80% of filovirus infectivity demonstrating for the first time the importance of endogenous expression of this protein for filovirus infection. Additionally, reduction of Axl expression decreased the ability of FPU inhibitors to block ZEBOV transduction, suggesting that the presence of Axl stimulates FPU uptake.

As Axl signaling has been predicted to activate PLC which in turn enhances FPU [85], we evaluated if ZEBOV entry was inhibited by PLC inhibitors. Indeed, we observed a reduction in ZEBOV entry in the presence of three different PLC inhibitors implicating PLC signaling in ZEBOV transduction in Axl-dependent cells, but not in cells such as Vero cells that do not require Axl for optimal filovirus transduction. We therefore propose that Axl expression enhances ZEBOV entry into SNB19s through PLC signaling leading to enhanced FPU. These studies therefore identify a potential mechanistic role for Axl in filovirus entry for the first time.

Our findings that the PI3K inhibitor LY-294,002 failed to inhibit filoviral-GP-dependent entry into Axl-dependent cell populations (**Fig. 38***A-B*), were surprising, as Saeed et al. have shown that PI3Ks are necessary for filoviral entry into VeroE6 cells [173]. However, we were able to confirm the findings of Saeed et al. that the PI3K/Akt signaling is important for ZEBOV entry into Vero cell lines (**Fig. 38***C-D*). While Vero cells express cell surface Axl, we and others have demonstrated that loss of plasma membrane expression of Axl has no effect on filovirus transduction into Vero cells [115, 160]. In total, our findings would suggest that pathways connecting Axl to FPU may be

disrupted in this cell line, and that filoviral signaling through PI3K is taking place through another, as yet unidentified surface molecule.

It should be noted that it has been shown that ectopic expression of Axl in poorly permissive Jurkat cells was demonstrated to provide a very modest (<1.25 fold) increase in ZEBOV infectivity suggesting the possibility that Axl may not be important for filovirus infection and replication [115]. These findings stand in contrast to our studies which demonstrate a significant role for Axl during ZEBOV infectivity. The discrepancy in the findings from the two studies may result from the absence of intact signaling pathways in Jurkat cells when Axl is ectopically expressed and underscores the importance of evaluating the function of a protein within its native environment.

<div align="center">**Indirect Axl engagement by filoviruses**</div>

<div align="center">**promotes viral fluid-phase uptake**</div>

This study provides compelling evidence that the presence of Axl stimulates FPU in SNB19 cells and other Axl-dependent cells. The mechanism of Axl activation by ZEBOV that leads to enhanced FPU remains unknown. No direct interaction between any filoviral GP and Axl or other TAM family member has been shown; however, indirect interactions may be occurring. Consistent with this possibility, we demonstrated that filovirus pseudovirions do interact with the TAM ligand Gas6. The possibility also exists that Axl may be capable of acting in concert with other TAM family molecules to elicit ZEBOV entry. However, we have failed to detect either of the other two TAM family members, Dtk and Mer on the surface of the Axl-dependent cell populations SNB19s and Hffs (data not shown).

We hypothesize that Axl-dependent uptake of filoviruses occurs through a novel mechanism involving three steps: 1) filoviral-GP expression on the surface of infected cells causing phosphatidyl serine (PS) flipping, generating virions that display PS on their surface and 2) the Axl ligand Gas6 interacting with virion associated PS, allowing

virion/Gas6 complexes to bind to Axl and 3) these interactions lead to signaling through Axl leading to increased rates of FPU enhancing productive virus uptake (**Fig. 43**).

We believe that the first step toward filoviral usage of Axl as a receptor involves phosphatidyl serine (PS) flipping on the surface of the infected cells. PS expression on the outer leaflet of enveloped virion membranes was first shown to occur for the poxvirus, vaccinia virus [81]. At that time, however, it was only hypothesized that the PS contained in the viral envelope was actually obtained from the host plasma membrane during viral budding. A current member of this laboratory has recently successfully shown that expression of either full length or mucin-domain deleted ZEBOV-GP induces flipping of plasma membrane PS from the cytoplasmic leaflet to the cell surface (data not shown). This seems to be specific to viral-GPs, as other cellular GPs serving as controls such as human CD4, or the cellular receptor for EIAV (equine ELR1) do not induce this flipping (data not shown).

Following filoviral infection, viral replication leading to filoviral GP expression on the surface of infected cells causes PS flipping. In turn, we believe that this allows for the generation of virions that display PS on their surface. Others in the lab have shown that PS is present on the surface of the budded pseudovirions (data not shown). These studies were performed by assessing Annexin V binding to PS on the outer surface of the budded fluorescently labeled EBOV pseudovirions (data not shown).

Finally, we hypothesize that once the filovirions have budded, the exposed PS on the outer leaflet of the viral membrane is capable of interacting with exogenous Gas6, therefore leading to filovirion-GP-expressing binding to Gas6. The binding of Axl ligand Gas6 with virion associated PS, allows virion/Gas6 complexes to bind to Axl, and these interactions ultimately lead to signaling through Axl. In turn, this leads to increased rates of FPU, thus enhancing productive virus uptake.

We are currently attempting to identify regions of full length ZEBOV-GP that are responsible for PS flipping. After this is completed, we will investigate the signaling

pathway(s) that are activated by indirect virus binding to Axl. Studies are planned to study the PLC signaling that leads to enhanced FPU of filovirions. In total, these studies will provide a more thorough understanding of the novel role of Axl in filovirus entry and will aid in development of novel antiviral therapies during filovirus infection. These studies will also provide a foundation for future *in vivo* mechanistic Axl studies during infectious filoviral entry.
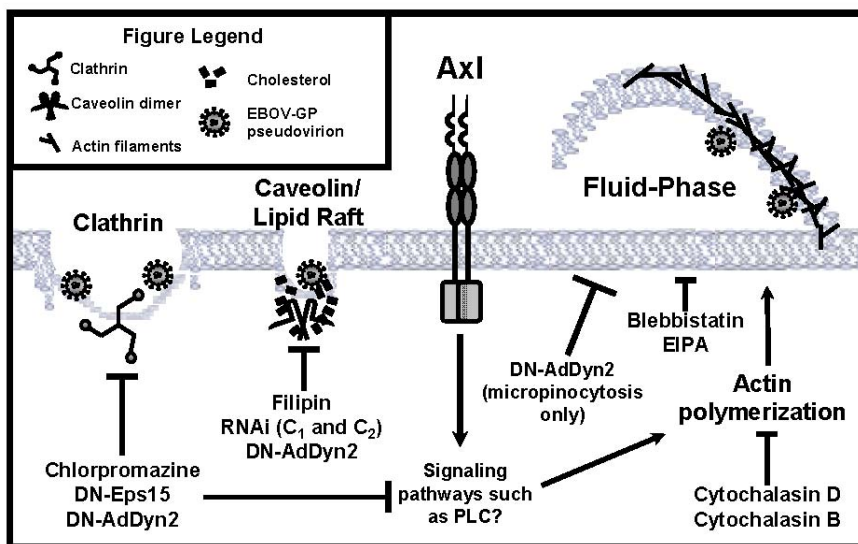
Figure 42. Model for ZEBOV-GP-dependent entry into Axl-dependent cells.
ZEBOV-GP-mediated entry into Axl-dependent cells occurs through multiple
mechanisms as evidenced by the use of biochemical inhibitors, dominant-negative
forms of endocytic proteins and RNAi. These routes of entry include the use of
clathrin coated pits, caveolae, lipid rafts, macropinocytosis, micropinocytosis and
possibly other forms of FPU. Inhibition of ZEBOV-GP-mediated entry by each of the
endocytic inhibitors was incomplete, indicating that multiple entry mechanisms are
used by ZEBOV-GP within one cell population. Axl signaling through PLC but not
PI3K promotes efficient ZEBOV-GP-mediated entry in Axl-dependent cells,
indicating that Axl is capable of serving as a signaling platform through which
ZEBOV-GP indirectly mediates entry via FPU.
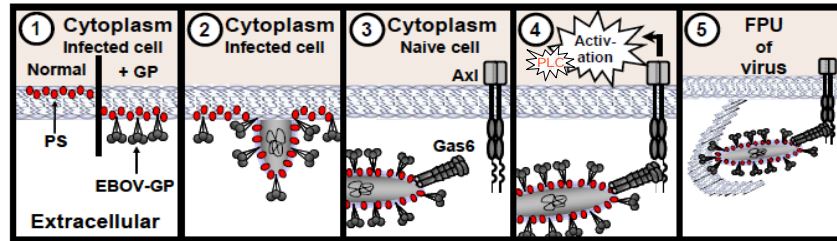
Figure 43. Model for Axl-mediated entry of EBOV. 1) Expression of EBOV-GP on the host plasma membrane during EBOV infection leads to membrane PS flipping. **2)** Subsequent virion budding allows incorporation of PS onto the viral membrane. **3)** The N-terminus of Gas6 binds the PS containing viral membrane. **4)** The C-terminus of Gas6 then binds the ectodomain of Axl, leading to Axl activation and signaling through PLC. **5)** Activated Axl leads to FPU of EBOV.

REFERENCES

1.   Sanchez A., C. A. L., Feldmann H. , Genetic Analysis Of Filoviruses Indicates That They Are More Closely Related To Paramyxoviruses Than To Rhabdoviruses. *unpublished data* **1991**.

2.   Feldmann, H.; Klenk, H. D.; Sanchez, A., Molecular biology and evolution of filoviruses. *Arch Virol Suppl* **1993,** *7*, 81-100.

3.   Suzuki, Y.; Gojobori, T., The origin and evolution of Ebola and Marburg viruses. *Mol Biol Evol* **1997,** *14* (8), 800-6.

4.   Richman, D. D.; Cleveland, P. H.; McCormick, J. B.; Johnson, K. M., Antigenic analysis of strains of Ebola virus: identification of two Ebola virus serotypes. *J Infect Dis* **1983,** *147* (2), 268-71.

5.   Kiley, M. P.; Cox, N. J.; Elliott, L. H.; Sanchez, A.; DeFries, R.; Buchmeier, M. J.; Richman, D. D.; McCormick, J. B., Physicochemical properties of Marburg virus: evidence for three distinct virus strains and their relationship to Ebola virus. *J Gen Virol* **1988,** *69 (Pt 8)*, 1957-67.

6.   Feldmann, H.; Muhlberger, E.; Randolf, A.; Will, C.; Kiley, M. P.; Sanchez, A.; Klenk, H. D., Marburg virus, a filovirus: messenger RNAs, gene order, and regulatory elements of the replication cycle. *Virus Res* **1992,** *24* (1), 1-19.

7.   Sanchez, A.; Trappier, S. G.; Mahy, B. W.; Peters, C. J.; Nichol, S. T., The virion glycoproteins of Ebola viruses are encoded in two reading frames and are expressed through transcriptional editing. *Proc Natl Acad Sci U S A* **1996,** *93* (8), 3602-7.

8.   Dolnik, O.; Kolesnikova, L.; Becker, S., Filoviruses: Interactions with the host cell. *Cellular and Molecular Life Sciences* **2008,** *65* (5), 756-776.

9.   Kuhn, J. H., Filoviruses. A compendium of 40 years of epidemiological, clinical, and laboratory studies. *Arch Virol Suppl* **2008,** *20*, 13-360.

10.   Yang, Z. Y.; Duckers, H. J.; Sullivan, N. J.; Sanchez, A.; Nabel, E. G.; Nabel, G. J., Identification of the Ebola virus glycoprotein as the main viral determinant of vascular cell cytotoxicity and injury. *Nat Med* **2000,** *6* (8), 886-9.

11.   Adam, B.; Lins, L.; Stroobant, V.; Thomas, A.; Brasseur, R., Distribution of hydrophobic residues is crucial for the fusogenic properties of the Ebola virus GP2 fusion peptide. *J Virol* **2004,** *78* (4), 2131-6.

12.   Formenty, P.; Hatz, C.; Le Guenno, B.; Stoll, A.; Rogenmoser, P.; Widmer, A., Human infection due to Ebola virus, subtype Cote d'Ivoire: clinical and biologic presentation. *J Infect Dis* **1999,** *179 Suppl 1*, S48-53.

13.   Le Guenno, B.; Formenty, P.; Boesch, C., Ebola virus outbreaks in the Ivory Coast and Liberia, 1994-1995. *Curr Top Microbiol Immunol* **1999,** *235*, 77-84.

14.   Towner, J. S.; Sealy, T. K.; Khristova, M. L.; Albarino, C. G.; Conlan, S.; Reeder, S. A.; Quan, P. L.; Lipkin, W. I.; Downing, R.; Tappero, J. W.; Okware, S.; Lutwama, J.; Bakamutumaho, B.; Kayiwa, J.; Comer, J. A.; Rollin, P. E.; Ksiazek, T. G.; Nichol, S. T., Newly discovered ebola virus associated with hemorrhagic fever outbreak in Uganda. *PLoS Pathog* **2008,** *4* (11), e1000212.

15.   Calain, P.; Monroe, M. C.; Nichol, S. T., Ebola virus defective interfering particles and persistent infection. *Virology* **1999,** *262* (1), 114-28.

16.   Huang, Y.; Xu, L.; Sun, Y.; Nabel, G. J., The assembly of Ebola virus nucleocapsid requires virion-associated proteins 35 and 24 and posttranslational modification of nucleoprotein. *Mol Cell* **2002,** *10* (2), 307-16.

17.   Noda, T.; Aoyama, K.; Sagara, H.; Kida, H.; Kawaoka, Y., Nucleocapsid-like structures of Ebola virus reconstructed using electron tomography. *J Vet Med Sci* **2005,** *67* (3), 325-8.

18.   Noda, T.; Ebihara, H.; Muramoto, Y.; Fujii, K.; Takada, A.; Sagara, H.; Kim, J. H.; Kida, H.; Feldmann, H.; Kawaoka, Y., Assembly and budding of Ebolavirus. *PLoS Pathog* **2006,** *2* (9), e99.

19.   Watanabe, S.; Noda, T.; Kawaoka, Y., Functional mapping of the nucleoprotein of Ebola virus. *J Virol* **2006,** *80* (8), 3743-51.

20.   Modrof, J.; Muhlberger, E.; Klenk, H. D.; Becker, S., Phosphorylation of VP30 impairs ebola virus transcription. *J Biol Chem* **2002,** *277* (36), 33099-104.

21.   Hartlieb, B.; Muziol, T.; Weissenhorn, W.; Becker, S., Crystal structure of the C-terminal domain of Ebola virus VP30 reveals a role in transcription and nucleocapsid association. *Proc Natl Acad Sci U S A* **2007,** *104* (2), 624-9.

22.   John, S. P.; Wang, T.; Steffen, S.; Longhi, S.; Schmaljohn, C. S.; Jonsson, C. B., Ebola virus VP30 is an RNA binding protein. *J Virol* **2007,** *81* (17), 8967-76.

23.   Elliott, L. H.; Kiley, M. P.; McCormick, J. B., Descriptive analysis of Ebola virus proteins. *Virology* **1985,** *147* (1), 169-76.

24.   Ruigrok, R. W.; Schoehn, G.; Dessen, A.; Forest, E.; Volchkov, V.; Dolnik, O.; Klenk, H. D.; Weissenhorn, W., Structural characterization and membrane binding properties of the matrix protein VP40 of Ebola virus. *J Mol Biol* **2000,** *300* (1), 103-12.

25.   Timmins, J.; Schoehn, G.; Kohlhaas, C.; Klenk, H. D.; Ruigrok, R. W.; Weissenhorn, W., Oligomerization and polymerization of the filovirus matrix protein VP40. *Virology* **2003,** *312* (2), 359-68.

26.   Licata, J. M.; Johnson, R. F.; Han, Z.; Harty, R. N., Contribution of ebola virus glycoprotein, nucleoprotein, and VP24 to budding of VP40 virus-like particles. *J Virol* **2004,** *78* (14), 7344-51.

27.   Licata, J. M.; Simpson-Holley, M.; Wright, N. T.; Han, Z.; Paragas, J.; Harty, R. N., Overlapping motifs (PTAP and PPEY) within the Ebola virus VP40 protein function independently as late budding domains: involvement of host proteins TSG101 and VPS-4. *J Virol* **2003,** *77* (3), 1812-9.

28.   Timmins, J.; Scianimanico, S.; Schoehn, G.; Weissenhorn, W., Vesicular release of ebola virus matrix protein VP40. *Virology* **2001,** *283* (1), 1-6.

29.   Bukreyev, A. A.; Belanov, E. F.; Blinov, V. M.; Netesov, S. V., Complete nucleotide sequences of Marburg virus genes 5 and 6 encoding VP30 and VP24 proteins. *Biochem Mol Biol Int* **1995,** *35* (3), 605-13.

30.   Ruthel, G.; Demmin, G. L.; Kallstrom, G.; Javid, M. P.; Badie, S. S.; Will, A. B.; Nelle, T.; Schokman, R.; Nguyen, T. L.; Carra, J. H.; Bavari, S.; Aman, M. J., Association of ebola virus matrix protein VP40 with microtubules. *J Virol* **2005,** *79* (8), 4709-19.

31.   Becker, S.; Rinne, C.; Hofsass, U.; Klenk, H. D.; Muhlberger, E., Interactions of Marburg virus nucleocapsid proteins. *Virology* **1998,** *249* (2), 406-17.

32.   Bamberg, S.; Kolesnikova, L.; Moller, P.; Klenk, H. D.; Becker, S., VP24 of Marburg virus influences formation of infectious particles. *J Virol* **2005,** *79* (21), 13421-33.

33.   Valmas, C.; Grosch, M. N.; Schumann, M.; Olejnik, J.; Martinez, O.; Best, S. M.; Krahling, V.; Basler, C. F.; Muhlberger, E., Marburg virus evades interferon responses by a mechanism distinct from ebola virus. *PLoS Pathog 6* (1), e1000721.

34.   Mateo, M.; Reid, S. P.; Leung, L. W.; Basler, C. F.; Volchkov, V. E., Ebolavirus VP24 binding to karyopherins is required for inhibition of interferon signaling. *J Virol 84* (2), 1169-75.

35.   Moller, P.; Pariente, N.; Klenk, H. D.; Becker, S., Homo-oligomerization of Marburgvirus VP35 is essential for its function in replication and transcription. *J Virol* **2005,** *79* (23), 14876-86.

36.   Groseth, A.; Charton, J. E.; Sauerborn, M.; Feldmann, F.; Jones, S. M.; Hoenen, T.; Feldmann, H., The Ebola virus ribonucleoprotein complex: a novel VP30-L interaction identified. *Virus Res* **2009,** *140* (1-2), 8-14.

37.   Johnson, R. F.; McCarthy, S. E.; Godlewski, P. J.; Harty, R. N., Ebola virus VP35-VP40 interaction is sufficient for packaging 3E-5E minigenome RNA into virus-like particles. *J Virol* **2006,** *80* (11), 5135-44.

38.   Haasnoot, J.; de Vries, W.; Geutjes, E. J.; Prins, M.; de Haan, P.; Berkhout, B., The Ebola virus VP35 protein is a suppressor of RNA silencing. *PLoS Pathog* **2007,** *3* (6), e86.

39.   Basler, C. F.; Wang, X.; Muhlberger, E.; Volchkov, V.; Paragas, J.; Klenk, H. D.; Garcia-Sastre, A.; Palese, P., The Ebola virus VP35 protein functions as a type I IFN antagonist. *Proc Natl Acad Sci U S A* **2000,** *97* (22), 12289-94.

40.   Cardenas, W. B.; Loo, Y. M.; Gale, M., Jr.; Hartman, A. L.; Kimberlin, C. R.; Martinez-Sobrido, L.; Saphire, E. O.; Basler, C. F., Ebola virus VP35 protein binds double-stranded RNA and inhibits alpha/beta interferon production induced by RIG-I signaling. *J Virol* **2006,** *80* (11), 5168-78.

41.   Feng, Z.; Cerveny, M.; Yan, Z.; He, B., The VP35 protein of Ebola virus inhibits the antiviral effect mediated by double-stranded RNA-dependent protein kinase PKR. *J Virol* **2007,** *81* (1), 182-92.

42.   Towner, J. S.; Khristova, M. L.; Sealy, T. K.; Vincent, M. J.; Erickson, B. R.; Bawiec, D. A.; Hartman, A. L.; Comer, J. A.; Zaki, S. R.; Stroher, U.; Gomes da Silva, F.; del Castillo, F.; Rollin, P. E.; Ksiazek, T. G.; Nichol, S. T., Marburgvirus genomics and association with a large hemorrhagic fever outbreak in Angola. *J Virol* **2006,** *80* (13), 6497-516.

43.   Volchkov, V. E.; Volchkova, V. A.; Chepurnov, A. A.; Blinov, V. M.; Dolnik, O.; Netesov, S. V.; Feldmann, H., Characterization of the L gene and 5' trailer region of Ebola virus. *J Gen Virol* **1999,** *80 (Pt 2)*, 355-62.

44.   Volchkov, V. E.; Becker, S.; Volchkova, V. A.; Ternovoj, V. A.; Kotov, A. N.; Netesov, S. V.; Klenk, H. D., GP mRNA of Ebola virus is edited by the Ebola virus polymerase and by T7 and vaccinia virus polymerases. *Virology* **1995,** *214* (2), 421-30.

45.   Volchkova, V. A.; Feldmann, H.; Klenk, H. D.; Volchkov, V. E., The nonstructural small glycoprotein sGP of Ebola virus is secreted as an antiparallel-orientated homodimer. *Virology* **1998,** *250* (2), 408-14.

46.   Sanchez, A.; Yang, Z. Y.; Xu, L.; Nabel, G. J.; Crews, T.; Peters, C. J., Biochemical analysis of the secreted and virion glycoproteins of Ebola virus. *J Virol* **1998,** *72* (8), 6442-7.

47.   Falzarano, D.; Krokhin, O.; Wahl-Jensen, V.; Seebach, J.; Wolf, K.; Schnittler, H. J.; Feldmann, H., Structure-function analysis of the soluble glycoprotein, sGP, of Ebola virus. *Chembiochem* **2006,** *7* (10), 1605-11.

48.   Barrientos, L. G.; Martin, A. M.; Rollin, P. E.; Sanchez, A., Disulfide bond assignment of the Ebola virus secreted glycoprotein SGP. *Biochem Biophys Res Commun* **2004,** *323* (2), 696-702.

49.   Falzarano, D.; Krokhin, O.; Van Domselaar, G.; Wolf, K.; Seebach, J.; Schnittler, H. J.; Feldmann, H., Ebola sGP--the first viral glycoprotein shown to be C-mannosylated. *Virology* **2007,** *368* (1), 83-90.

50.   Ito, H.; Watanabe, S.; Takada, A.; Kawaoka, Y., Ebola virus glycoprotein: proteolytic processing, acylation, cell tropism, and detection of neutralizing antibodies. *J Virol* **2001,** *75* (3), 1576-80.

51.   Dolnik, O.; Volchkova, V.; Garten, W.; Carbonnelle, C.; Becker, S.; Kahnt, J.; Stroher, U.; Klenk, H. D.; Volchkov, V., Ectodomain shedding of the glycoprotein GP of Ebola virus. *Embo J* **2004,** *23* (10), 2175-84.

52.   Wool-Lewis, R. J.; Bates, P., Endoproteolytic processing of the ebola virus envelope glycoprotein: cleavage is not required for function. *J Virol* **1999,** *73* (2), 1419-26.

53.   Ascenzi, P.; Bocedi, A.; Heptonstall, J.; Capobianchi, M. R.; Di Caro, A.; Mastrangelo, E.; Bolognesi, M.; Ippolito, G., Ebolavirus and Marburgvirus: insight the Filoviridae family. *Mol Aspects Med* **2008,** *29* (3), 151-85.

54. Chandran, K.; Sullivan, N. J.; Felbor, U.; Whelan, S. P.; Cunningham, J. M., Endosomal proteolysis of the Ebola virus glycoprotein is necessary for infection. *Science* **2005,** *308* (5728), 1643-5.

55. Schornberg, K.; Matsuyama, S.; Kabsch, K.; Delos, S.; Bouton, A.; White, J., Role of endosomal cathepsins in entry mediated by the Ebola virus glycoprotein. *J Virol* **2006,** *80* (8), 4174-8.

56. White, J. M.; Delos, S. E.; Brecher, M.; Schornberg, K., Structures and mechanisms of viral membrane fusion proteins: multiple variations on a common theme. *Crit Rev Biochem Mol Biol* **2008,** *43* (3), 189-219.

57. Marsh, M.; Helenius, A., Virus entry: open sesame. *Cell* **2006,** *124* (4), 729-40.

58. Simmons, G.; Gosalia, D. N.; Rennekamp, A. J.; Reeves, J. D.; Diamond, S. L.; Bates, P., Inhibitors of cathepsin L prevent severe acute respiratory syndrome coronavirus entry. *Proc Natl Acad Sci U S A* **2005,** *102* (33), 11876-81.

59. Damico, R. L.; Crane, J.; Bates, P., Receptor-triggered membrane association of a model retroviral glycoprotein. *Proc Natl Acad Sci U S A* **1998,** *95* (5), 2580-5.

60. Hernandez, L. D.; Peters, R. J.; Delos, S. E.; Young, J. A.; Agard, D. A.; White, J. M., Activation of a retroviral membrane fusion protein: soluble receptor-induced liposome binding of the ALSV envelope glycoprotein. *J Cell Biol* **1997,** *139* (6), 1455-64.

61. Mothes, W.; Boerger, A. L.; Narayan, S.; Cunningham, J. M.; Young, J. A., Retroviral entry mediated by receptor priming and low pH triggering of an envelope glycoprotein. *Cell* **2000,** *103* (4), 679-89.

62. Albritton, L. M.; Tseng, L.; Scadden, D.; Cunningham, J. M., A putative murine ecotropic retrovirus receptor gene encodes a multiple membrane-spanning protein and confers susceptibility to virus infection. *Cell* **1989,** *57* (4), 659-66.

63. Ebert, D. H.; Deussing, J.; Peters, C.; Dermody, T. S., Cathepsin L and cathepsin B mediate reovirus disassembly in murine fibroblast cells. *J Biol Chem* **2002,** *277* (27), 24609-17.

64. Miyauchi, K.; Kim, Y.; Latinovic, O.; Morozov, V.; Melikyan, G. B., HIV enters cells via endocytosis and dynamin-dependent fusion with endosomes. *Cell* **2009,** *137* (3), 433-44.

65. Hogle, J. M., Poliovirus cell entry: common structural themes in viral cell entry pathways. *Annu Rev Microbiol* **2002,** *56*, 677-702.

66. Manicassamy, B.; Wang, J.; Jiang, H.; Rong, L., Comprehensive analysis of ebola virus GP1 in viral entry. *J Virol* **2005,** *79* (8), 4793-805.

67. Manicassamy, B.; Wang, J.; Rumschlag, E.; Tymen, S.; Volchkova, V.; Volchkov, V.; Rong, L., Characterization of Marburg virus glycoprotein in viral entry. *Virology* **2007,** *358* (1), 79-88.

68. Kuhn, J. H.; Radoshitzky, S. R.; Guth, A. C.; Warfield, K. L.; Li, W.; Vincent, M. J.; Towner, J. S.; Nichol, S. T.; Bavari, S.; Choe, H.; Aman, M. J.; Farzan, M., Conserved receptor-binding domains of Lake Victoria marburgvirus and Zaire ebolavirus bind a common receptor. *J Biol Chem* **2006,** *281* (23), 15951-8.

69. Chan, S. Y.; Ma, M. C.; Goldsmith, M. A., Differential induction of cellular detachment by envelope glycoproteins of Marburg and Ebola (Zaire) viruses. *J Gen Virol* **2000,** *81* (Pt 9), 2155-9.

70. Simmons, G.; Wool-Lewis, R. J.; Baribaud, F.; Netter, R. C.; Bates, P., Ebola virus glycoproteins induce global surface protein down-modulation and loss of cell adherence. *J Virol* **2002,** *76* (5), 2518-28.

71. Takada, A.; Watanabe, S.; Ito, H.; Okazaki, K.; Kida, H.; Kawaoka, Y., Downregulation of beta1 integrins by Ebola virus glycoprotein: implication for virus entry. *Virology* **2000,** *278* (1), 20-6.

72. Yonezawa, A.; Cavrois, M.; Greene, W. C., Studies of ebola virus glycoprotein-mediated entry and fusion by using pseudotyped human immunodeficiency virus type 1 virions: involvement of cytoskeletal proteins and enhancement by tumor necrosis factor alpha. *J Virol* **2005,** *79* (2), 918-26.

73. Swanson, J. A., Shaping cups into phagosomes and macropinosomes. *Nat Rev Mol Cell Biol* **2008,** *9* (8), 639-49.

74. Hewlett, L. J.; Prescott, A. R.; Watts, C., The coated pit and macropinocytic pathways serve distinct endosome populations. *J Cell Biol* **1994,** *124* (5), 689-703.

75. Amstutz, B.; Gastaldelli, M.; Kalin, S.; Imelli, N.; Boucke, K.; Wandeler, E.; Mercer, J.; Hemmi, S.; Greber, U. F., Subversion of CtBP1-controlled macropinocytosis by human adenovirus serotype 3. *Embo J* **2008,** *27* (7), 956-69.

76. Coyne, C. B.; Shen, L.; Turner, J. R.; Bergelson, J. M., Coxsackievirus entry across epithelial tight junctions requires occludin and the small GTPases Rab34 and Rab5. *Cell Host Microbe* **2007,** *2* (3), 181-92.

77. Matilainen, H.; Rinne, J.; Gilbert, L.; Marjomaki, V.; Reunanen, H.; Oker-Blom, C., Baculovirus entry into human hepatoma cells. *J Virol* **2005,** *79* (24), 15452-9.

78. Kee, S. H.; Cho, E. J.; Song, J. W.; Park, K. S.; Baek, L. J.; Song, K. J., Effects of endocytosis inhibitory drugs on rubella virus entry into VeroE6 cells. *Microbiol Immunol* **2004,** *48* (11), 823-9.

79. Liu, N. Q.; Lossinsky, A. S.; Popik, W.; Li, X.; Gujuluva, C.; Kriederman, B.; Roberts, J.; Pushkarsky, T.; Bukrinsky, M.; Witte, M.; Weinand, M.; Fiala, M., Human immunodeficiency virus type 1 enters brain microvascular endothelia by macropinocytosis dependent on lipid rafts and the mitogen-activated protein kinase signaling pathway. *J Virol* **2002,** *76* (13), 6689-700.

80. Marechal, V.; Prevost, M. C.; Petit, C.; Perret, E.; Heard, J. M.; Schwartz, O., Human immunodeficiency virus type 1 entry into macrophages mediated by macropinocytosis. *J Virol* **2001,** *75* (22), 11166-77.

81.   Mercer, J.; Helenius, A., Vaccinia virus uses macropinocytosis and apoptotic mimicry to enter host cells. *Science* **2008,** *320* (5875), 531-5.

82.   Karjalainen, M.; Kakkonen, E.; Upla, P.; Paloranta, H.; Kankaanpaa, P.; Liberali, P.; Renkema, G. H.; Hyypia, T.; Heino, J.; Marjomaki, V., A Raft-derived, Pak1-regulated entry participates in alpha2beta1 integrin-dependent sorting to caveosomes. *Mol Biol Cell* **2008,** *19* (7), 2857-69.

83.   Nicola, A. V.; McEvoy, A. M.; Straus, S. E., Roles for endocytosis and low pH in herpes simplex virus entry into HeLa and Chinese hamster ovary cells. *J Virol* **2003,** *77* (9), 5324-32.

84.   Gu, H.; Botelho, R. J.; Yu, M.; Grinstein, S.; Neel, B. G., Critical role for scaffolding adapter Gab2 in Fc gamma R-mediated phagocytosis. *J Cell Biol* **2003,** *161* (6), 1151-61.

85.   Amyere, M.; Payrastre, B.; Krause, U.; Van Der Smissen, P.; Veithen, A.; Courtoy, P. J., Constitutive macropinocytosis in oncogene-transformed fibroblasts depends on sequential permanent activation of phosphoinositide 3-kinase and phospholipase C. *Mol Biol Cell* **2000,** *11* (10), 3453-67.

86.   Donepudi, M.; Resh, M. D., c-Src trafficking and co-localization with the EGF receptor promotes EGF ligand-independent EGF receptor activation and signaling. *Cell Signal* **2008,** *20* (7), 1359-67.

87.   Conner, S. D.; Schmid, S. L., Regulated portals of entry into the cell. *Nature* **2003,** *422* (6927), 37-44.

88.   Cao, H.; Chen, J.; Awoniyi, M.; Henley, J. R.; McNiven, M. A., Dynamin 2 mediates fluid-phase micropinocytosis in epithelial cells. *J Cell Sci* **2007,** *120* (Pt 23), 4167-77.

89.   Parton, R. G.; Simons, K., The multiple faces of caveolae. *Nat Rev Mol Cell Biol* **2007,** *8* (3), 185-94.

90.   Sanchez, A., Analysis of filovirus entry into vero e6 cells, using inhibitors of endocytosis, endosomal acidification, structural integrity, and cathepsin (B and L) activity. *J Infect Dis* **2007,** *196 Suppl 2*, S251-8.

91.   Empig, C. J.; Goldsmith, M. A., Association of the caveola vesicular system with cellular entry by filoviruses. *J Virol* **2002,** *76* (10), 5266-70.

92.   Grant, B. D.; Donaldson, J. G., Pathways and mechanisms of endocytic recycling. *Nat Rev Mol Cell Biol* **2009,** *10* (9), 597-608.

93.   Brindley, M. A.; Maury, W., Equine infectious anemia virus entry occurs through clathrin-mediated endocytosis. *J Virol* **2008,** *82* (4), 1628-37.

94.   Bhattacharyya, S.; Warfield, K. L.; Ruthel, G.; Bavari, S.; Aman, M. J.; Hope, T. J., Ebola virus uses clathrin-mediated endocytosis as an entry pathway. *Virology*.

95.   Chan, S. Y.; Speck, R. F.; Ma, M. C.; Goldsmith, M. A., Distinct mechanisms of entry by envelope glycoproteins of Marburg and Ebola (Zaire) viruses. *J Virol* **2000,** *74* (10), 4933-7.

96.   Turell, M. J.; Bressler, D. S.; Rossi, C. A., Short report: lack of virus replication in arthropods after intrathoracic inoculation of Ebola Reston virus. *Am J Trop Med Hyg* **1996,** *55* (1), 89-90.

97.   Dowling, W.; Thompson, E.; Badger, C.; Mellquist, J. L.; Garrison, A. R.; Smith, J. M.; Paragas, J.; Hogan, R. J.; Schmaljohn, C., Influences of glycosylation on antigenicity, immunogenicity, and protective efficacy of ebola virus GP DNA vaccines. *J Virol* **2007,** *81* (4), 1821-37.

98.   Lin, G.; Simmons, G.; Pohlmann, S.; Baribaud, F.; Ni, H.; Leslie, G. J.; Haggarty, B. S.; Bates, P.; Weissman, D.; Hoxie, J. A.; Doms, R. W., Differential N-linked glycosylation of human immunodeficiency virus and Ebola virus envelope glycoproteins modulates interactions with DC-SIGN and DC-SIGNR. *J Virol* **2003,** *77* (2), 1337-46.

99.   Jeffers, S. A.; Sanders, D. A.; Sanchez, A., Covalent modifications of the ebola virus glycoprotein. *J Virol* **2002,** *76* (24), 12463-72.

100.   Dolnik, O.; Kolesnikova, L.; Becker, S., Filoviruses: Interactions with the host cell. *Cell Mol Life Sci* **2008,** *65* (5), 756-76.

101.   Hoenen, T.; Groseth, A.; Falzarano, D.; Feldmann, H., Ebola virus: unravelling pathogenesis to combat a deadly disease. *Trends Mol Med* **2006,** *12* (5), 206-15.

102.   Cambi, A.; Koopman, M.; Figdor, C. G., How C-type lectins detect pathogens. *Cell Microbiol* **2005,** *7* (4), 481-8.

103.   Marzi, A.; Moller, P.; Hanna, S. L.; Harrer, T.; Eisemann, J.; Steinkasserer, A.; Becker, S.; Baribaud, F.; Pohlmann, S., Analysis of the interaction of Ebola virus glycoprotein with DC-SIGN (dendritic cell-specific intercellular adhesion molecule 3-grabbing nonintegrin) and its homologue DC-SIGNR. *J Infect Dis* **2007,** *196 Suppl 2*, S237-46.

104.   Marzi, A.; Gramberg, T.; Simmons, G.; Moller, P.; Rennekamp, A. J.; Krumbiegel, M.; Geier, M.; Eisemann, J.; Turza, N.; Saunier, B.; Steinkasserer, A.; Becker, S.; Bates, P.; Hofmann, H.; Pohlmann, S., DC-SIGN and DC-SIGNR interact with the glycoprotein of Marburg virus and the S protein of severe acute respiratory syndrome coronavirus. *J Virol* **2004,** *78* (21), 12090-5.

105.   Simmons, G.; Reeves, J. D.; Grogan, C. C.; Vandenberghe, L. H.; Baribaud, F.; Whitbeck, J. C.; Burke, E.; Buchmeier, M. J.; Soilleux, E. J.; Riley, J. L.; Doms, R. W.; Bates, P.; Pohlmann, S., DC-SIGN and DC-SIGNR bind ebola glycoproteins and enhance infection of macrophages and endothelial cells. *Virology* **2003,** *305* (1), 115-23.

106.   Takada, A.; Fujioka, K.; Tsuiji, M.; Morikawa, A.; Higashi, N.; Ebihara, H.; Kobasa, D.; Feldmann, H.; Irimura, T.; Kawaoka, Y., Human macrophage C-type lectin specific for galactose and N-acetylgalactosamine promotes filovirus entry. *J Virol* **2004,** *78* (6), 2943-7.

107.   Alvarez, C. P.; Lasala, F.; Carrillo, J.; Muniz, O.; Corbi, A. L.; Delgado, R., C-type lectins DC-SIGN and L-SIGN mediate cellular entry by Ebola virus in cis and in trans. *J Virol* **2002,** *76* (13), 6841-4.

108. Baribaud, F.; Doms, R. W.; Pohlmann, S., The role of DC-SIGN and DC-SIGNR in HIV and Ebola virus infection: can potential therapeutics block virus transmission and dissemination? *Expert Opin Ther Targets* **2002,** *6* (4), 423-31.

109. Geijtenbeek, T. B.; van Kooyk, Y., Pathogens target DC-SIGN to influence their fate DC-SIGN functions as a pathogen receptor with broad specificity. *APMIS* **2003,** *111* (7-8), 698-714.

110. Arnaout, M. A.; Mahalingam, B.; Xiong, J. P., Integrin structure, allostery, and bidirectional signaling. *Annu Rev Cell Dev Biol* **2005,** *21*, 381-410.

111. Schornberg, K. L.; Shoemaker, C. J.; Dube, D.; Abshire, M. Y.; Delos, S. E.; Bouton, A. H.; White, J. M., Alpha5beta1-integrin controls ebolavirus entry by regulating endosomal cathepsins. *Proc Natl Acad Sci U S A* **2009,** *106* (19), 8003-8.

112. Chan, S. Y.; Empig, C. J.; Welte, F. J.; Speck, R. F.; Schmaljohn, A.; Kreisberg, J. F.; Goldsmith, M. A., Folate receptor-alpha is a cofactor for cellular entry by Marburg and Ebola viruses. *Cell* **2001,** *106* (1), 117-26.

113. Sinn, P. L.; Hickey, M. A.; Staber, P. D.; Dylla, D. E.; Jeffers, S. A.; Davidson, B. L.; Sanders, D. A.; McCray, P. B., Jr., Lentivirus vectors pseudotyped with filoviral envelope glycoproteins transduce airway epithelia from the apical surface independently of folate receptor alpha. *J Virol* **2003,** *77* (10), 5902-10.

114. Simmons, G.; Rennekamp, A. J.; Chai, N.; Vandenberghe, L. H.; Riley, J. L.; Bates, P., Folate receptor alpha and caveolae are not required for Ebola virus glycoprotein-mediated viral infection. *J Virol* **2003,** *77* (24), 13433-8.

115. Shimojima, M.; Takada, A.; Ebihara, H.; Neumann, G.; Fujioka, K.; Irimura, T.; Jones, S.; Feldmann, H.; Kawaoka, Y., Tyro3 family-mediated cell entry of Ebola and Marburg viruses. *J Virol* **2006,** *80* (20), 10109-16.

116. Shimojima, M.; Ikeda, Y.; Kawaoka, Y., The mechanism of Axl-mediated Ebola virus infection. *J Infect Dis* **2007,** *196 Suppl 2*, S259-63.

117. Linger, R. M.; Keating, A. K.; Earp, H. S.; Graham, D. K., TAM receptor tyrosine kinases: biologic functions, signaling, and potential therapeutic targeting in human cancer. *Adv Cancer Res* **2008,** *100*, 35-83.

118. Hafizi, S.; Dahlback, B., Gas6 and protein S. Vitamin K-dependent ligands for the Axl receptor tyrosine kinase subfamily. *FEBS J* **2006,** *273* (23), 5231-44.

119. Jaluria, P.; Chu, C.; Betenbaugh, M.; Shiloach, J., Cells by design: a mini-review of targeting cell engineering using DNA microarrays. *Mol Biotechnol* **2008,** *39* (2), 105-11.

120. Melaragno, M. G.; Cavet, M. E.; Yan, C.; Tai, L. K.; Jin, Z. G.; Haendeler, J.; Berk, B. C., Gas6 inhibits apoptosis in vascular smooth muscle: role of Axl kinase and Akt. *J Mol Cell Cardiol* **2004,** *37* (4), 881-7.

121. Brindley, M. A.; Hughes, L.; Ruiz, A.; McCray, P. B., Jr.; Sanchez, A.; Sanders, D. A.; Maury, W., Ebola virus glycoprotein 1: identification of residues important for binding and postbinding events. *J Virol* **2007,** *81* (14), 7702-9.

122. Neumann, G.; Feldmann, H.; Watanabe, S.; Lukashevich, I.; Kawaoka, Y., Reverse genetics demonstrates that proteolytic processing of the Ebola virus glycoprotein is not essential for replication in cell culture. *J Virol* **2002,** *76* (1), 406-10.

123. Watanabe, S.; Takada, A.; Watanabe, T.; Ito, H.; Kida, H.; Kawaoka, Y., Functional importance of the coiled-coil of the Ebola virus glycoprotein. *J Virol* **2000,** *74* (21), 10194-201.

124. Quinn, K.; Brindley, M. A.; Weller, M. L.; Kaludov, N.; Kondratowicz, A.; Hunt, C. L.; Sinn, P. L.; McCray, P. B., Jr.; Stein, C. S.; Davidson, B. L.; Flick, R.; Mandell, R.; Staplin, W.; Maury, W.; Chiorini, J. A., Rho GTPases modulate entry of Ebola virus and vesicular stomatitis virus pseudotyped vectors. *J Virol* **2009,** *83* (19), 10176-86.

125. Sinn, P. L.; Goreham-Voss, J. D.; Arias, A. C.; Hickey, M. A.; Maury, W.; Chikkanna-Gowda, C. P.; McCray, P. B., Jr., Enhanced gene expression conferred by stepwise modification of a nonprimate lentiviral vector. *Hum Gene Ther* **2007,** *18* (12), 1244-52.

126. Johnson, R. F.; Bell, P.; Harty, R. N., Effect of Ebola virus proteins GP, NP and VP35 on VP40 VLP morphology. *Virol J* **2006,** *3*, 31.

127. Johnston, J. C.; Gasmi, M.; Lim, L. E.; Elder, J. H.; Yee, J. K.; Jolly, D. J.; Campbell, K. P.; Davidson, B. L.; Sauter, S. L., Minimum requirements for efficient transduction of dividing and nondividing cells by feline immunodeficiency virus vectors. *J Virol* **1999,** *73* (6), 4991-5000.

128. Takada, A.; Robison, C.; Goto, H.; Sanchez, A.; Murti, K. G.; Whitt, M. A.; Kawaoka, Y., A system for functional analysis of Ebola virus glycoprotein. *Proc Natl Acad Sci U S A* **1997,** *94* (26), 14764-9.

129. Johannsdottir, H. K.; Mancini, R.; Kartenbeck, J.; Amato, L.; Helenius, A., Host cell factors and functions involved in vesicular stomatitis virus entry. *J Virol* **2009,** *83* (1), 440-53.

130. Imported case of Marburg hemorrhagic fever - Colorado, 2008. *MMWR Morb Mortal Wkly Rep* **2009,** *58* (49), 1377-81.

131. Leroy, E. M.; Kumulungui, B.; Pourrut, X.; Rouquet, P.; Hassanin, A.; Yaba, P.; Delicat, A.; Paweska, J. T.; Gonzalez, J. P.; Swanepoel, R., Fruit bats as reservoirs of Ebola virus. *Nature* **2005,** *438* (7068), 575-6.

132. Towner, J. S.; Amman, B. R.; Sealy, T. K.; Carroll, S. A.; Comer, J. A.; Kemp, A.; Swanepoel, R.; Paddock, C. D.; Balinandi, S.; Khristova, M. L.; Formenty, P. B.; Albarino, C. G.; Miller, D. M.; Reed, Z. D.; Kayiwa, J. T.; Mills, J. N.; Cannon, D. L.; Greer, P. W.; Byaruhanga, E.; Farnon, E. C.; Atimnedi, P.; Okware, S.; Katongole-Mbidde, E.; Downing, R.; Tappero, J. W.; Zaki, S. R.; Ksiazek, T. G.; Nichol, S. T.; Rollin, P. E., Isolation of genetically diverse Marburg viruses from Egyptian fruit bats. *PLoS Pathog* **2009,** *5* (7), e1000536.

133.   Towner, J. S.; Pourrut, X.; Albarino, C. G.; Nkogue, C. N.; Bird, B. H.; Grard, G.;
        Ksiazek, T. G.; Gonzalez, J. P.; Nichol, S. T.; Leroy, E. M., Marburg virus
        infection detected in a common African bat. *PLoS ONE* **2007,** *2* (1), e764.

134.   Gonzalez, J. P.; Pourrut, X.; Leroy, E., Ebolavirus and other filoviruses. *Curr Top
        Microbiol Immunol* **2007,** *315*, 363-87.

135.   Groseth, A.; Feldmann, H.; Strong, J. E., The ecology of Ebola virus. *Trends
        Microbiol* **2007,** *15* (9), 408-16.

136.   Swanepoel, R.; Smit, S. B.; Rollin, P. E.; Formenty, P.; Leman, P. A.; Kemp, A.;
        Burt, F. J.; Grobbelaar, A. A.; Croft, J.; Bausch, D. G.; Zeller, H.; Leirs, H.;
        Braack, L. E.; Libande, M. L.; Zaki, S.; Nichol, S. T.; Ksiazek, T. G.; Paweska, J.
        T., Studies of reservoir hosts for Marburg virus. *Emerg Infect Dis* **2007,** *13* (12),
        1847-51.

137.   Pourrut, X.; Souris, M.; Towner, J. S.; Rollin, P. E.; Nichol, S. T.; Gonzalez, J. P.;
        Leroy, E., Large serological survey showing cocirculation of Ebola and Marburg
        viruses in Gabonese bat populations, and a high seroprevalence of both viruses in
        Rousettus aegyptiacus. *BMC Infect Dis* **2009,** *9*, 159.

138.   van der Poel, W. H.; Lina, P. H.; Kramps, J. A., Public health awareness of
        emerging zoonotic viruses of bats: a European perspective. *Vector Borne
        Zoonotic Dis* **2006,** *6* (4), 315-24.

139.   Kuzmin, I. V.; Niezgoda, M.; Franka, R.; Agwanda, B.; Markotter, W.; Breiman,
        R. F.; Shieh, W. J.; Zaki, S. R.; Rupprecht, C. E., Marburg virus in fruit bat,
        Kenya. *Emerg Infect Dis 16* (2), 352-4.

140.   Patnaik, S. K.; Stanley, P., Lectin-resistant CHO glycosylation mutants. *Methods
        Enzymol* **2006,** *416*, 159-82.

141.   Chen, W.; Stanley, P., Five Lec1 CHO cell mutants have distinct Mgat1 gene
        mutations that encode truncated N-acetylglucosaminyltransferase I. *Glycobiology*
        2003, *13* (1), 43-50.

142.   Eckhardt, M.; Gotza, B.; Gerardy-Schahn, R., Mutants of the CMP-sialic acid
        transporter causing the Lec2 phenotype. *J Biol Chem* **1998,** *273* (32), 20189-95.

143.   Oelmann, S.; Stanley, P.; Gerardy-Schahn, R., Point mutations identified in Lec8
        Chinese hamster ovary glycosylation mutants that inactivate both the UDP-
        galactose and CMP-sialic acid transporters. *J Biol Chem* **2001,** *276* (28), 26291-
        300.

144.   Kingsley, D. M.; Kozarsky, K. F.; Hobbie, L.; Krieger, M., Reversible defects in
        O-linked glycosylation and LDL receptor expression in a UDP-Gal/UDP-GalNAc
        4-epimerase deficient mutant. *Cell* **1986,** *44* (5), 749-59.

145.   Tian, E.; Ten Hagen, K. G.; Shum, L.; Hang, H. C.; Imbert, Y.; Young, W. W.,
        Jr.; Bertozzi, C. R.; Tabak, L. A., An inhibitor of O-glycosylation induces
        apoptosis in NIH3T3 cells and developing mouse embryonic mandibular tissues. *J
        Biol Chem* **2004,** *279* (48), 50382-90.

146. Yan, Y.; Jung, Y. T.; Wu, T.; Kozak, C. A., Role of receptor polymorphism and glycosylation in syncytium induction and host range variation of ecotropic mouse gammaretroviruses. *Retrovirology* **2008,** *5*, 2.

147. Gramberg, T.; Hofmann, H.; Moller, P.; Lalor, P. F.; Marzi, A.; Geier, M.; Krumbiegel, M.; Winkler, T.; Kirchhoff, F.; Adams, D. H.; Becker, S.; Munch, J.; Pohlmann, S., LSECtin interacts with filovirus glycoproteins and the spike protein of SARS coronavirus. *Virology* **2005,** *340* (2), 224-36.

148. Park, J. O.; Chang, K. H.; Lee, H. H.; Chung, I. S., Biochemical analysis of Hyphantria cunea NPV attachment to Spodoptera frugiperda 21 cells. *Cytotechnology* **1999,** *31* (1-2), 159-163.

149. Ferreira, L.; Villar, E.; Munoz-Barroso, I., Gangliosides and N-glycoproteins function as Newcastle disease virus receptors. *Int J Biochem Cell Biol* **2004,** *36* (11), 2344-56.

150. Stevenson, R. A.; Huang, J. A.; Studdert, M. J.; Hartley, C. A., Sialic acid acts as a receptor for equine rhinitis A virus binding and infection. *J Gen Virol* **2004,** *85* (Pt 9), 2535-43.

151. Wang, J.; Babcock, G. J.; Choe, H.; Farzan, M.; Sodroski, J.; Gabuzda, D., N-linked glycosylation in the CXCR4 N-terminus inhibits binding to HIV-1 envelope glycoproteins. *Virology* **2004,** *324* (1), 140-50.

152. Wool-Lewis, R. J.; Bates, P., Characterization of Ebola virus entry by using pseudotyped viruses: identification of receptor-deficient cell lines. *J Virol* **1998,** *72* (4), 3155-60.

153. Yang, Z.; Delgado, R.; Xu, L.; Todd, R. F.; Nabel, E. G.; Sanchez, A.; Nabel, G. J., Distinct cellular interactions of secreted and transmembrane Ebola virus glycoproteins. *Science* **1998,** *279* (5353), 1034-7.

154. Sullivan, N.; Yang, Z. Y.; Nabel, G. J., Ebola virus pathogenesis: implications for vaccines and therapies. *J Virol* **2003,** *77* (18), 9733-7.

155. Nguyen, E. K.; Nemerow, G. R.; Smith, J. G., Direct evidence from single-cell analysis that human alpha-defensins block adenovirus uncoating to neutralize infection. *J Virol*.

156. Swimm, A. I.; Bornmann, W.; Jiang, M.; Imperiale, M. J.; Lukacher, A. E.; Kalman, D., Abl-family Tyrosine Kinases Regulate Sialylated Ganglioside Receptors for Polyomavirus. *J Virol*.

157. Ho, H. T.; Fan, L.; Nowicka-Sans, B.; McAuliffe, B.; Li, C. B.; Yamanaka, G.; Zhou, N.; Fang, H.; Dicker, I.; Dalterio, R.; Gong, Y. F.; Wang, T.; Yin, Z.; Ueda, Y.; Matiskella, J.; Kadow, J.; Clapham, P.; Robinson, J.; Colonno, R.; Lin, P. F., Envelope conformational changes induced by human immunodeficiency virus type 1 attachment inhibitors prevent CD4 binding and downstream entry events. *J Virol* **2006,** *80* (8), 4017-25.

158. Newhouse, E. I.; Xu, D.; Markwick, P. R.; Amaro, R. E.; Pao, H. C.; Wu, K. J.; Alam, M.; McCammon, J. A.; Li, W. W., Mechanism of glycan receptor recognition and specificity switch for avian, swine, and human adapted influenza

virus hemagglutinins: a molecular dynamics perspective. *J Am Chem Soc* **2009,** *131* (47), 17430-42.

159.   Alexander, L.; Zhang, S.; McAuliffe, B.; Connors, D.; Zhou, N.; Wang, T.; Agler, M.; Kadow, J.; Lin, P. F., Inhibition of envelope-mediated CD4+-T-cell depletion by human immunodeficiency virus attachment inhibitors. *Antimicrob Agents Chemother* **2009,** *53* (11), 4726-32.

160.   Brindley, M. A., C. L. Hunt, A. Kondratowicz, J. Bowman, P. Sinn, P. B. McCray, K. Quinn, M. L. Weller, J. A. Chiorini, and W. Maury., A requirement for Axl-mediated signaling during Ebolavirus transduction into some cells. *Submitted* **2009**.

161.   Hevey, M.; Negley, D.; Schmaljohn, A., Characterization of monoclonal antibodies to Marburg virus (strain Musoke) glycoprotein and identification of two protective epitopes. *Virology* **2003,** *314* (1), 350-7.

162.   Wang, G.; Slepushkin, V.; Zabner, J.; Keshavjee, S.; Johnston, J. C.; Sauter, S. L.; Jolly, D. J.; Dubensky, T. W., Jr.; Davidson, B. L.; McCray, P. B., Jr., Feline immunodeficiency virus vectors persistently transduce nondividing airway epithelia and correct the cystic fibrosis defect. *J Clin Invest* **1999,** *104* (11), R55-62.

163.   Kao, A. W.; Ceresa, B. P.; Santeler, S. R.; Pessin, J. E., Expression of a dominant interfering dynamin mutant in 3T3L1 adipocytes inhibits GLUT4 endocytosis without affecting insulin signaling. *J Biol Chem* **1998,** *273* (39), 25450-7.

164.   Ivanov, A. I., Pharmacological inhibition of endocytic pathways: is it specific enough to be useful? *Methods Mol Biol* **2008,** *440*, 15-33.

165.   Sun, X.; Yau, V. K.; Briggs, B. J.; Whittaker, G. R., Role of clathrin-mediated endocytosis during vesicular stomatitis virus entry into host cells. *Virology* **2005,** *338* (1), 53-60.

166.   Cureton, D. K.; Massol, R. H.; Saffarian, S.; Kirchhausen, T. L.; Whelan, S. P., Vesicular stomatitis virus enters cells through vesicles incompletely coated with clathrin that depend upon actin for internalization. *PLoS Pathog* **2009,** *5* (4), e1000394.

167.   Doherty, G. J.; McMahon, H. T., Mechanisms of Endocytosis. *Annu Rev Biochem* **2009**.

168.   Hooper, N. M., Detergent-insoluble glycosphingolipid/cholesterol-rich membrane domains, lipid rafts and caveolae (review). *Mol Membr Biol* **1999,** *16* (2), 145-56.

169.   Orlandi, P. A.; Fishman, P. H., Filipin-dependent inhibition of cholera toxin: evidence for toxin internalization and activation through caveolae-like domains. *J Cell Biol* **1998,** *141* (4), 905-15.

170.   Sieczkarski, S. B.; Whittaker, G. R., Dissecting virus entry via endocytosis. *J Gen Virol* **2002,** *83* (Pt 7), 1535-45.

171.   Mercer, J.; Helenius, A., Virus entry by macropinocytosis. *Nat Cell Biol* **2009,** *11* (5), 510-20.

172.   Peterson, J. R.; Mitchison, T. J., Small molecules, big impact: a history of chemical inhibitors and the cytoskeleton. *Chem Biol* **2002,** *9* (12), 1275-85.

173.   Saeed, M. F.; Kolokoltsov, A. A.; Freiberg, A. N.; Holbrook, M. R.; Davey, R. A., Phosphoinositide-3 kinase-Akt pathway controls cellular entry of Ebola virus. *PLoS Pathog* **2008,** *4* (8), e1000141.

174.   Schaeffer, E.; Soros, V. B.; Greene, W. C., Compensatory link between fusion and endocytosis of human immunodeficiency virus type 1 in human CD4 T lymphocytes. *J Virol* **2004,** *78* (3), 1375-83.

175.   Basta-Kaim, A.; Budziszewska, B.; Jaworska-Feil, L.; Tetich, M.; Leskiewicz, M.; Kubera, M.; Lason, W., Chlorpromazine inhibits the glucocorticoid receptor-mediated gene transcription in a calcium-dependent manner. *Neuropharmacology* **2002,** *43* (6), 1035-43.

176.   Lipid second messengers. *Journal of Cellular Biochemistry* **1994,** *56* (S18D), 19-63.

177.   Gekle, M.; Freudinger, R.; Mildenberger, S., Inhibition of Na+-H+ exchanger-3 interferes with apical receptor-mediated endocytosis via vesicle fusion. *J Physiol* **2001,** *531* (Pt 3), 619-29.

178.   Gekle, M.; Drumm, K.; Mildenberger, S.; Freudinger, R.; Gassner, B.; Silbernagl, S., Inhibition of Na+-H+ exchange impairs receptor-mediated albumin endocytosis in renal proximal tubule-derived epithelial cells from opossum. *J Physiol* **1999,** *520 Pt 3*, 709-21.

179.   Binder, M. D.; Kilpatrick, T. J., TAM receptor signalling and demyelination. *Neurosignals* **2009,** *17* (4), 277-87.

180.   Towner, J. S.; Rollin, P. E.; Bausch, D. G.; Sanchez, A.; Crary, S. M.; Vincent, M.; Lee, W. F.; Spiropoulou, C. F.; Ksiazek, T. G.; Lukwiya, M.; Kaducu, F.; Downing, R.; Nichol, S. T., Rapid diagnosis of Ebola hemorrhagic fever by reverse transcription-PCR in an outbreak setting and assessment of patient viral load as a predictor of outcome. *J Virol* **2004,** *78* (8), 4330-41.

181.   Steele, K. E.; Anderson, A. O.; Mohamadzadeh, M., Fibroblastic reticular cells and their role in viral hemorrhagic fevers. *Expert Rev Anti Infect Ther* **2009,** *7* (4), 423-35.

182.   Akhtar, J.; Shukla, D., Viral entry mechanisms: cellular and viral mediators of herpes simplex virus entry. *FEBS J* **2009,** *276* (24), 7228-36.

183.   Kondratowicz, A., Patrick L. Sinn, Kathrina Quinn, Robert A. Davey, Paul D. Rennert, Melinda Brindley, Catherine L. Hunt, Nicholas J. Lennemann, Lindsay M. Sandersfeld, Melodie Weller, Paul B. McCray, Jr., John A.Chiorini and Wendy Maury, T-cell immunoglobulin and mucin domain protein 1 (TIM-1) is a receptor for Ebola and Marburg virus. *Nature* **2010,** *Under review*.

184.   Connolly, B. M.; Steele, K. E.; Davis, K. J.; Geisbert, T. W.; Kell, W. M.; Jaax, N. K.; Jahrling, P. B., Pathogenesis of experimental Ebola virus infection in guinea pigs. *J Infect Dis* **1999,** *179 Suppl 1*, S203-17.

185. Gibb, T. R.; Bray, M.; Geisbert, T. W.; Steele, K. E.; Kell, W. M.; Davis, K. J.; Jaax, N. K., Pathogenesis of experimental Ebola Zaire virus infection in BALB/c mice. *J Comp Pathol* **2001,** *125* (4), 233-42.

186. Bray, M.; Hatfill, S.; Hensley, L.; Huggins, J. W., Haematological, biochemical and coagulation changes in mice, guinea-pigs and monkeys infected with a mouse-adapted variant of Ebola Zaire virus. *J Comp Pathol* **2001,** *125* (4), 243-53.

187. Geisbert, T. W.; Jahrling, P. B.; Hanes, M. A.; Zack, P. M., Association of Ebola-related Reston virus particles and antigen with tissue lesions of monkeys imported to the United States. *J Comp Pathol* **1992,** *106* (2), 137-52.